

---

# TECHNICAL REPORT

## PREDICTING CATCHMENT SCALE PROCESSES, MOUNT LOFTY RANGES, SOUTH AUSTRALIA

2010/17

---

### DISCLAIMER

The Department for Water and its employees do not warrant or make any representation regarding the use, or results of use of the information contained herein as to its correctness, accuracy, reliability, currency or otherwise. The Department for Water and its employees expressly disclaim all liability or responsibility to any person using the information or advice





---

# **PREDICTING CATCHMENT SCALE PROCESSES, MOUNT LOFTY RANGES, SOUTH AUSTRALIA**

---

**Dragana Zulfic<sup>1</sup>, Tania Wilson<sup>2</sup>, Adrian Costar<sup>1</sup> and Luke Mortimer<sup>3</sup>**

**Science, Monitoring and Information Division  
Department for Water**

**May 2010**

**Technical Report DFW 2010/17**

1. Science, Monitoring and Information Division, Department for Water, South Australia
2. Geological Survey Branch, Minerals and Energy Resources Division, Department of Primary Industries and Resources, South Australia
3. School of the Environment, Flinders University of South Australia

## **Science, Monitoring and Information Division**

Department for Water

25 Grenfell Street, Adelaide

GPO Box 2834, Adelaide SA 5001

Telephone	National	(08) 8463 6946
	International	+61 8 8463 6946
Fax	National	(08) 8463 6999
	International	+61 8 8463 6999
Website	<a href="http://www.waterforgood.sa.gov.au">www.waterforgood.sa.gov.au</a>	

### **Disclaimer**

The Department for Water and its employees do not warrant or make any representation regarding the use, or results of the use, of the information contained herein as regards to its correctness, accuracy, reliability, currency or otherwise. The Department for Water and its employees expressly disclaims all liability or responsibility to any person using the information or advice. Information contained in this document is correct at the time of writing.

### **© Government of South Australia, through the Department for Water 2010**

This work is Copyright. Apart from any use permitted under the Copyright Act 1968 (Cwlth), no part may be reproduced by any process without prior written permission obtained from the Department for Water. Requests and enquiries concerning reproduction and rights should be directed to the Chief Executive, Department for Water, GPO Box 2834, Adelaide SA 5001.

ISBN 978-1-921528-86-6

### **Preferred way to cite this publication**

Zulfic D, Wilson T, Costar A and Mortimer L, 2010, *Predicting catchment scale processes, Mount Lofty Ranges, South Australia*, DFW Technical Report 2010/17, Government of South Australia, through Department for Water, Adelaide

Download this document at: <http://www.waterconnect.sa.gov.au/TechnicalPublications/Pages/default.aspx>

---

## PREFACE

---

On July 1<sup>st</sup> 2010, the Department for Water replaced the former Department of Water, Land and Biodiversity Conservation. The Department of Water, Land and Biodiversity Conservation and the abbreviation 'DWLBC' are referred to in several instances in this report. The reader is advised that these terms are retained in certain contexts within this document in order to provide a correct historical account of the investigation and the production of the technical report document.



---

# FOREWORD

---

South Australia's Department for Water leads the management of our most valuable resource—water.

Water is fundamental to our health, our way of life and our environment. It underpins growth in population and our economy—and these are critical to South Australia's future prosperity.

High quality science and monitoring of our State's natural water resources is central to the work that we do. This will ensure we have a better understanding of our surface and groundwater resources so that there is sustainable allocation of water between communities, industry and the environment.

Department for Water scientific and technical staff continue to expand their knowledge of our water resources through undertaking investigations, technical reviews and resource modelling.

Scott Ashby  
CHIEF EXECUTIVE  
DEPARTMENT FOR WATER

---

## ACKNOWLEDGEMENTS

---

The authors wish to thank Enys Watt for her time and effort in compiling numerous data sets of well yields and well depths required for this study.

---

# CONTENTS

---

<b>PREFACE</b> .....	<b>III</b>
<b>FOREWORD</b> .....	<b>V</b>
<b>ACKNOWLEDGEMENTS</b> .....	<b>VI</b>
<b>SUMMARY</b> .....	<b>1</b>
<b>1. INTRODUCTION</b> .....	<b>3</b>
<b>2. GEOLOGICAL SETTING</b> .....	<b>4</b>
<b>3. METHODOLOGY</b> .....	<b>5</b>
3.1. SITE SELECTION AND FIELD DATA COLLECTION .....	5
3.2. STRUCTURAL ANALYSIS.....	8
3.3. CURRENT DAY STRESS REGIME .....	8
3.4. YIELD ANALYSIS .....	10
<b>4. RESULTS</b> .....	<b>11</b>
4.1. STRUCTURAL ANALYSIS.....	11
4.2. CURRENT DAY STRESS REGIME .....	18
4.3. YIELD ANALYSIS .....	23
<b>5. DISCUSSION AND CONCLUSIONS</b> .....	<b>29</b>
<b>6. RECOMMENDATIONS</b> .....	<b>31</b>
<b>APPENDICES</b> .....	<b>32</b>
A. STEREOGRAPHIC PROJECTION .....	32
B. FRACTURE SPACING ANALYSIS .....	61
<b>UNITS OF MEASUREMENT</b> .....	<b>73</b>
<b>GLOSSARY</b> .....	<b>74</b>
<b>REFERENCES</b> .....	<b>76</b>

---

## CONTENTS

---

### LIST OF FIGURES

Figure 1	Example of the site selection process using subdivision into structural domains (red lines), followed by representative sites selected based on lithological variations within each domain (circles).....	6
Figure 2	Geological map and location of measured sites .....	7
Figure 3	The World Stress Map stress regime classifications and their associated styles of faulting (from Heidbach et al. 2008) .....	9
Figure 4	Conceptual fracture network model showing upper, transition and lower zones .....	10
Figure 5	Dominant fracture sets stereographic projection .....	11
Figure 6	Lithology and dominant fracture set orientations plotted as strike, dip and dip direction .....	13
Figure 7	Distribution of historical seismic activity, earthquake magnitudes and $S_H$ azimuth estimates in southern South Australia (from Quigley, 2006). .....	18
Figure 8	In-situ stress field indicators within the Adelaide Geosyncline, including the method, quality ranking, stress regime and orientations of the principal horizontal stress axis ( $S_H$ ) (from Heidbach et al., 2008) .....	19
Figure 9	Map of dominant fracture orientations relative to the maximum principal stress direction. Figure includes summarised results from the Zones of Influence sub-program (Costar et al., 2008).....	21
Figure 10	Geological map and location of wells with well yields.....	25

### LIST OF TABLES

Table 1	Summary of dominant fracture orientations for the central Mount Lofty Ranges .....	14
Table 2	World Stress Map 2008 quality ranked stress field data for the entire Adelaide Geosyncline (Heidbach et al., 2008).....	20
Table 3	Analysis of the relationship between yield and depth; results summary .....	23

---

## SUMMARY

---

The Mount Lofty Ranges (MLR) are located within the southern portion of the Adelaide Geosyncline, which is a Neoproterozoic to Cambrian age, thick (>10 km), rift-related basin complex (Preiss, 2000). Sedimentary rocks were deposited in a fault controlled, north-northwest-trending extensional basin over several phases of rifting and marine transgression–regression cycles (Preiss, 1995, 2000).

During the late Miocene period (<6 Ma), a new phase of tectonic activity commenced which continues to affect southeastern Australia today. This new, and ongoing, tectonic phase was initiated by coupling and/or convergence between the Pacific and Australia plates (Hillis and Reynolds, 2000; Sandiford et al., 2004).

Conceptualisation of groundwater flow in a fractured rock environment required several assumptions regarding fracture network development and the structural geology at a regional or catchment scale. One of the assumptions was that groundwater flow directions are preferentially controlled by one or more dominant fracture sets.

Mapped geological formations and specific units throughout the MLR were assessed and grouped according to similar lithological characteristics. Since fracture distribution and density typically varies across a fold structure and with lithological variations, the region was subdivided into structural domains. The study area extends from Mt Crawford in the north to the vicinity of Mt Compass in the south, and the hills face zone on the eastern margins of metropolitan Adelaide eastwards to Monarto, an area of ~2500 km<sup>2</sup>.

Fracture orientation, fracture spacing and bedding measured at 84 sites have indicated a tendency for fractures to be orientated NNE, with moderate to steep easterly dips where bedding exhibits a significant role in controlling the orientation of the dominant fracture sets throughout the MLR. This is consistent with the findings of the Zones of Influence sub-program (Costar et al., 2008), and correlates with the preferential groundwater flow path.

All fracture sets collectively allow the flow of groundwater in the direction of the regional hydraulic gradient. However, on a sub-regional or local scale, groundwater flow is highly variable and dependent on rock type, geological structure, fracture aperture and density.

Fracture spacing analyses indicate increased fracture spacing with increased competency of the rock type. Competent units such as the high-grade metamorphic basement of the Barossa Complex, Adelaidean quartzites and Cambrian turbidites, typically have average fracture spacings greater than 6 cm, whilst units of lesser competency, such as siltstones, exhibit much closer fracture spacings averaging 1–3 cm.

The current day stress regime does not appear to exert a significant influence over preferential flow directions in shallow fractured rock aquifers; unloading and weathering has a much greater influence on the development of fractures and their density at shallow crustal levels.

The conceptual fracture network model for the study area can be broadly divided into a densely fractured weathered upper zone (0–100 m), a less-fractured transitional zone (100–200 m) and a broadly fractured lower zone (>200 m). The extreme high-yielding characteristics (>60 L/s) are likely to be associated with densely fractured fault zones.

Consistently low yields observed in the Cambrian turbidites, compared to Adelaidean metasediments, may be a result of erosion of the upper weathered section of the sequence, which is consistent with

---

## SUMMARY

---

results indicating uplift and unloading producing higher yields at shallow depths in the Adelaidean metasediments.

---

# 1. INTRODUCTION

---

The MLR provide important surface water and groundwater resources for domestic, industrial and agricultural purposes locally, as well as metropolitan Adelaide's reticulated water supply. As such, water allocations in these areas need to be actively managed to ensure that current and future uses of these resources are sustainable and that the environment is also recognised as a user of the resource.

The National Water Initiative (NWI) funded project *Improve the knowledge of groundwater flow mechanisms in fractured rock aquifers in the Mount Lofty Ranges, Northern Adelaide Plains, and Kangaroo Island* aims to improve decision-making processes on the allocation of groundwater resources in fractured rock aquifers (FRAs) by increasing the understanding of groundwater flow mechanisms in these systems. Predicting Catchment Scale Processes, Mount Lofty Ranges, South Australia is one of four sub-programs conducted over a period of four years, between 2004 and 2010.

The fractured rock aquifer systems are characterised by high spatial variability in hydraulic conductivity, making traditional hydraulic methods for estimating groundwater flow difficult to apply. Due to the heterogeneous nature of these systems, there is a lack of predictive capability at regional scales.

The current project includes detailed structural mapping at the catchment scale, and the analysis of obtained information on fracture orientations, spacing and connectivity. The purpose of the project is to determine consistent geological and structural characteristics within a catchment and ascertain which regions in the MLR are favourable for groundwater flow based on these measured fracture set orientations. The concept that past and present stress regimes play a controlling role in the development of FRAs has been established for many years and was considered in the structural analysis. The final element of the project was to analyse the relationship between yield and lithology in order to qualitatively estimate fracture density.

---

## 2. GEOLOGICAL SETTING

---

The Mount Lofty Ranges are located within the southern portion of the Adelaide Geosyncline, which is a Neoproterozoic to Cambrian age, thick (>10 km), rift-related basin complex (Preiss, 2000). Sedimentary rocks were deposited in a fault controlled, north-northwest-trending extensional basin over several phases of rifting and marine transgression–regression cycles (Preiss, 1995, 2000). During the middle-late Cambrian Delamerian Orogeny, these rocks were subjected to low-grade, greenschist-facies metamorphism and three deformation events ( $D_1$ – $D_3$ ). This was a major episode of crustal shortening leading to strongly contractional, west-verging, thrust faulting and NNW-trending folding (Preiss, 2000). From the Delamerian Orogeny until the late Miocene period the Adelaide Geosyncline remained relatively tectonically stable (Preiss, 1995).

As southern Australia entered the late Miocene period (<6 Ma), a new phase of tectonic activity commenced which continues to affect southeastern Australia today. This new, and ongoing, tectonic phase was initiated by coupling and/or convergence between the Pacific and Australia plates (Hillis and Reynolds, 2000; Sandiford et al., 2004).

---

## 3. METHODOLOGY

---

The concept that past and present stress regimes play a controlling role in the development of FRAs has been established for many years (Barton et al., 1995; NRC, 1996; Ferrill et al., 1999). For example, palaeostress regimes play a significant role in the primary development of fractures and fracture permeability during episodes of rock deformation, whilst present-day stress regimes may superimpose a secondary influence on pre-existing fracture networks by further deforming them.

Exactly how a fracture network will behave under an applied stress regime depends upon many factors; however, relationships have been established between the hydraulic behaviour of fractures, their geometry, orientation and the in-situ stress field (Barton et al., 1995; Zhang et al., 1996; Ferrill et al., 1999). Fluid flow through fractures is linked to tectonic stress and deformation via changes in permeability and storage, whilst tectonic stress and deformation is linked to fluid flow via changes in fluid pressure and effective stress (NRC, 1996).

Conceptualisation of groundwater flow in a fractured rock environment requires several assumptions regarding fracture network development and the structural geology at a regional or catchment scale. Studies of contaminant transport in FRAs have highlighted that groundwater flow is focused along major fracture sets with a preferred orientation (Mortimer et al., 2008a,b). Additionally, potentiometric surfaces of FRAs at a catchment scale have long been recognised as not accurately reflecting groundwater flow directions at a local scale.

Given this, a reasonable assumption regarding FRAs is that groundwater flow directions are preferentially controlled by one or more dominant fracture sets. Furthermore, the development of these dominant fracture sets, their orientation, spacing and interconnectivity, will be largely controlled by the deformation history, lithology and competency variations of the rocks throughout the catchment.

### **3.1. SITE SELECTION AND FIELD DATA COLLECTION**

Mapped geological formations and specific units throughout the MLR were assessed and grouped according to similar lithological characteristics. Grouped formations and units were displayed using GIS, providing a spatial distribution of rocks with common lithological properties.

Fracture distribution and density typically varies across a fold structure and with lithological variations. As such, the region was subdivided into structural domains (Fig 1), with a total of 130 sites initially selected as being representative of different lithologies occurring within each domain.

Due to the sparse nature of outcrop throughout some areas of the MLR, a reconnaissance field survey was undertaken to locate and record locations of outcrop suitable for fracture analysis. A GPS navigation system was connected to a laptop displaying a geological map with the selected sites in order to locate outcrop as near as possible to the initial preferred locations. Over 150 sites were recorded, however a significant number could not be analysed due to access issues in roadside cuttings.

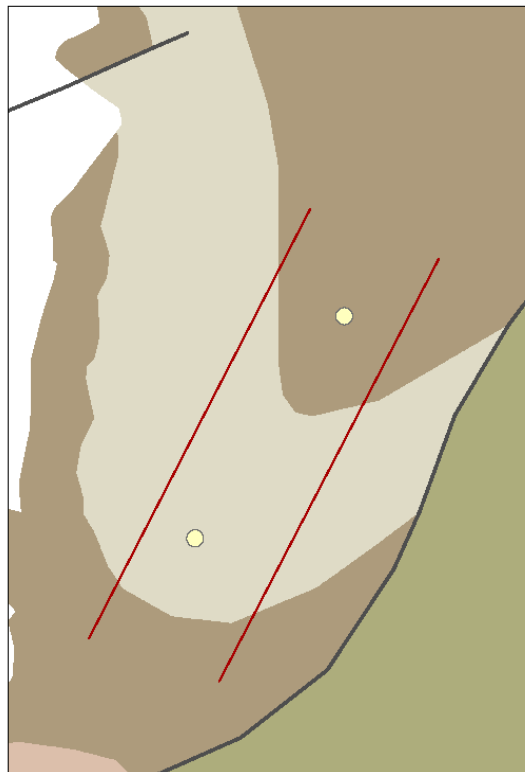


**Figure 1** Example of the site selection process using subdivision into structural domains (red lines), followed by representative sites selected based on lithological variations within each domain (circles)

From this initial reconnaissance, a total of 84 sites throughout the MLR were studied with measurements of fracture orientation (strike/dip/dip direction), fracture spacing and, where present, bedding and/or schistosity (Fig 2). The study area extends from Mt Crawford in the north to the vicinity of Mt Compass in the south, and the hills face zone on the eastern margins of metropolitan Adelaide eastwards to Monarto, an area of ~2500 km<sup>2</sup>.

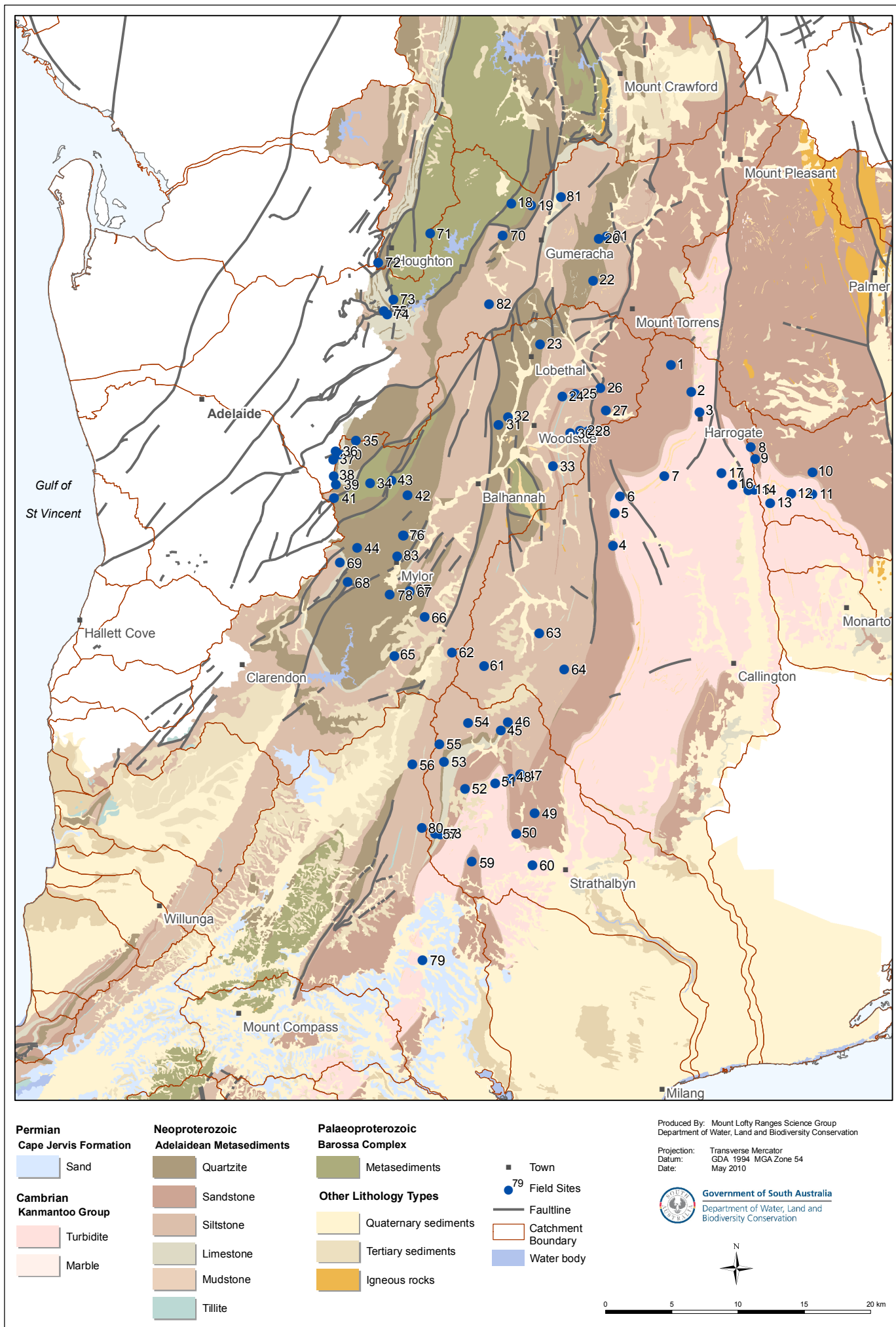


Figure 2. Geological map and location of measured sites

### **3.2. STRUCTURAL ANALYSIS**

Fracture orientation data for each site were plotted as poles on equal area, lower hemisphere stereonet using the program Stereostat V1.2. The data were contoured using 1% area contouring and an inverse square smoothing function, and subsequently analysed for dominant fracture orientation. A dominant fracture orientation was determined for each site and a representative great circle girdle added manually to the stereographic projection. Bedding and schistosity orientations, where present, were also added to the projections as great circle girdles. An assessment of whether the dominant fracture orientation was parallel to bedding was made and results summarised. In addition, all dominant fracture set data were combined in a single stereographic projection and contoured separately.

Strike, dip and dip direction information for each dominant fracture set was plotted spatially using GIS and overlain on the lithological properties coverage. This map was then used to compare dominant fracture orientation information for each site with bedding, regional geological structures, the current day stress regime, aquifer yield and results from the Zones of Influence sub-program from this project (Costar et al., 2008).

Fracture spacing information, specifically the distance between two consecutive fractures within the same fracture set, was collected during fieldwork. These data were used in a frequency analysis to determine the average spacing of dominant fracture sets occurring at each site, and was subsequently compared to lithology.

### **3.3. CURRENT DAY STRESS REGIME**

Stress ( $\sigma$ ) is quantified as force per unit area and arises at all scales throughout the Earth's crust from several sources including the weight of overlying rocks, tectonic forces, fluid pressures, thermal loading and other geological phenomena such as volcanic activity and igneous intrusions (Hobbs et al., 1976). Generally, stress fields are inhomogeneous and defined in simplified terms by three mutually orthogonal principal axes of stress, namely the vertical principal stress ( $\sigma_v$ ) and the maximum and minimum horizontal principal axes of stress ( $\sigma_H$  and  $\sigma_h$ , respectively). Far-field crustal stress regimes are classified using the Andersonian scheme, which relates the three major styles of faulting in the crust to the three major arrangements of the principal axes of stress (Anderson, 1951). These three major stress regimes are: (a) normal faulting stress regime where  $\sigma_v > \sigma_H > \sigma_h$ ; (b) strike-slip faulting stress regime where  $\sigma_H > \sigma_v > \sigma_h$ ; and (c) thrust faulting stress regime where  $\sigma_H > \sigma_h > \sigma_v$  (Fig 3).

Stress-dependant permeability of deep-seated, fractured rocks is well documented in studies relating to hydrocarbon and geothermal reservoirs, as well as nuclear repositories. In particular, in-situ stress fields are known to exert a significant control on fluid flow patterns in fractured rocks with low matrix permeability. For example, in a key study of deep (>1.7 km) boreholes, Barton et al. (1995) found that permeability manifests itself as fluid flow focused along fractures favourably aligned within the in-situ stress field, and that if fractures are critically stressed, this can impart a significant anisotropy to the permeability of a fractured rock mass. Preferential flow occurs along fractures that are orientated orthogonal to the minimum principal stress direction (due to low normal stress), or inclined  $\sim 30^\circ$  to the maximum principal stress direction (due to shear dilation).

Stress acting on a fracture plane can be resolved into normal and shear stresses, which are the components of stress that act normal and parallel to a plane, respectively. In a fractured rock mass, these stresses are highly coupled and can cause fractures to deform, with the potential rate of fracture deformation considered to be greatest at shallow depths where lower confining pressures result in a lesser amount of contact between fracture walls ("fracture stiffness") (NRC, 1996). This would imply that stress-dependent fracture permeability may be expected to be greatest at shallow depths where groundwater is typically extracted. Conversely, the potential influence of stress on fracture permeability

## METHODOLOGY

at shallow depths might also be less effective as lower confining pressures are less likely to cause fractures to be critically stressed. This last point is perhaps the main reason why the effects of stress fields are largely ignored in shallow depth hydrogeological investigations.

Earthquake focal mechanisms and fault kinematic analyses have been used to determine the current day stress regime for the MLR (Love, 1999, 2001).

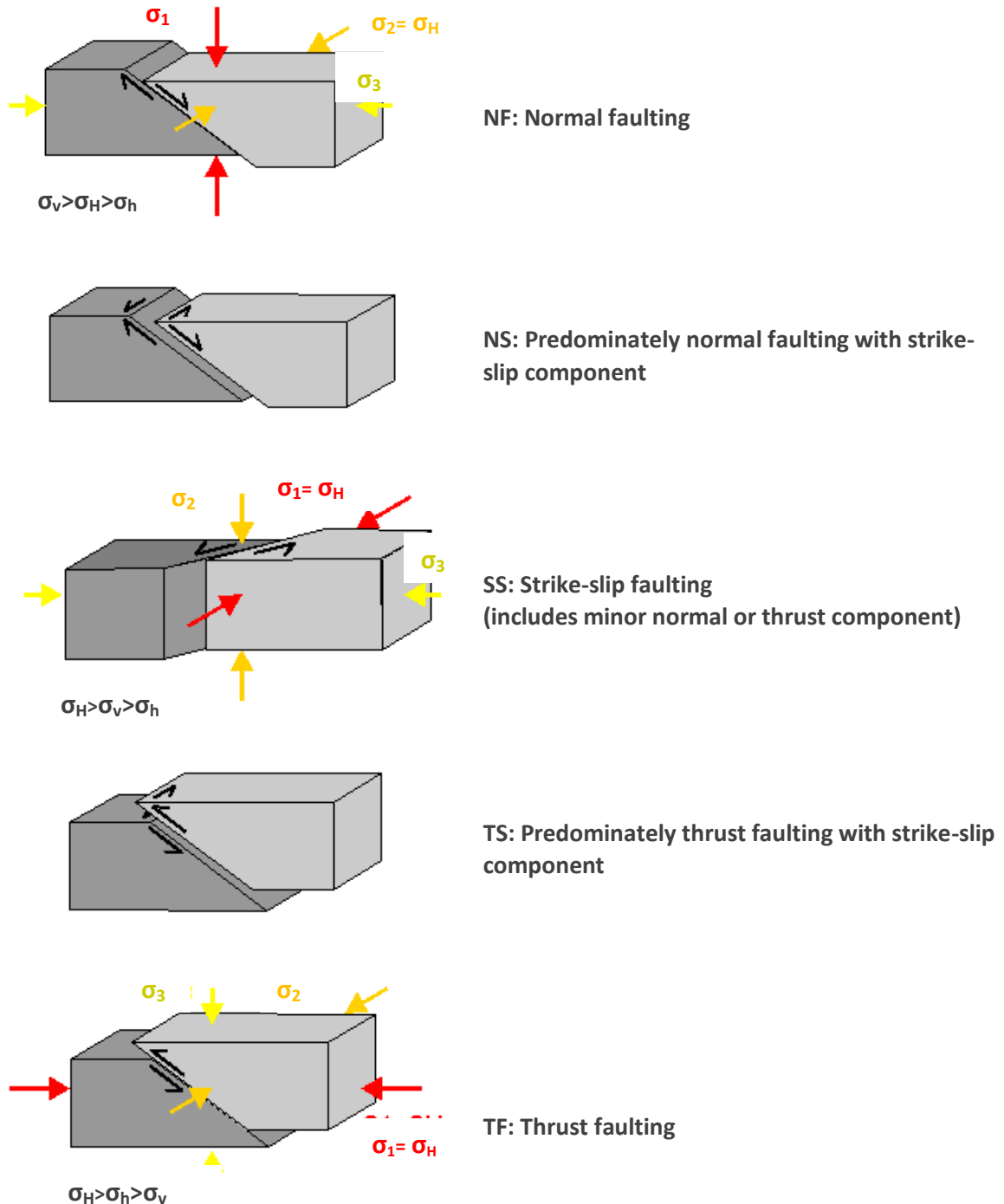


**Figure 3** The World Stress Map stress regime classifications and their associated styles of faulting (from Heidbach et al. 2008)

### 3.4. YIELD ANALYSIS

The conceptual fracture network model consists of a densely fractured, weathered upper zone, a less-fractured transitional zone and a broadly fractured lower zone, as seen in Figure 4. Dashed lines denote the persistent, dense, bedding planes whilst the solid lines represent typical joint sets. With increasing depth there is a trend of decreasing fracture density based upon a reduction in the number of fracture sets against a persistent background of high-density bedding planes. The primary cause of this decreasing fracture density trend with depth is attributed to the effects of uplift and unloading.

This model has been used in the shallow FRAs in the Clare Valley area to analyse the relationship between depth, fracture density and well yields. This study concluded that the direction of maximum hydraulic conductivity is aligned with the strike of the steeply dipping bedding and that there are two distinct, shallow, upper and lower groundwater flow systems in the Clare Valley (Love, 2003).

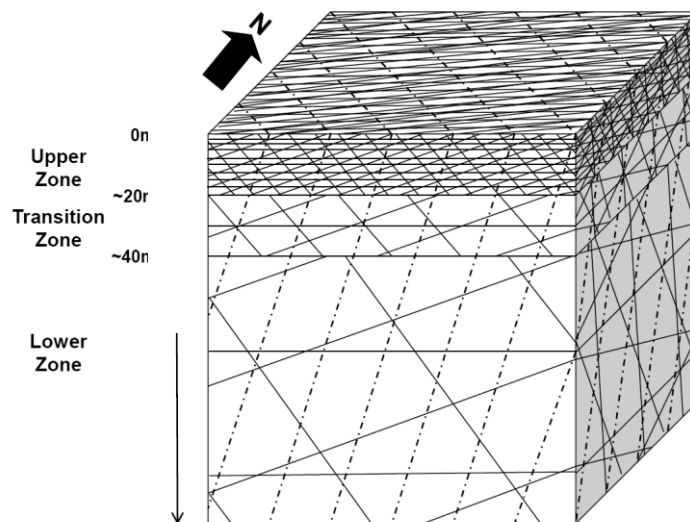


**Figure 4** Conceptual fracture network model showing upper, transition and lower zones

Based on the assumption that these effects of uplift and unloading are widespread across the entire MLR, this conceptual fracture network model has been adopted for the MLR study area. In addition, information on specific geological formations and lithology was applied to the adopted model in order to identify relationship between depth, yield, fracture density and lithology.

Yield versus depth plotted for each lithology type was analysed to determine:

- the distinctive depth at which yield stops increasing for each lithology type, from which the conceptual fracture network model for the southern MLR area will be determined,
- the relationship between maximum yield and depth as a function of weathering or unloading,
- the relationship between yield and lithology to qualitatively estimate fracture density.

## 4. RESULTS

### 4.1. STRUCTURAL ANALYSIS

Fracture orientation, fracture spacing and bedding, where present, were measured at 84 sites throughout the MLR (Fig 5). A summary of fracture details, bedding and schistosity information is presented in Table 1.

All data were plotted as poles on equal area, lower hemisphere stereonet using the program Stereostat V1.2. The data have been contoured using 1% area contouring and an inverse square smoothing function, and subsequently analysed (Appendix A). In addition, the dominant fracture orientations for each site have been plotted as poles and contoured separately (Fig 6).

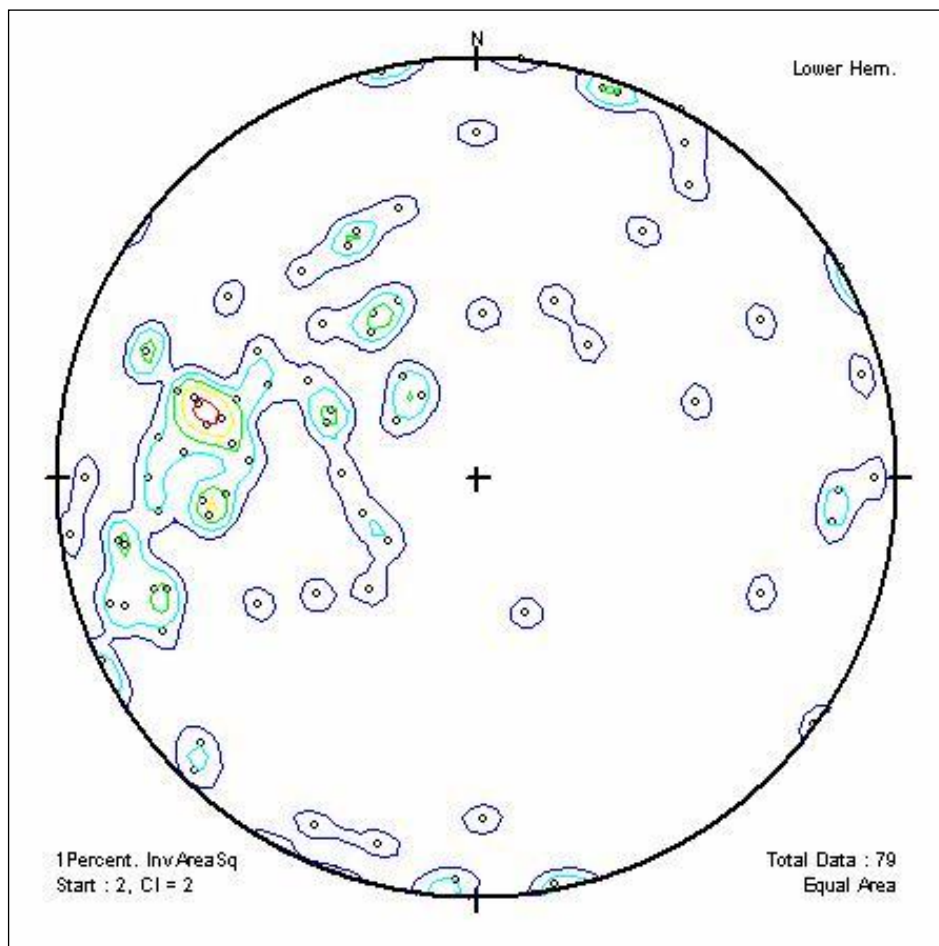


**Figure 5** Dominant fracture sets stereographic projection

This plot highlights the scattered and variable orientation of the dominant fracture sets, which is not unexpected given the large sampling area, variable lithologies and structural complexity throughout the MLR. Figure 6 does however, indicate a broad clustering of poles in the NW quadrant of the stereonet with an average orientation of  $014/56^{\circ}$  E.

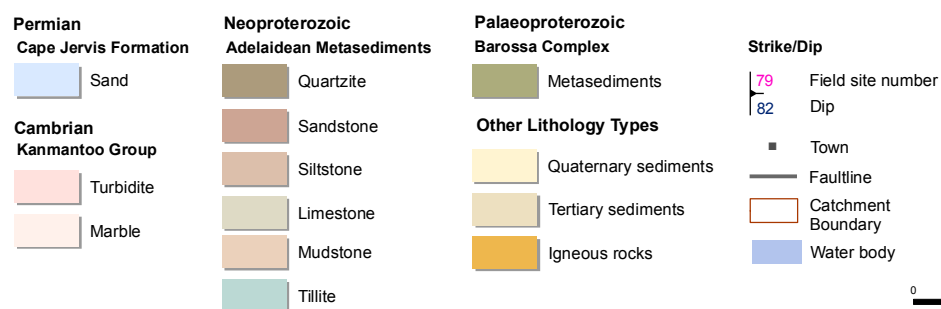
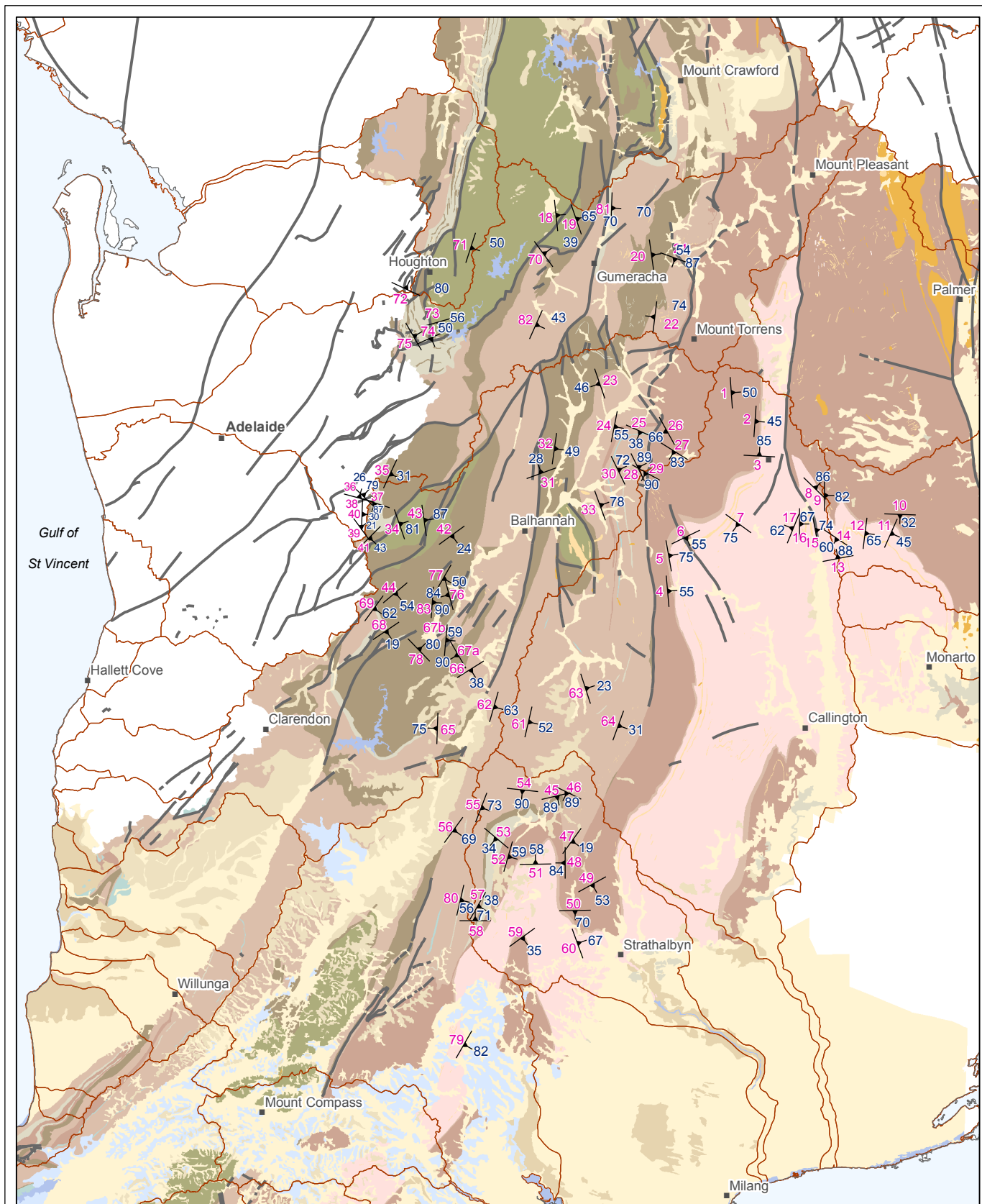
---

## RESULTS

---

An analysis of the parallelism between bedding and the dominant fracture set at each site was also undertaken. Of the 51 sites where bedding was observed, 40 sites exhibited a dominant fracture set parallel to bedding, and at 11 sites the dominant fracture set was not parallel to bedding (Table 1). Sites where dominant fracture orientation was not parallel to bedding often exhibited fractures parallel to schistosity. For the remaining sites, bedding was not observed due to lithology type or metamorphic grade.

Overall, this field work indicated a tendency for fractures throughout the MLR to be orientated NNE with moderate to steep easterly dips, with bedding providing a significant role in controlling the orientation of the dominant fracture sets.



Produced By: Mount Lofty Ranges Science Group  
 Department of Water, Land and Biodiversity Conservation  
 Projection: Transverse Mercator  
 Datum: GDA 1984 MGA Zone 54  
 Date: May 2010

**Government of South Australia**  
 Department of Water, Land and Biodiversity Conservation



Figure 6. Lithology and dominant fracture set orientations plotted as strike, dip and dip direction

## RESULTS

**Table 1** Summary of dominant fracture orientations for the central Mount Lofty Ranges

Site	Fracture Sets Total	Dominant Orientation	n Total	n Dominant	Bedding Parallel	Strike-CDSR Difference	Fracture Spacing (cm)	Lithology	Geology	Comments
1	3	176/50 E	34	16	Yes	66	>6	Sandstone	Backstairs Passage Fm	
2	3	184/45 E	16	9	Yes	74	3–5	Siltstone	Talisker Formation	
3	2	093/85 N	32	22	No	17	2–3, >6	Turbidite	Tapanappa Formation	
4	4	175/55 E	28	28	Yes	65	0–2	Siltstone	Backstairs Passage Fm	
5	3	170/75 E	30	13		60	0–1	Turbidite	Tapanappa Formation	Parallel to schistosity
6	3	064/55 S	26	16		46	>6	Turbidite	Tapanappa Formation	Parallel to schistosity
7	3	126/75 S	26	14	No	16	>6	Turbidite	Tapanappa Formation	
8	2	134/86 E	15	13		24	>6	Sandstone	Backstairs Passage Fm	
9	2	180/82 E	20	12		70	>6	Sandstone	Backstairs Passage Fm	Parallel to schistosity
10	2	092/32 S	34	24	Yes	18	0–1	Sandstone	Backstairs Passage Fm	
11	4	024/45 E	14	6		86	>6	Turbidite	Tapanappa Formation	Parallel to schistosity
12	2	007/65 E	22	18	No	103	>6	Turbidite	Tapanappa Formation	
13	2	079/88 N	17	9		31	>6	Turbidite	Tapanappa Formation	
14	3	124/60 W	15	8		14	>6	Turbidite	Tapanappa Formation	
15	3	169/74 E	31	23		59	2–3	Turbidite	Tapanappa Formation	
16	4	180/67 E	26	9	Yes	70	>6	Turbidite	Tapanappa Formation	
17	4	022/62 W	21	9		88	>6	Turbidite	Tapanappa Formation	
18	4	174/65 E	53	24	Yes	64	>6	Metasediments	Barossa Complex	Parallel to schistosity
19	6	161/70 N	36	15	Yes	51	>6	Quartzite	Aldgate sandstone	
20	4	172/54 E	42	24	Yes	62	0–1	Quartzite	Stonyfell Quartzite	
21	2	110/87 S	18	12		0	>6	Quartzite	Stonyfell Quartzite	
22	4	007/74 W	47	22	No	103	>6	Quartzite	Stonyfell Quartzite	
23	4	161/46 S	33	12		51	>6	Quartzite	Stonyfell Quartzite	
24	3	011/55 E	52	30	Yes	99	1–3	Sandstone	Belair Subgroup	
25	5	114/38 S	30	8	Yes	4	1–2	Siltstone	Belair Subgroup	
26	2	151/66 W	25	14		41	>6	Sandstone	Mitcham Quartzite	

## RESULTS

Site	Fracture Sets Total	Dominant Orientation	n Total	n Dominant	Bedding Parallel	Strike-CDSR Difference	Fracture Spacing (cm)	Lithology	Geology	Comments
27	2	122/83 S	29	15	No	12	>6	Sandstone	Backstairs Passage Fm	Orthogonal fracture set parallel to S <sub>0</sub>
28	3	154/89 E	37	23	Yes	44	5–6	Siltstone	Tarcowie Siltstone	
29	3	119/90	33	12	No	9	>6	Siltstone	Tarcowie Siltstone	
30	3	154/72 E	31	16		44	>6	Limestone	Brighton Limestone	
31	3	070/28 N	40	24	Yes	40	1–2	Quartzite	Stonyfell Quartzite	
32	2	008/49 E	79	62	Yes	102	0–1	Quartzite	Stonyfell Quartzite	Parallel to schistosity
33	2	160/78 E	48	43	Yes	50	0–1	Sandstone	Mitcham Quartzite	
34	3	161/81 E	28	13		51	>6	Metasediments	Barossa Complex	
35	3	025/31E	45	20	Yes	85	>6	Quartzite	Basket Range Sandstone	
36	3	105/79 N	19	9	No	5	>6	Quartzite	Stonyfell Quartzite	
37	2	108/87 S	27	18	No	2	5–6	Quartzite	Stonyfell Quartzite	
38	3	002/26 E	50	35	Yes	108	0–1	Quartzite	Stonyfell Quartzite	
39	3	144/21 N	24	9		34	>6	Quartzite	Stonyfell Quartzite	Possible conjugate joint set
40	3	134/30 E	49	26	Yes	24	1–2	Limestone	Mundallio Subgroup	
41	2	045/43 S	39	31	Yes	65	0–1	Quartzite	Stonyfell Quartzite	
42	3	054/24 E	28	20	Yes	56	1–3	Quartzite	Aldgate Sandstone	
43	1	172/87 E	12	12		62	>6	Metasediments	Barossa Complex	Parallel to schistosity
44	3	050/54 S	34	19	Yes	60	>6	Quartzite	Aldgate Sandstone	
45	4	077/89 S	33	14		33	0–1	Quartzite	ABC Range Quartzite	
46	4	036/89 W	21	10		74	>6	Quartzite	ABC Range Quartzite	
47	4	036/19 E	42	34	Yes	74	1–2	Siltstone	Ulupa Siltstone	
48	6	180/84 W	79	23	Yes	70	0–1	Sandstone	Backstairs Passage Fm	
49	5	061/53 E	42	19		49	2–3	Sandstone	Backstairs Passage Fm	
50	3	089/70 N	45	22	Yes	21	2–3	Siltstone	Talisker Formation	
51	2	015/58 E	18	12		95	>6	Turbidite	Tapanappa Formation	
52	3	016/59 E	19	13	Yes	94	>6	Sandstone	Backstairs Passage Fm	
53	4	130/34 W	55	23		20	0–2	Quartzite	ABC Range Quartzite	
54	2	096/90	17	10		14	>6	Siltstone	Tarcowie Siltstone	

## RESULTS

Site	Fracture Sets Total	Dominant Orientation	n Total	n Dominant	Bedding Parallel	Strike-CDSR Difference	Fracture Spacing (cm)	Lithology	Geology	Comments
55	3	021/73 E	26	10	Yes	89	0–1	Siltstone	Ulupa Siltstone	
56	4	036/69 E	69	43	Yes	74	1–2	Siltstone	Belair Subgroup	
57	2	030/38 N	40	30	Yes	80	0–2	Siltstone	Ulupa Siltstone	
58	3	090/71 E	15	8	Yes	20	3–4	Limestone	Normanville Group	
59	2	054/35 E	15	9	Yes	56	>6	Sandstone	Balquhider Formation	
60	3	160/67 E	16	8		50	>6	Turbidite	Tapanappa Formation	
61	3	013/52 E	37	27	Yes	97	1–2	Siltstone	Tarcowie Siltstone	
62	4	016/63 E	62	41	Yes	94	0–1	Siltstone	Saddleworth Formation	
63	3	162/23 E	42	26	Yes	52	0–1	Siltstone	Tapley Hill Formation	
64	2	020/31 S	10	7		90	>6	Siltstone	Ulupa Siltstone	
65	2	002/75 W	11	6		108	>6	Quartzite	Aldgate Sandstone	Fracture sets orthogonal
66	2	058/38 E	18	11	Yes	52	0–1	Siltstone	Woolshed Flat Shale	
67A	2	150/90	31	24	Yes	40	0–3	Quartzite	Aldgate Sandstone	
67B	2	005/59 E	22	16		105	>6	Quartzite	Aldgate Sandstone	
68	4	056/19 E	38	11	Yes	54	>6	Quartzite	Aldgate Sandstone	
69	2	036/62 E	15	10	Yes	74	0–1	Siltstone	Woolshed Flat Shale	
70	2	144/39 E	28	19	Yes	34	2–4	Quartzite	Stonyfell Quartzite	
71	2	018/50 E	31	26	Yes	92	>6	Metasediments	Barossa Complex	
72	3	115/80 N	67	30		5	1–2	Quartzite	Aldgate Sandstone	
73	3	074/56 SE	25	13	No	36	>6	Quartzite	Aldgate Sandstone	
74	3	066/38 S	27	10		44	>6	Limestone	Montacute Dolomite	
75	2	150/50E	40	29	Yes	40	3–4	Limestone	Skillogalee Dolomite	
76	1	165/84 W	12	12	No	55	>6	Quartzite	Aldgate Sandstone	
77	2	030/50 E	30	16	Yes	80	1–2	Quartzite	Aldgate Sandstone	Both fracture sets dominate outcrop
78	3	136/80 E	21	13	No	26	>6	Quartzite	Aldgate Sandstone	
79	5	030/82 E	39	15	Yes	80	>6	Turbidite	Tapanappa Formation	Parallel to schistosity
80	6	013/56 E	95	54	Yes	97	1–2	Siltstone	Tarcowie Siltstone	Parallel to schistosity
81	15	002/66 E	410	32	Yes	108	1–2	Siltstone	Woolshed Flat Shale	Parallel to schistosity

---

## RESULTS

---

Site	Fracture Sets Total	Dominant Orientation	n Total	n Dominant	Bedding Parallel	Strike-CDSR Difference	Fracture Spacing (cm)	Lithology	Geology	Comments
82	23	024/48 E	150	16	Yes	86	1-2	Siltstone	Saddleworth Formation	
83	16	004/90	81	13	No	106	>6	Quartzite	Aldgate Sandstone	Parallel to schistosity

## 4.2. CURRENT DAY STRESS REGIME

Determination of the current day stress regime indicates that the MLR is currently under the influence of horizontal, approximately WNW–ESE directed compression and is seismically active as shown in Figure 7 (Love, 1999, 2001).

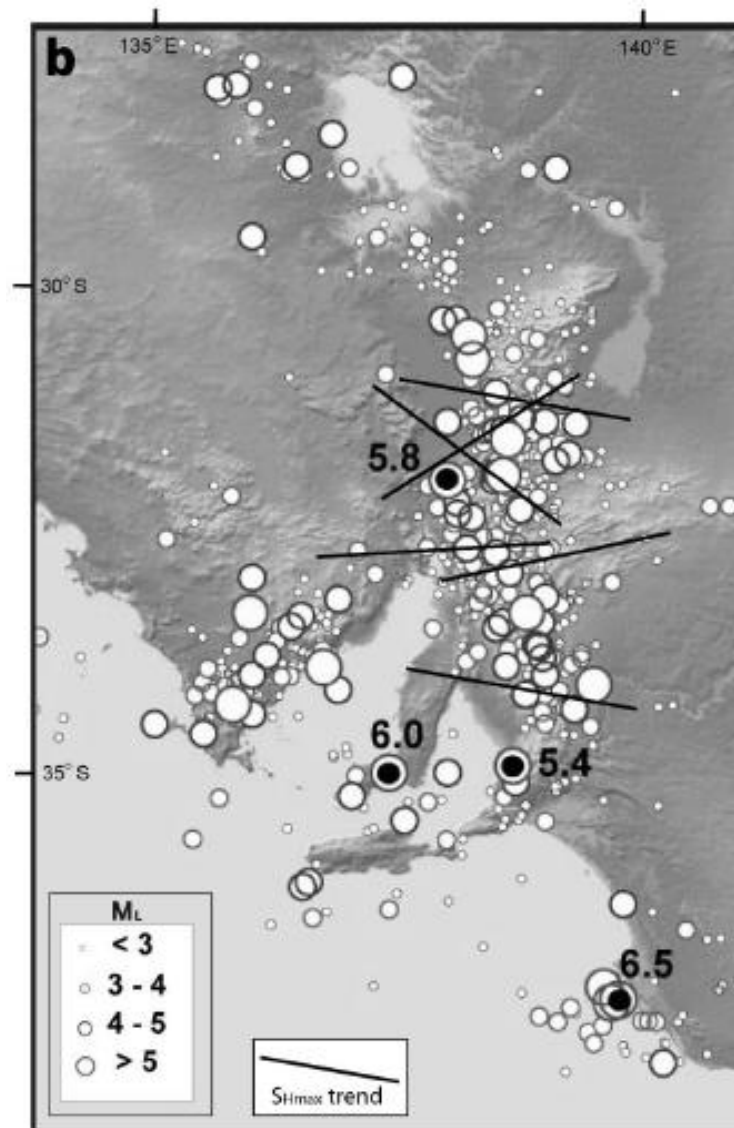


**Figure 7** Distribution of historical seismic activity, earthquake magnitudes and  $S_H$  azimuth estimates in southern South Australia (from Quigley, 2006).

Evidence from earthquake focal mechanisms and fault kinematic analyses suggests that the MLR is currently under the influence of a thrust fault stress regime with an  $S_H$  azimuth of  $110^\circ$  (D. Love, PIRSA, pers. comm, 2009). A compilation of the World Stress Map 2008 data release for all quality ranked in-situ stress field data for the entire Adelaide Geosyncline is illustrated in Figure 8 and Table 2.

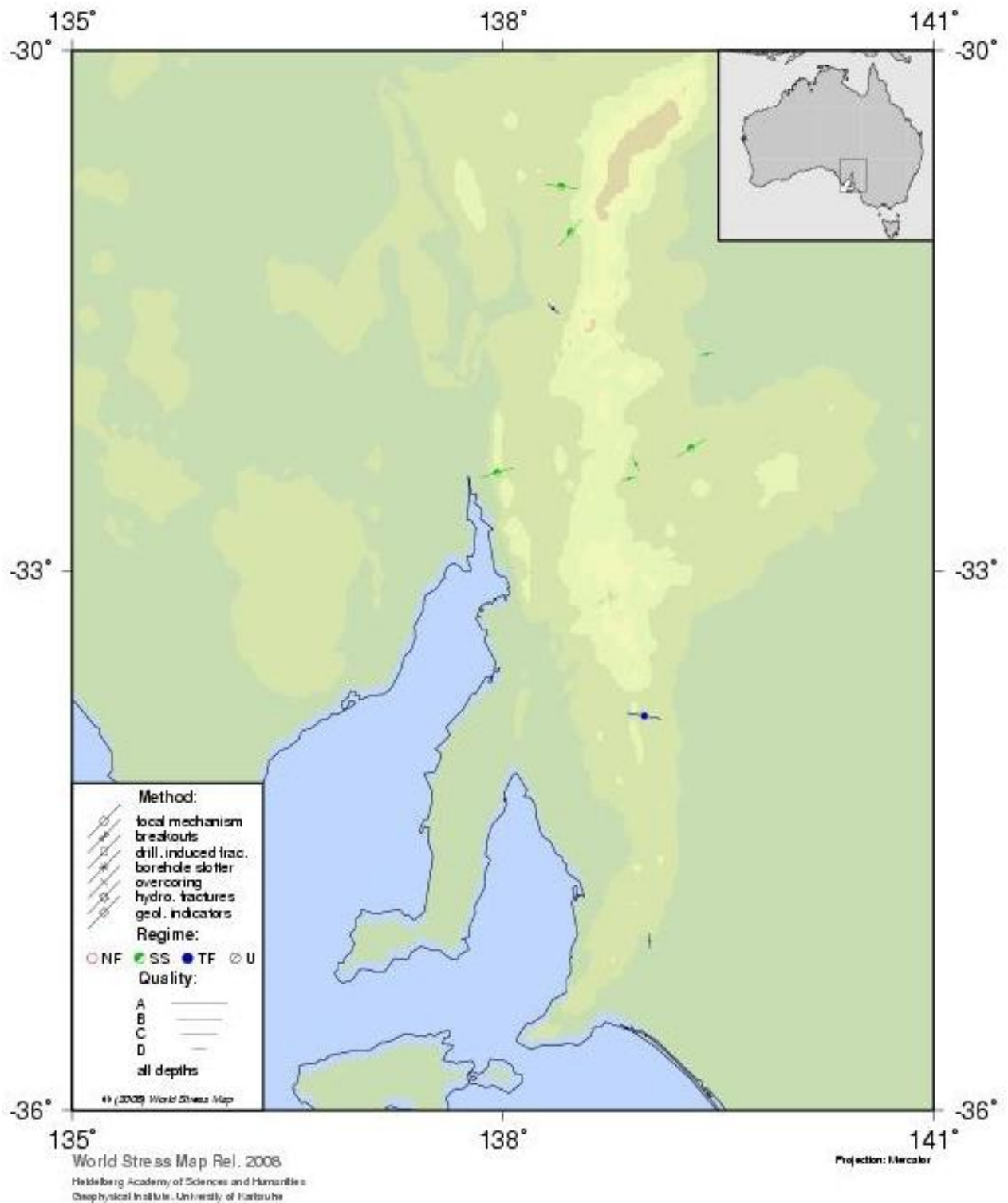


**Figure 8** In-situ stress field indicators within the Adelaide Geosyncline, including the method, quality ranking, stress regime and orientations of the principal horizontal stress axis ( $S_H$ ) (from Heidbach et al., 2008)

## RESULTS

**Table 2 World Stress Map 2008 quality ranked stress field data for the entire Adelaide Geosyncline (Heidbach et al., 2008)**

Latitude	Longitude	S <sub>H</sub> azimuth (°)	Type	Quality	Regime	Depth (km)
-35.07	139.02	173	OC	D	U	0.058
-30.794	138.405	97	FMS	C	SS	20
-32.476	138.878	76	FMS	D	SS	6.8
-32.389	138.923	153	FMS	D	SS	16.4
-32.3	139.31	59	FMS	C	SS	15
-31.06	138.47	41	FMS	C	SS	10
-32.44	137.96	74	FMS	C	SS	5
-31.76	139.42	86	FMS	D	SS	5
-33.816	138.984	100	FMS	C	TF	20.4
-35.845	135.687	147	BO	C	U	2.593
-35.591	135.35	99	BO	A	U	2.594
-35.604	135.817	130	BO	D	U	2.556
-31.5	138.35	130	FMA	D	TF	3

Method types include BO=borehole breakout, FMS=single focal mechanism, FMA=composite focal mechanism average and OC=overcoring; Stress regime classifications include SS=strike-slip, TF=thrust fault and U=unknown (see also Figure 8).

A comparison of the current day stress regime to dominant fracture set orientations measured throughout the MLR was undertaken (Fig 9). Findings from this analysis indicate that dominant fracture orientations optimally aligned with the maximum principal stress direction of 110°, either parallel to 110° (low normal stress) or inclined at ~30° (shear dilation), only occurs at a total of 11 sites. This suggests that the current day stress regime imparts only a minimal influence over preferential fluid flow directions in the FRAs of the MLR.

A comparison of dominant fracture orientations to results from the Zones of Influence sub-program exhibit a good correlation in some regions of the MLR, however correlations are not consistent between the two data sets (Costar et al., 2008).

Fracture spacing data collected during fieldwork was used in a frequency analysis to determine the average spacing of dominant fracture sets at each site (Appendix B). Additionally, this data were compared to lithology and is summarised in Table 1. In general, results indicate increased fracture spacing with increased competency of the rock type. Competent units such as the high-grade metamorphic basement of the Barossa Complex, Adelaidean quartzites and Cambrian turbidites, typically have average fracture spacings greater than 6 cm, whilst units of lesser competency such as siltstones, exhibit much closer fracture spacings averaging between 1 and 3 cm.

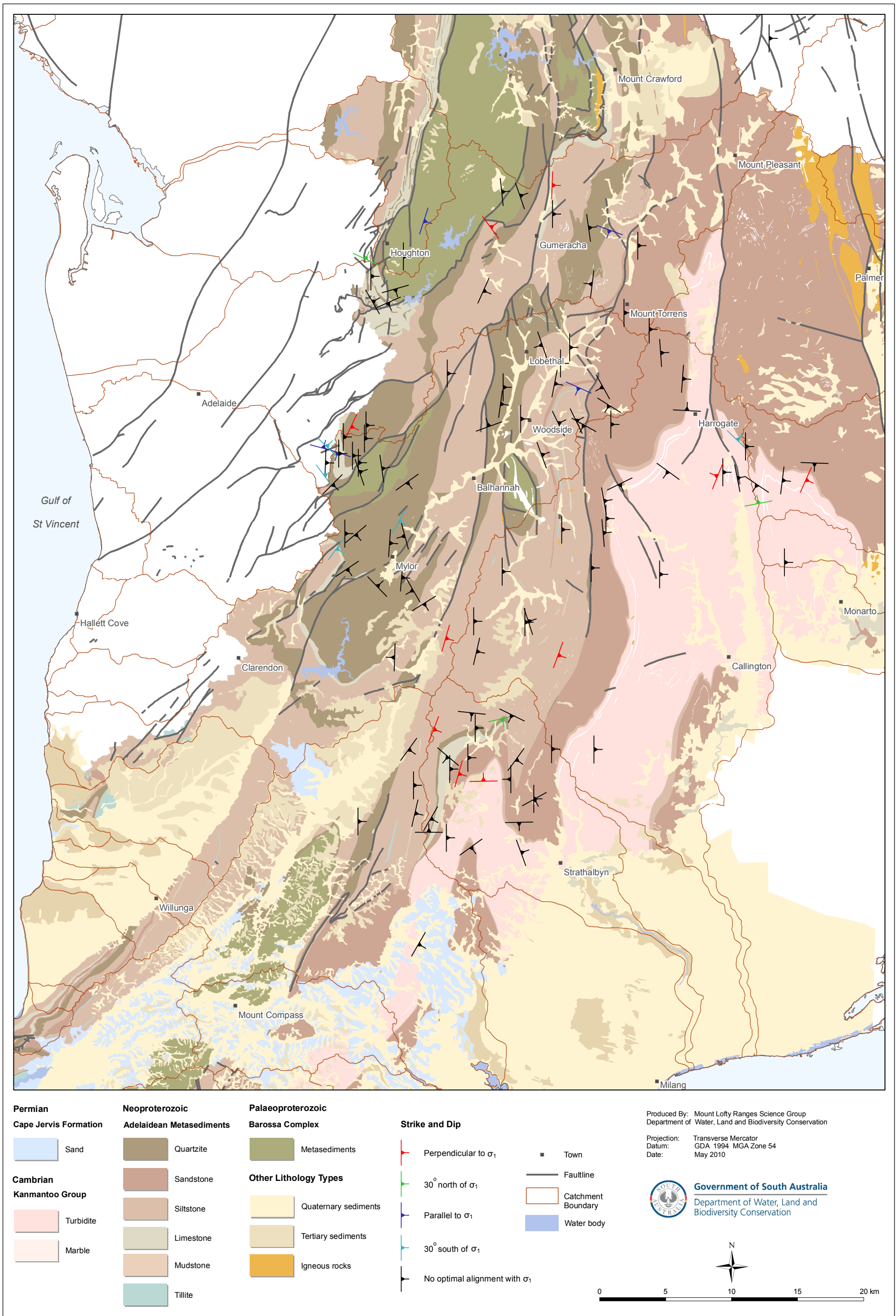


Figure 9. Map of dominant fracture orientations relative to the maximum principal stress direction, Figure includes summarised results from the Zones of influence sub-program (Costar et al., 2008)



### 4.3. YIELD ANALYSIS

As discussed in the methodology section, the conceptual MLR fracture network model consists of a densely fractured weathered upper zone, less fractured transitional zone and a broadly fractured lower zone. With increasing depth, there is a trend of decreasing fracture density based upon a reduction in the number of joint sets and a further increase in yields is expected.

SA Geodata (state water well data base) records were used to obtain information on water cuts and respective well yields collected during drilling. A search returned 2890 wells in the study area of ~2500 km<sup>2</sup> that contained this information (Fig 10), with more than 8200 records as a result of multiple water cuts in each well. These wells were plotted over the lithological coverage, and respective lithological units were assigned to each well.

Within the MLR, individual geological formations typically contain sandstone and siltstone units. Given this, well yields were compared to lithological variations rather than specific geological formations.

Of all well records analysed, siltstone, quartzite and sandstone had the largest sample populations of 4211, 1750 and 1454, respectively (Table 3), confirming that these metasedimentary rocks provide most groundwater supplies. Other lithological formations are presented as an order of magnitude less, with ~200–400 samples.

**Table 3 Analysis of the relationship between yield and depth; results summary**

Lithology	Yield zone	Sample number	Depth (m)	Yield max (L/s)	Yield, majority sample up to (L/s)
Siltstone	Upper zone	4211	120	80	20
	Transition zone		120–200	40	10
	Lower zone		200–300	20	10
Sandstone	Upper zone	1454	100	40	20
	Transition zone		100–250	40	10
	Lower zone		250–300	20	5
Quartzite	Upper zone	1750	100	40	20
	Transition zone		100–200	30	10
	Lower zone		200–300	10	
Turbidite	Upper zone	215	120	15	10
	Lower zone		120–160	5	
Metasediments	Upper zone	415	100	14	8
	Lower zone		100–200	8	4
Limestone	Upper zone	166	100	15	12
	Lower zone		100–200	10	

Based on a change in cumulative well yield with depth, the upper, transition and lower zones are observed in siltstone, sandstone and quartzite units. However, the transition zone was not distinctive in the Barossa Complex metasediments, Adelaidean limestone or Cambrian turbiditic units. An analysis of the relationship between well yield and depth, determining at which depth the cumulative yield stops increasing, shows that yields in the siltstone increased to a maximum of 80 L/s at about 120 m, with the majority of the sample population being 20–40 L/s (Fig 11A, Table 3). The transition zone is between 120 and 200 m, with maximum yields being ~40 L/s, and the majority of yields recorded being 5–10 L/s. A few samples were found in the lower zone between 200 and 300 m in depth, with yields generally up to 10 L/s.

---

## RESULTS

---

Wells completed in sandstone and quartzite show an almost identical relationship between change of yield with depth, resulting in the upper zone being between 0 and 100 m, and the transition zone being 100–250 m and 100–200 m for sandstone and quartzite, respectively (Fig 11B,C). The maximum cumulative yields are very similar — up to 40 L/s in the upper zone, 30–40 L/s in the transition zone and 10–20 L/s in the lower zone, where lower yields at greater depths are observed in quartzites. The majority of samples are up to 10 and 20 L/s in the transition and upper zones, respectively. Both quartzites and sandstones have quite similar characteristics to siltstones, which occasionally display very high yields. The extreme high-yielding characteristics can be associated with zones of major faulting, combined with zones of dense fracturing.

The Barossa Complex metasediments, Adelaidean limestone and Cambrian turbidites are lower yielding, with maximum yields of ~15 L/s and significantly smaller distribution, and therefore do not provide the same level of confidence in the yield analysis. These lithological units only have distinct upper and lower zones; the upper zone in the former being from 0 to 120 m, and the two latter formations having a shallower upper zone between 0 and 100 m. The maximum yields are ~15 L/s in all units, less than 5 L/s below 120 m depth in turbidites, and less than 8 and 10 L/s in the Barossa complex and limestone, respectively (Fig 11D,E,F).

Table 3 demonstrates that while the lower limit of the upper zone for all lithological units is ~100 m, the lower limit of the transitional zone varies between 160 and 250 m, with 200 m being the upper depth of the lower zone for four lithology types analysed.

It can be concluded that the conceptual fracture network model for the southern MLR is consistent with that used in the Clare Valley study (Love, 2003). It consists of a densely fractured weathered upper zone (0–100 m), less fractured transitional zone (100–200 m) and a broadly fractured lower zone (>200 m).

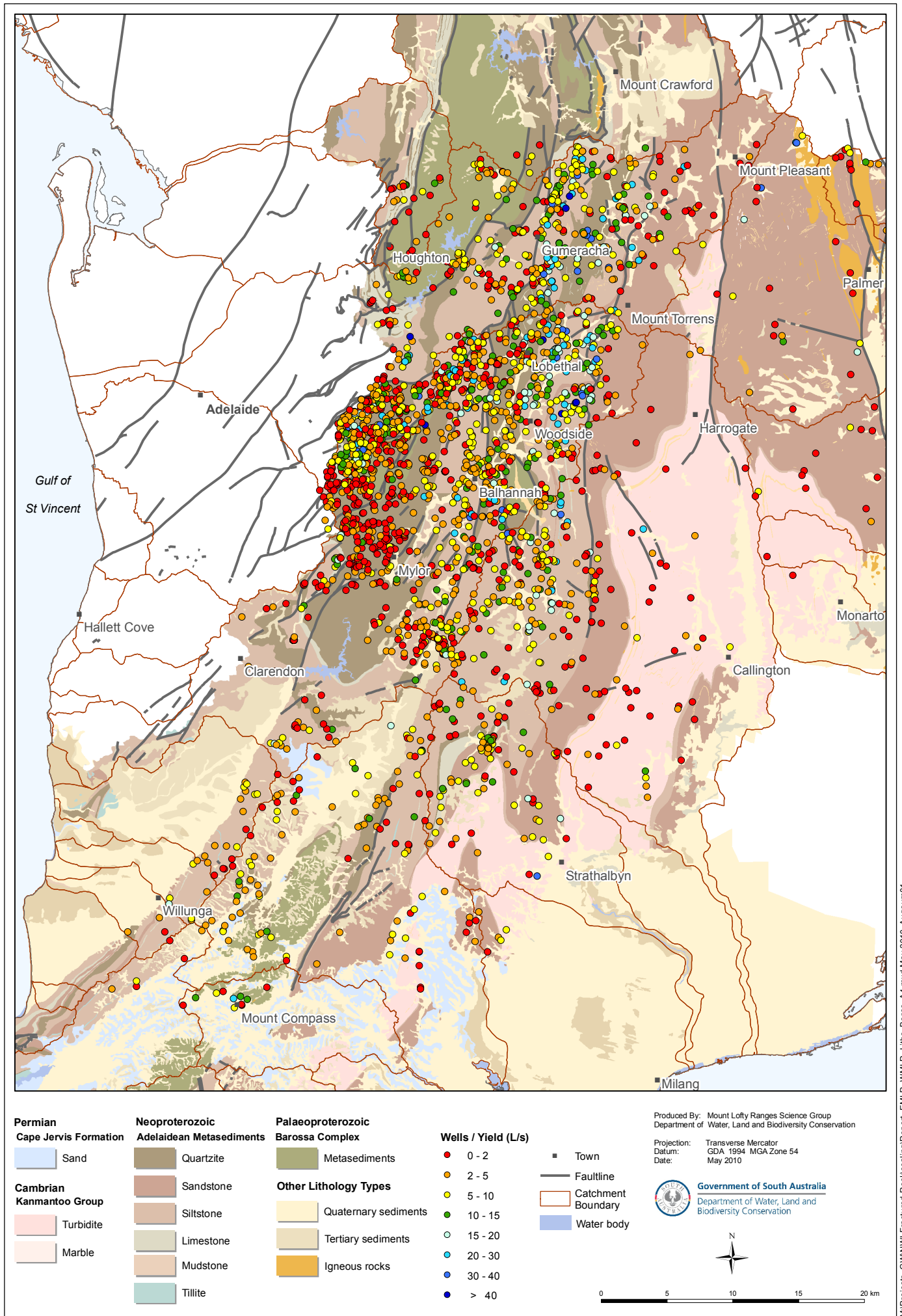
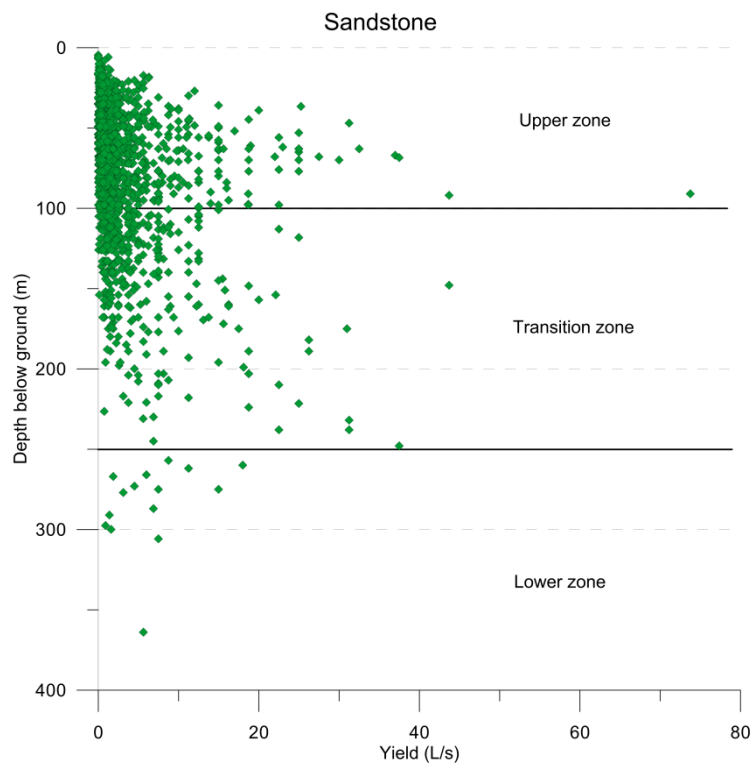
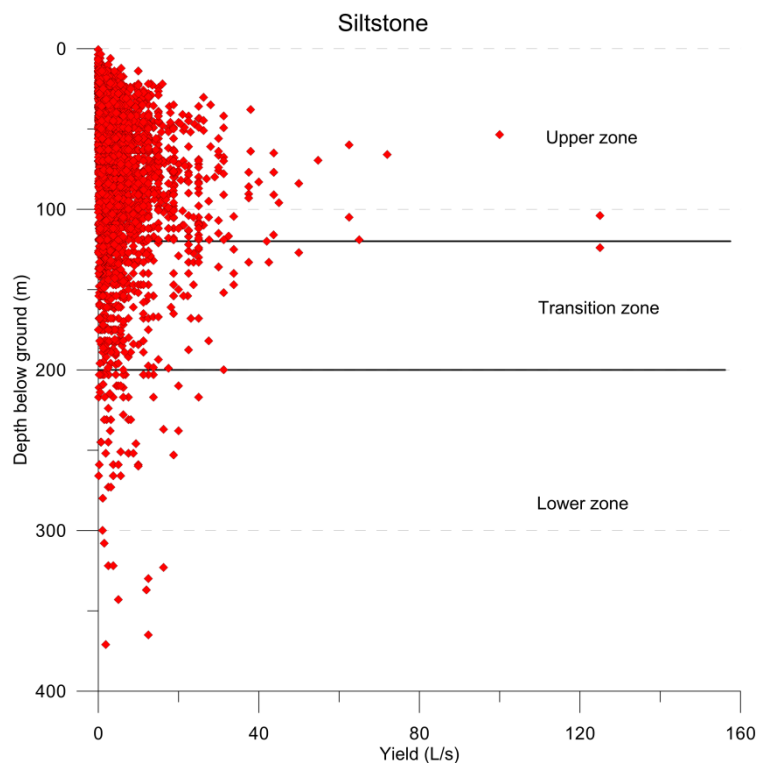
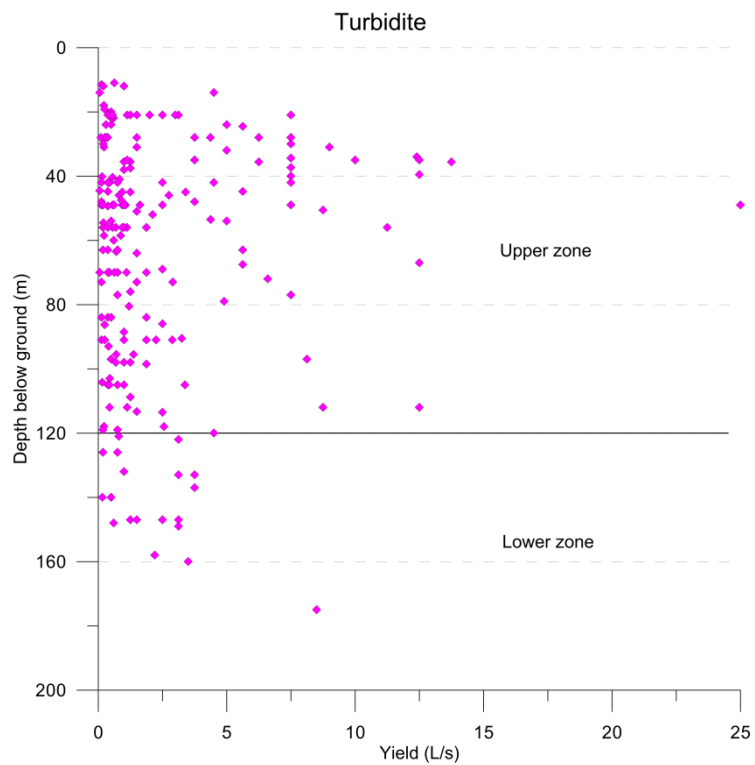
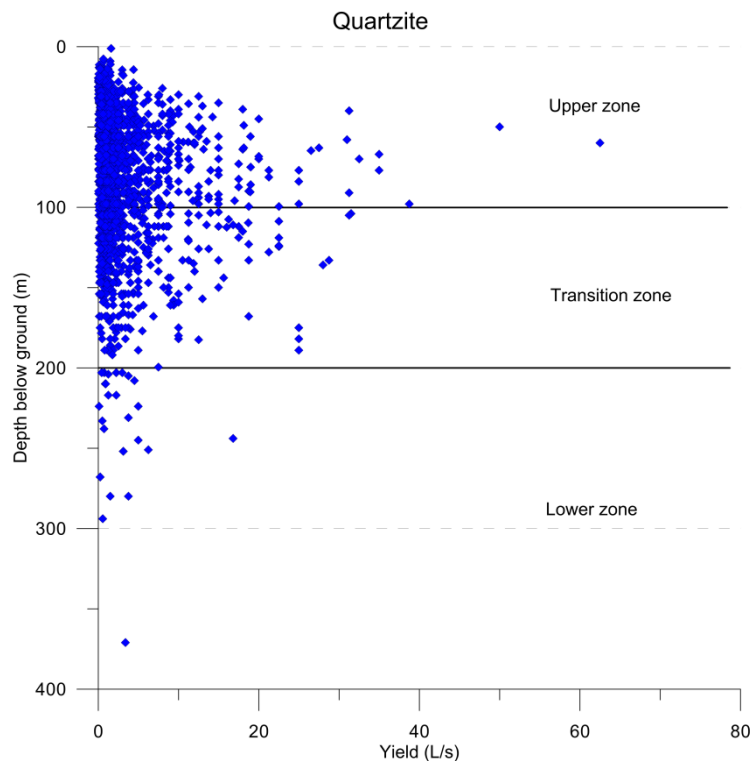


Figure 10. Geological map and location of wells with well yields





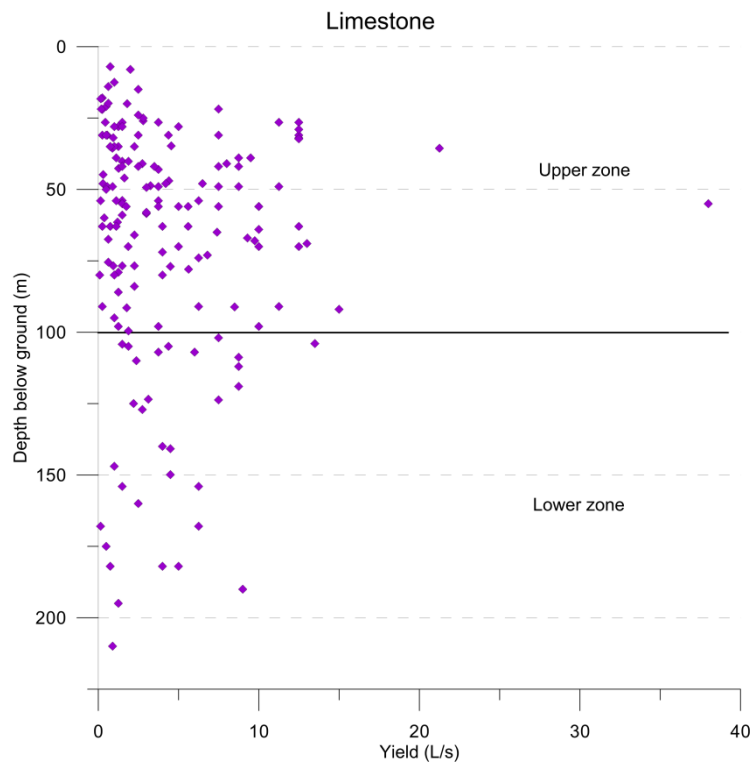
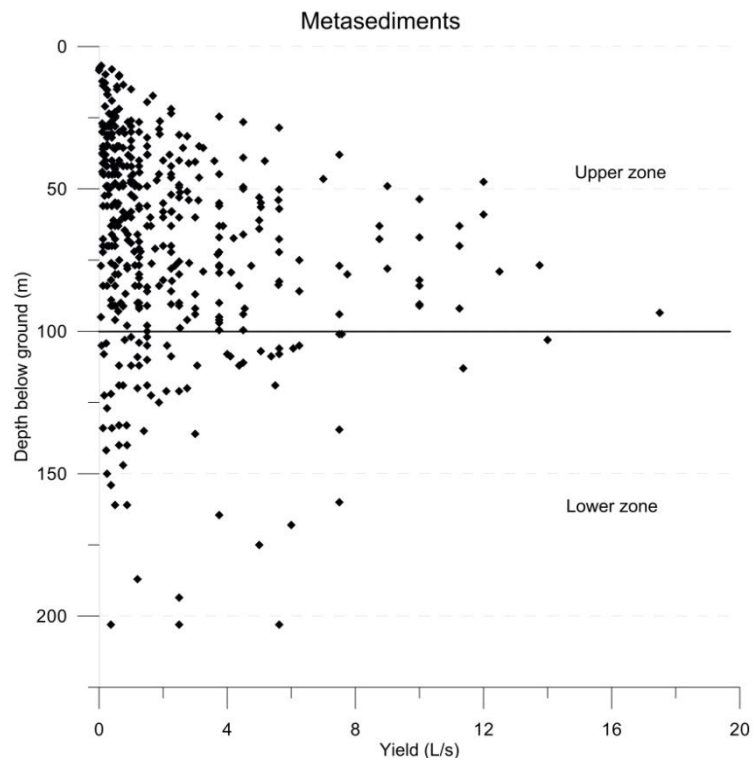


Figure 11 (A,B,C,D,E &F) Relationship between yield and depth with lithological variations

---

## 5. DISCUSSION AND CONCLUSIONS

---

Fracture orientation, fracture spacing and bedding measured at 84 sites were plotted as poles on equal area, lower hemisphere stereonet, which highlighted the scattered and variable orientation of the dominant fracture sets. This is not necessarily unexpected given the large sampling area, variable lithologies and structural complexity throughout the MLR. It did however, indicate a broad clustering of poles in the NW quadrant of the stereonet with an average orientation of 014/56° E.

An analysis of the parallelism between bedding and the dominant fracture set at each site was also undertaken. Of the 51 sites where bedding could be observed, 40 sites exhibited the dominant fracture set parallel to bedding. Dominant fractures were often parallel to schistosity at the other 11 sites. For the remaining sites, bedding was not observed due to lithological type or metamorphic grade.

Overall, this has indicated a tendency for fractures to be orientated NNE with moderate to steep easterly dips where bedding exhibits a significant role in controlling the orientation of the dominant fracture sets throughout the MLR.

Studies into stress-dependent fracture permeability processes within the MLR have found that the contemporary in-situ stress field has a significant influence on the hydraulics of pre-existing fractures. In particular, within the upper ~0–1.0 km, there is a pronounced anisotropic permeability orientation that favours steeply dipping to vertical fractures. Their enhanced permeability is in response to far-field, isotropic, lateral relaxation of the rock mass. As this stress field is more or less isotropic, there is no preferred strike orientation. The direction of maximum hydraulic conductivity is often coincidental with the strike of bedding, as bedding planes are often steeply dipping and the densest and most extensive mechanical planes within the rock mass. The effects of uplift and unloading also results in an increase in fracture density and bulk hydraulic conductivity close to the present-day surface. At depths below the effects of uplift and unloading (>1.0 km), it is expected that fracture permeability will favour shallow-dipping to horizontal fractures. The major bounding faults of the MLR are currently tectonically active and, by corollary, are also hydraulically active.

In general, the conceptual fracture network model consists of a densely fractured weathered upper zone, a less-fractured transitional zone and a broadly fractured lower zone. With increasing depth, there is a trend of decreasing fracture density based upon a reduction in the number of joint sets, and no increase in yields with depth is expected.

Analysis of the relationship between yield and depth at which the yield stops increasing shows that in the siltstone formations, yields increase to a maximum of 80 L/s at about 120 m, with the majority of yields observed to be between 20 and 40 L/s. The transition zone is between 120 and 200 m, while a few records on well yields were found to be in the lower zone, between 200 and 300 m in depth.

Wells completed in sandstone and quartzite units show an almost identical relationship between change of yield with depth, with the upper zone being between 0 and 100 m, and the transition zone being 100–250 m and 100–200 m for sandstone and quartzite, respectively. The maximum yields are very similar for both lithologies, with lower yields at greater depths being observed in quartzites. Both quartzites and sandstones have quite similar characteristics to siltstones, which only occasionally display very high yields when associated with zones of major faulting.

The Barossa Complex metasediments, Cambrian turbidites and Adelaidean limestone are lower yielding units with maximum yields of ~15 L/s and significantly smaller spatial distribution. These lithological units only have distinct upper and lower zones, the upper zone in the former being from 0 to 120 m, and the two latter units having a shallower upper zone between 0 and 100 m.

---

## DISCUSSION AND CONCLUSIONS

---

The investigations and analyses resulted in the following findings:

The current day stress regime does not appear to exert a significant influence over preferential flow directions in shallow FRAs. Results indicate that unloading and weathering have a much greater influence on the development of fractures and their density at shallow crustal levels.

Dominant fracture set orientations in the study area are typically orientated NNE with moderate to steep easterly dips, and are parallel to bedding. Deviations from this dominant strike pattern are most likely due to variations in bedding orientation associated with hinge zones of major regional synclines and anticlines.

Bedding parallel fractures appear to be the dominant fracture set, consistent with the findings of the Zones of Influence sub-project, and correlates with the preferential groundwater flow path. Orientations of the dominant hydraulically conductive sub-vertical fractures are consistent with regional trends.

All fracture sets collectively allow the flow of groundwater in the direction of the regional hydraulic gradient. However, on a sub-regional or local scale, groundwater flow is highly variable and dependent on rock type, geological structure, fracture aperture and density.

Fracture spacing analyses indicate increased fracture spacing with increased competency of the rock type. Competent units, such as the high-grade metamorphic basement of the Barossa Complex, Adelaidean quartzites and Cambrian turbidites, typically have average fracture spacings greater than 6 cm, whilst units of lesser competency, such as siltstones, exhibit much closer fracture spacings averaging 1–3 cm.

The conceptual fracture network model for the study area can be broadly divided into a densely fractured weathered upper zone (0–100 m), a less-fractured transitional zone (100–200 m), and a broadly fractured lower zone (>200 m). The extreme high-yielding characteristics (>60 L/s) may be associated with densely fractured fault zones.

The consistently low yields observed in the Cambrian turbidites, compared to Adelaidean metasediments, may be a result of erosion of the upper weathered section of the sequence. This suggestion is consistent with results indicating uplift and unloading producing higher yields at shallow depths in the Adelaidean metasediments.

---

## 6. RECOMMENDATIONS

---

Data presented in this report provide a baseline data set for the FRAs of the MLR. An increase in both structural orientation data and preferential flow direction information is recommended for future investigations. The baseline data set requires denser data populations to address localised variations in order to improve the confidence level in management recommendations.

Due to the complex distribution of fractures in almost every rock type, no single method can unambiguously map fractures and their capacity for fluid movement. Using integrated interpretations from a number of methods will lead to a greater understanding of the characterisation of subsurface flow in recharge zones, and can be used to define orientation of fractures in terms of strike and dip, as well as broadly defining bulk electric resistivity, bulk porosity and hydraulic conductivity.

The findings of this project also lead to recommendations for cost-effective drilling. Any new drilling that is to take place should consider the general observations made about fracture spacing and lithology, as well as the results of the yield versus depth analysis. Yields should be monitored during drilling to ensure that the well is drilled to the most effective depth without entering the transitional (lower yielding) zone, to provide a more economical method of well construction.

---

# APPENDICES

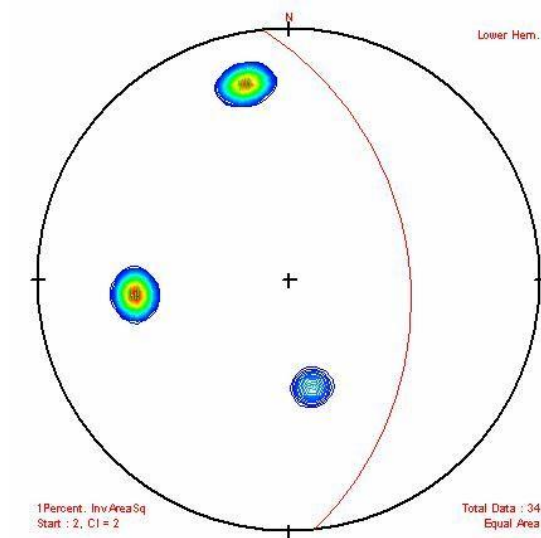
---

## A. *STEREOGRAPHIC PROJECTION*

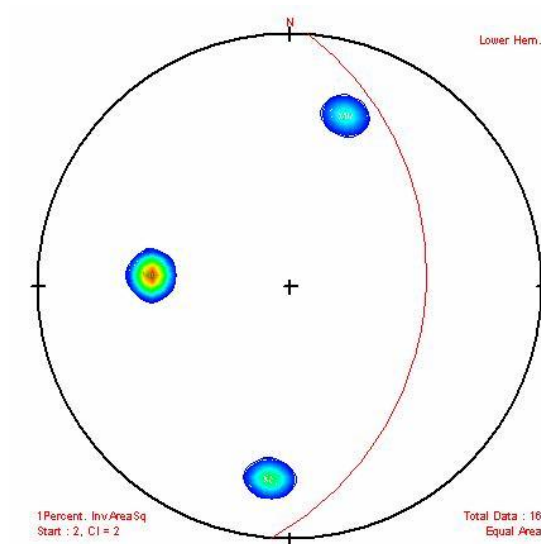
Red great circle girdle — dominant fracture orientation

Black great circle girdle — bedding

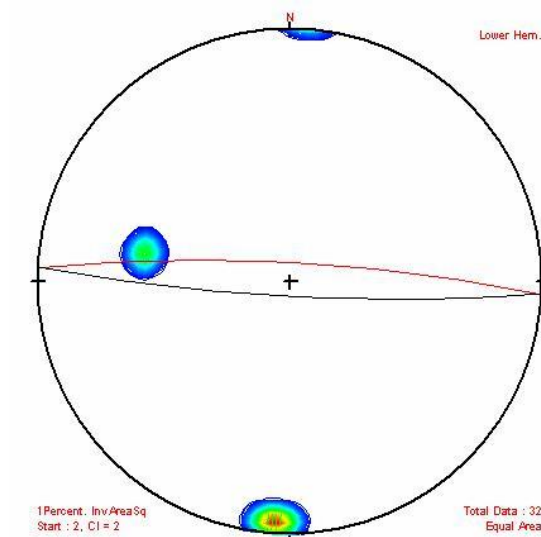
Blue great circle girdle — schistosity



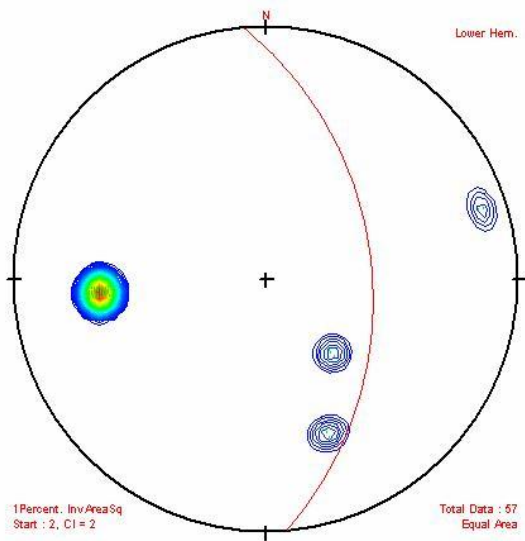
Site 1



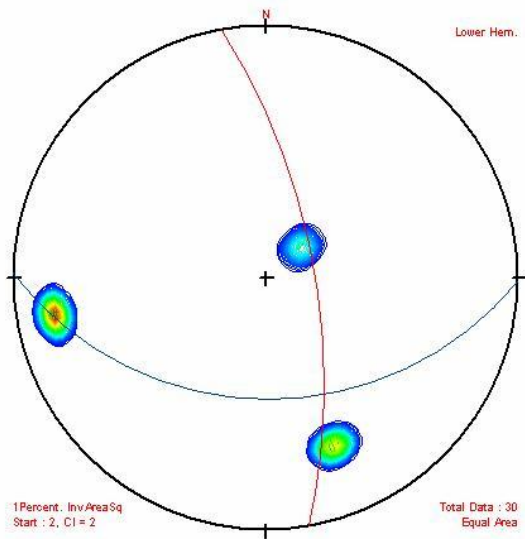
Site 2



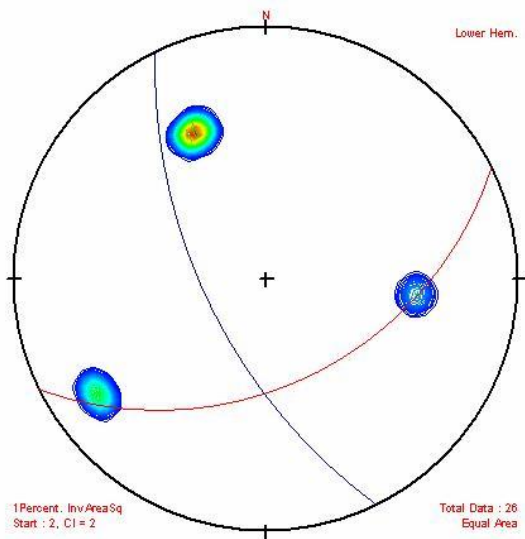
Site 3



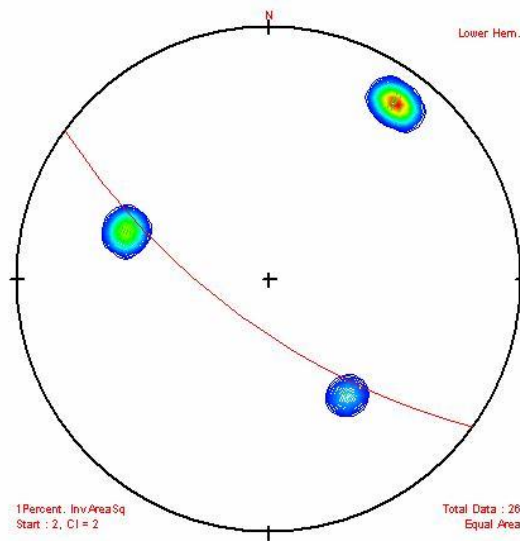
Site 4



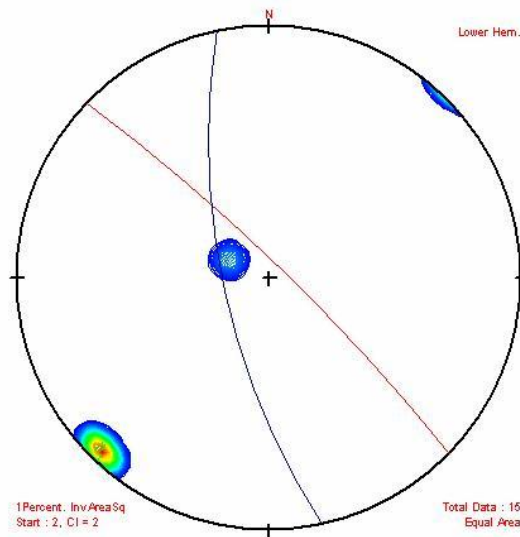
Site 5



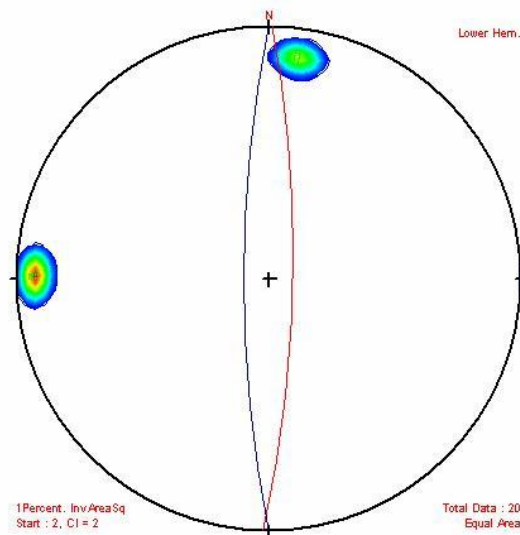
Site 6



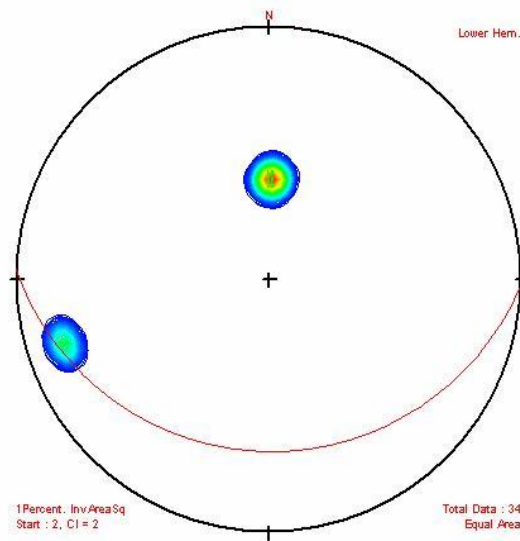
Site 7



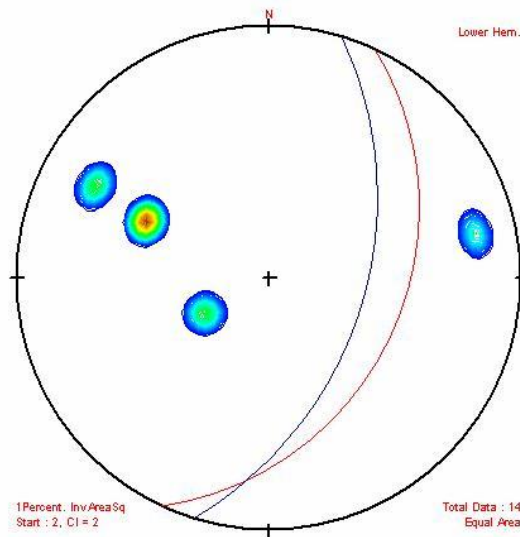
Site 8



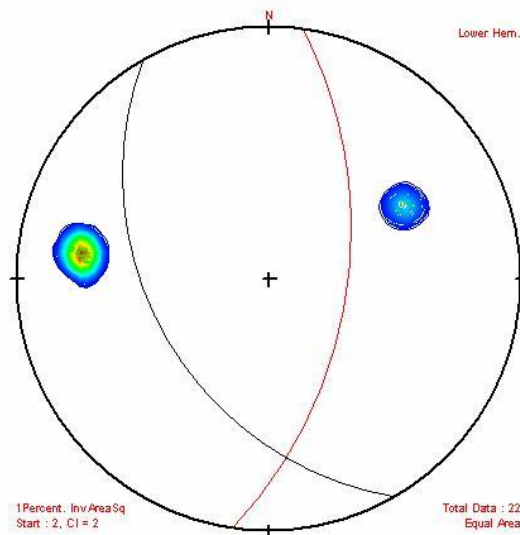
Site 9



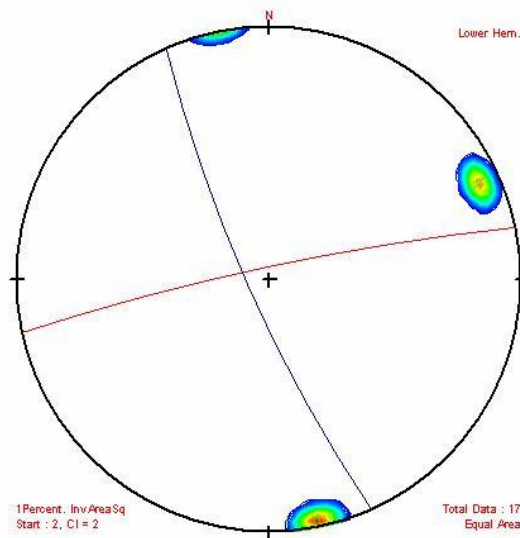
Site 10



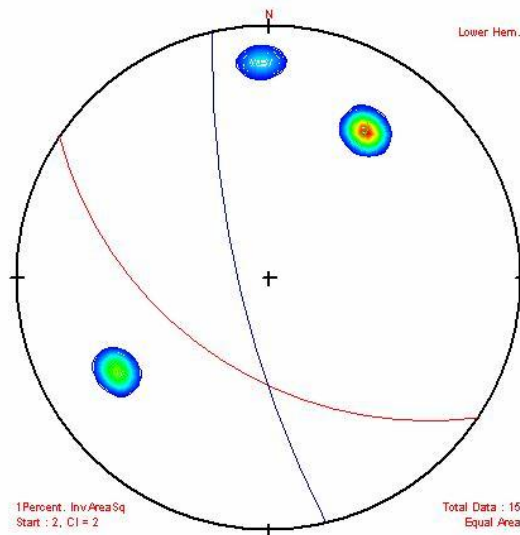
Site 11



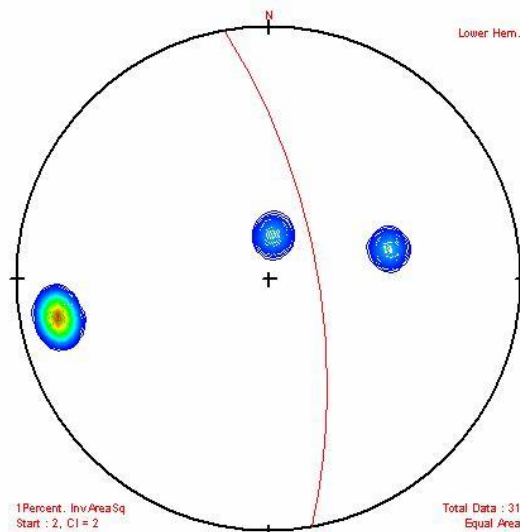
Site 12



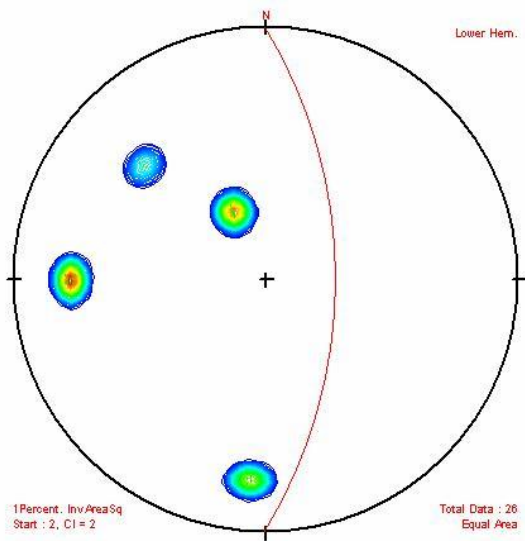
Site 13



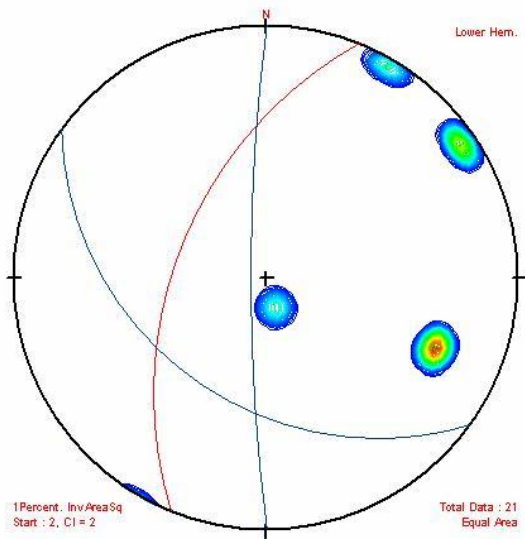
Site 14



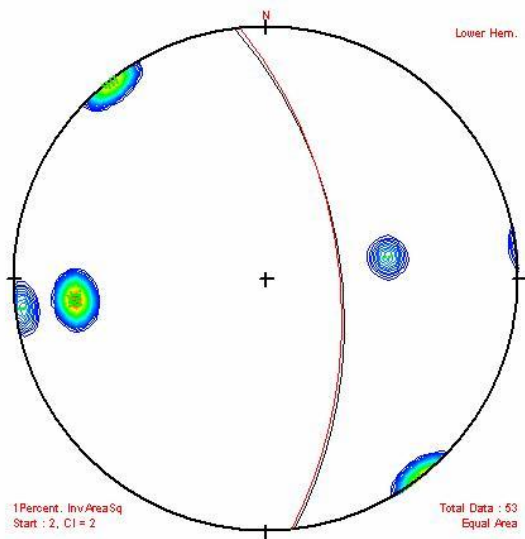
Site 15



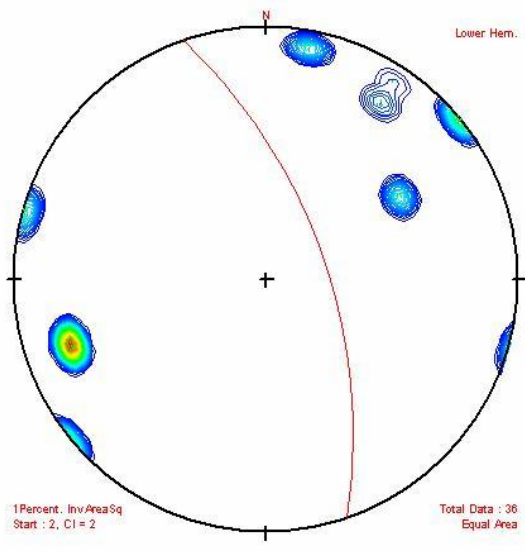
Site 16



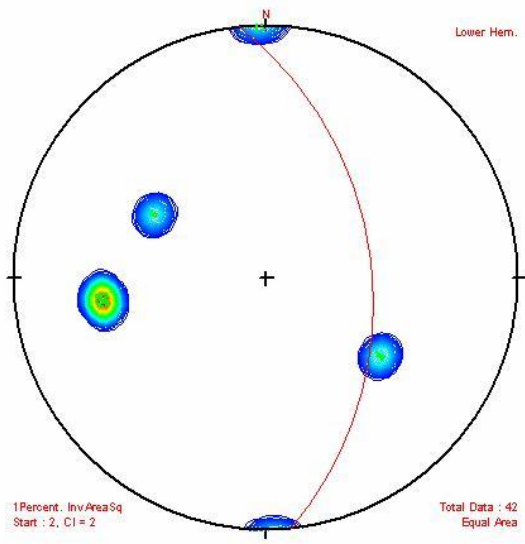
Site 17



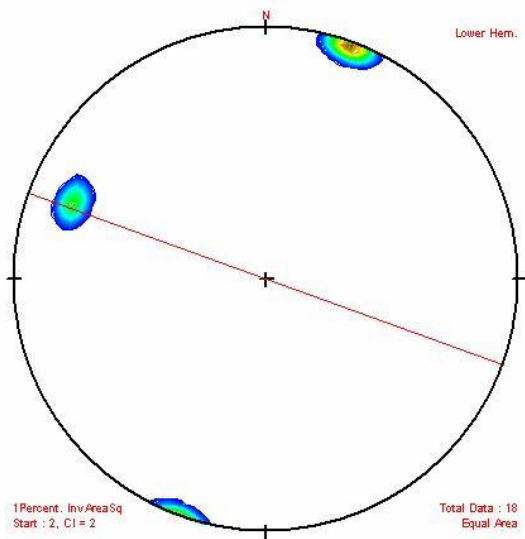
Site 18



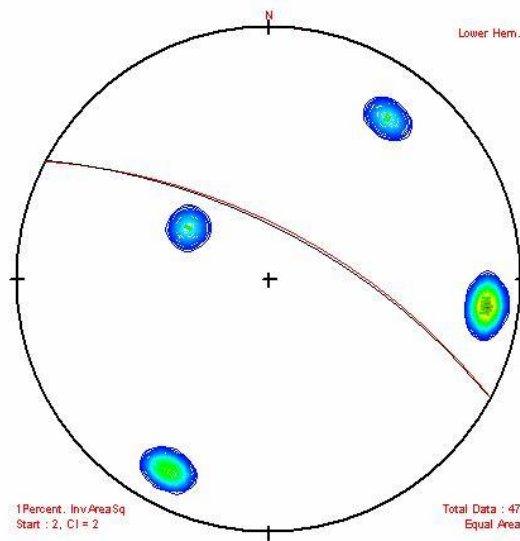
Site 19



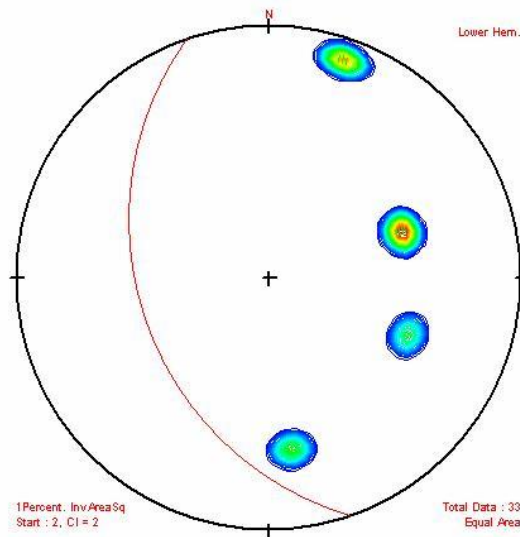
Site 20



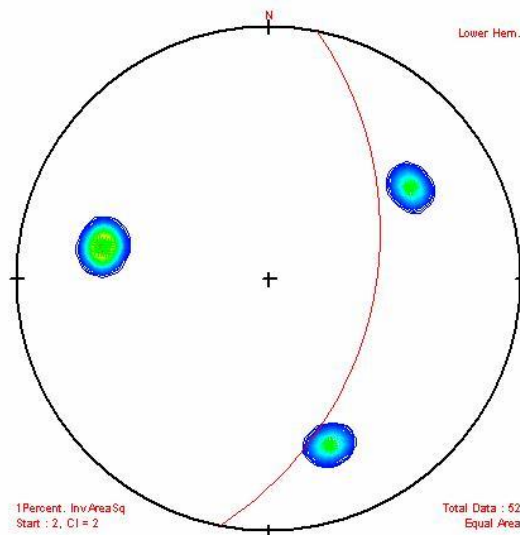
Site 21



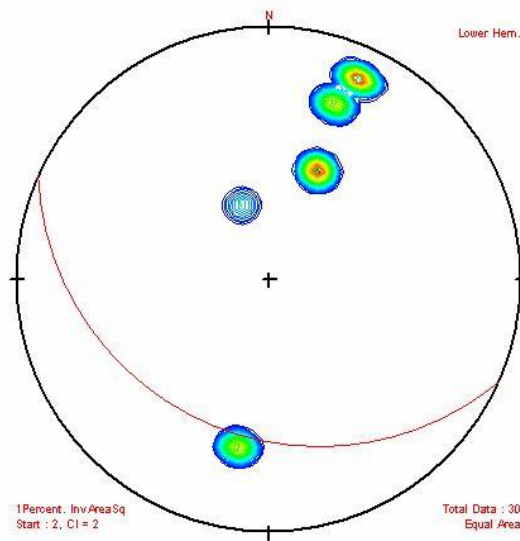
Site 22



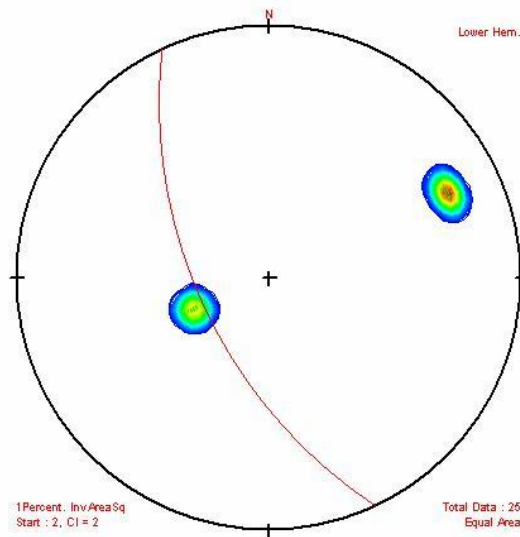
Site 23



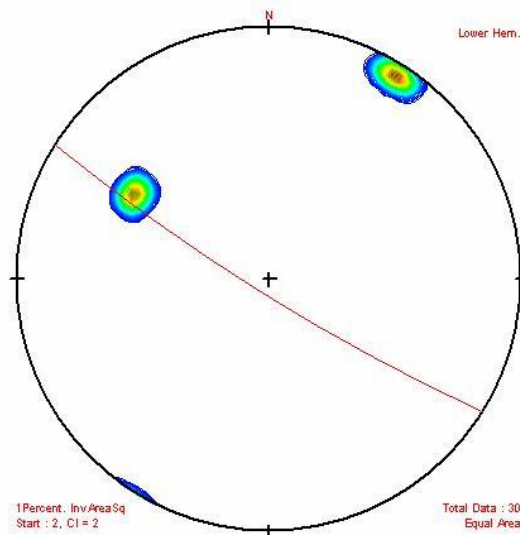
Site 24



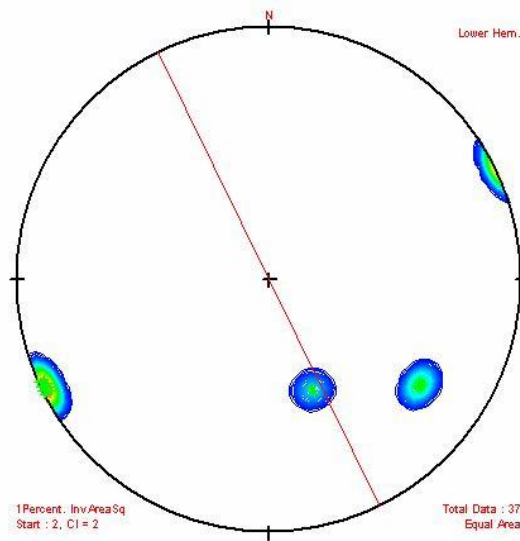
Site 25



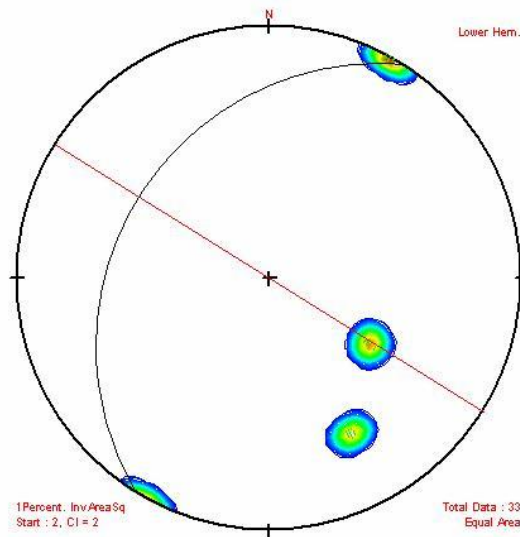
Site 26



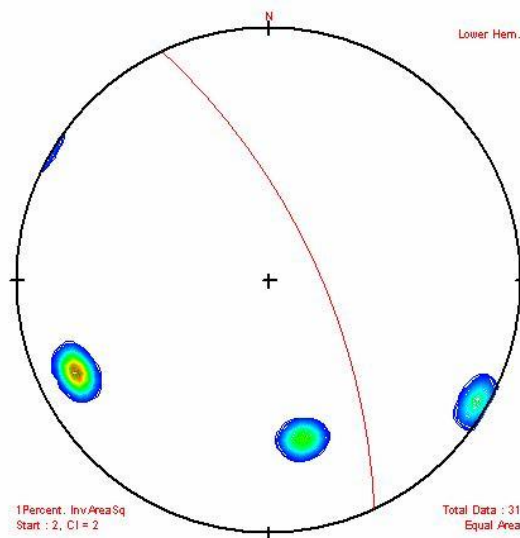
Site 27



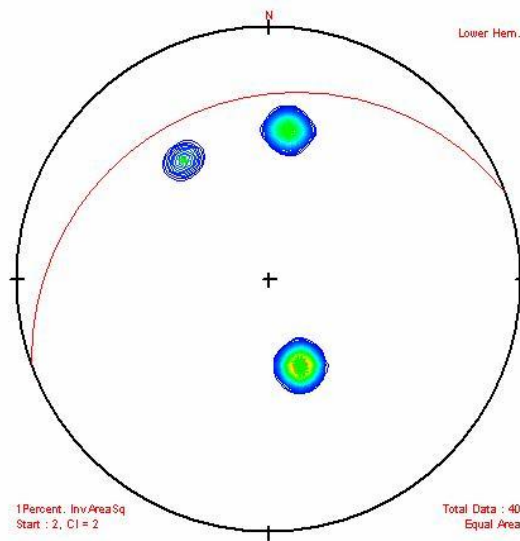
Site 28



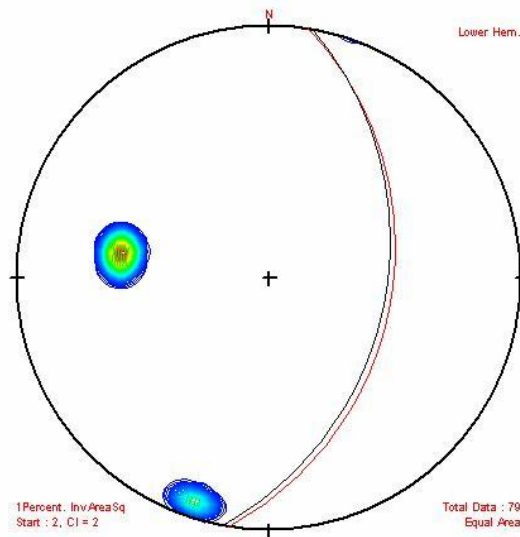
Site 29



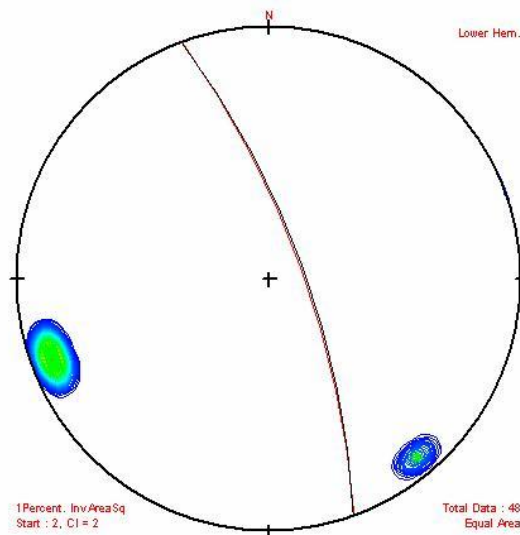
Site 30



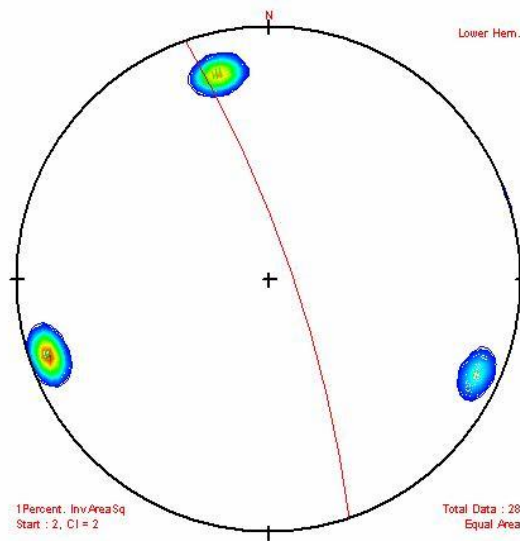
Site 31



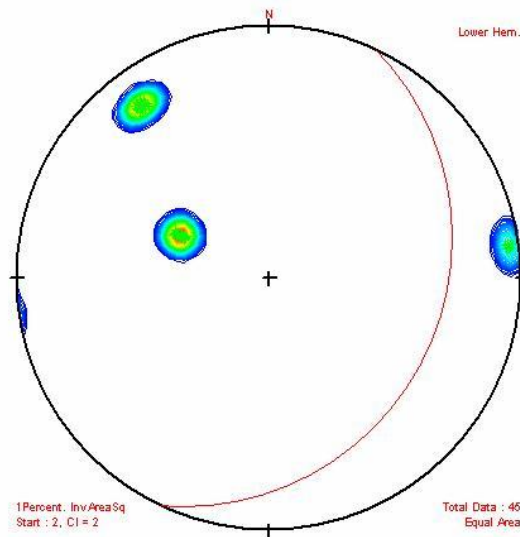
Site 32



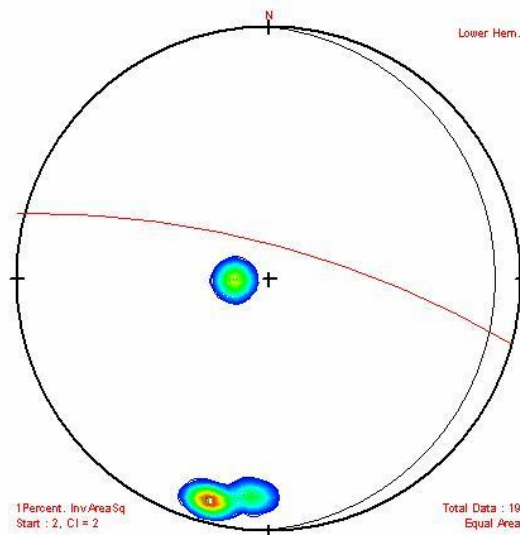
Site 33



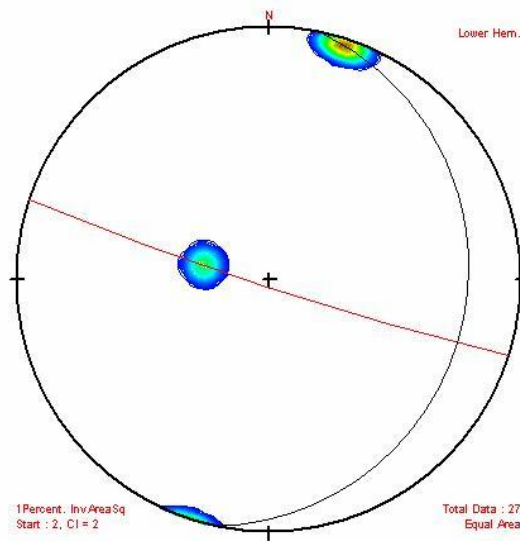
Site 34



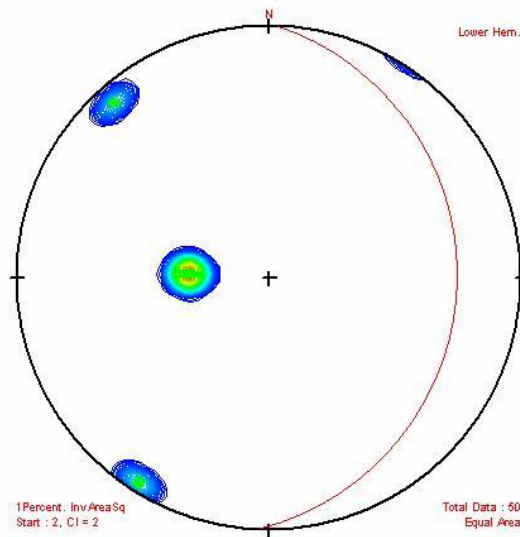
Site 35



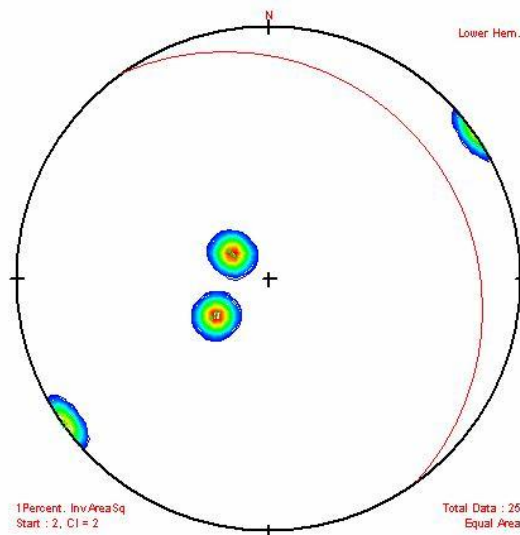
Site 36



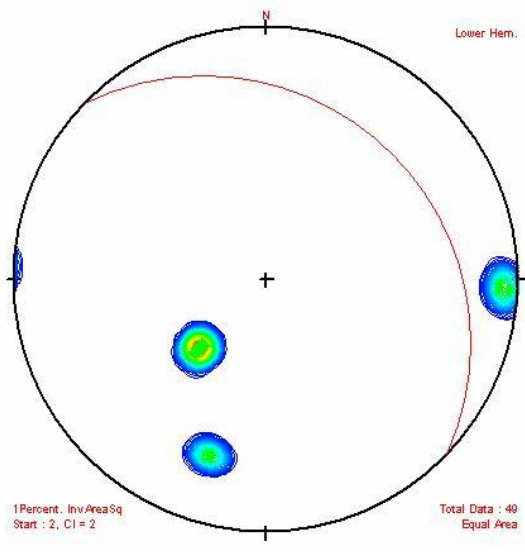
Site 37



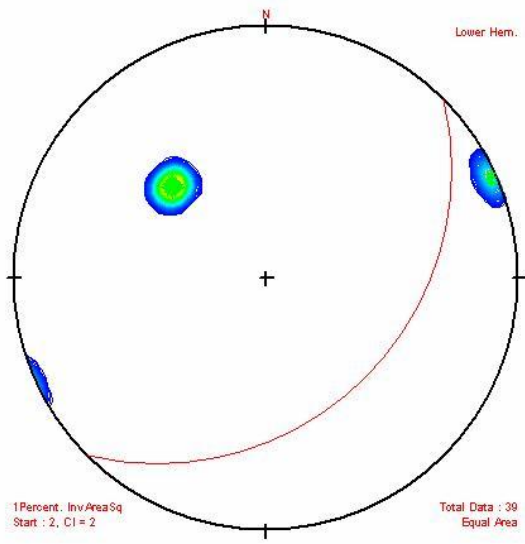
Site 38



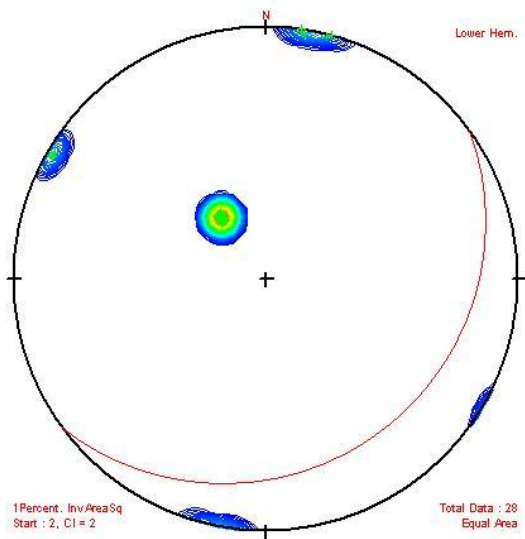
Site 39



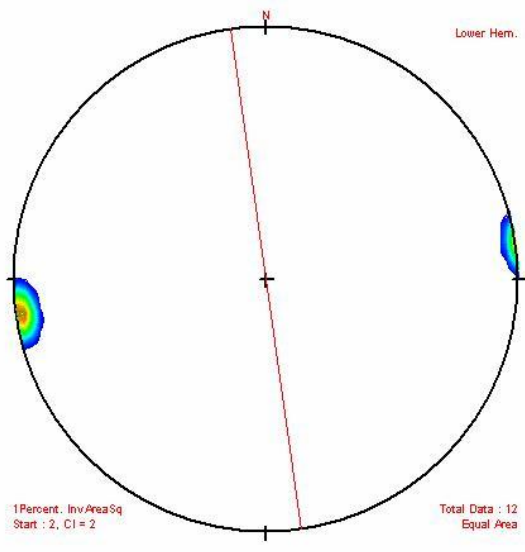
Site 40



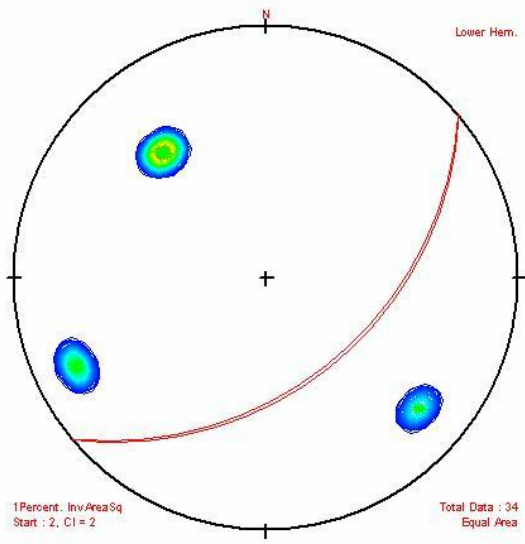
Site 41



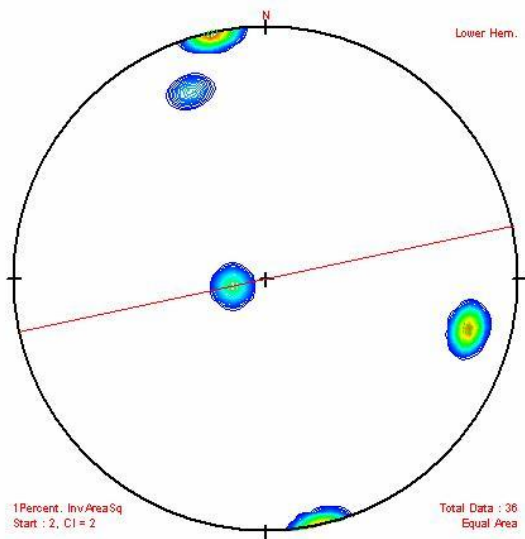
Site 42



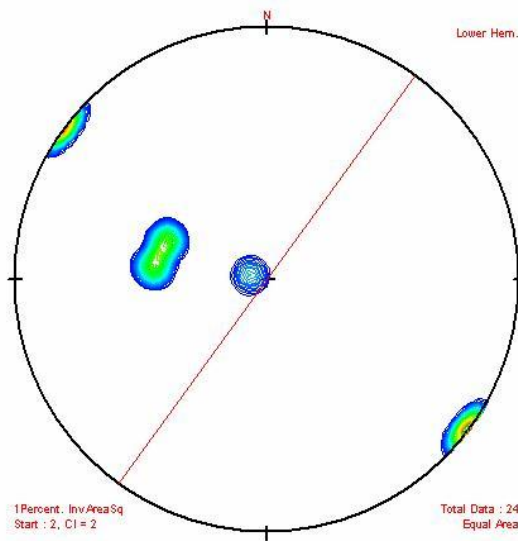
Site 43



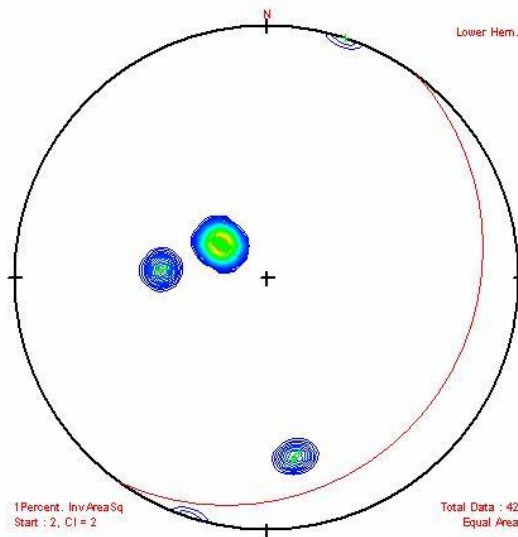
Site 44



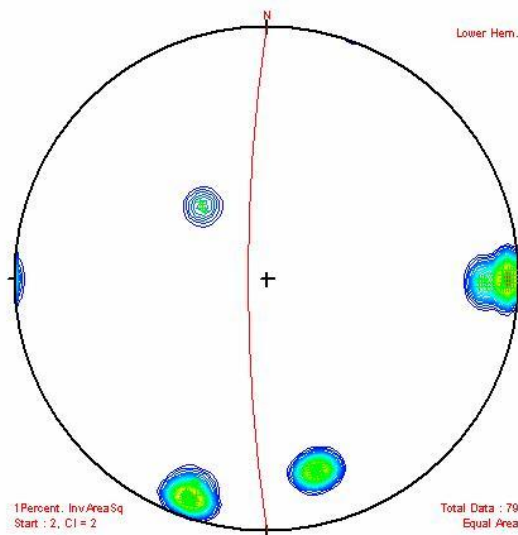
Site 45



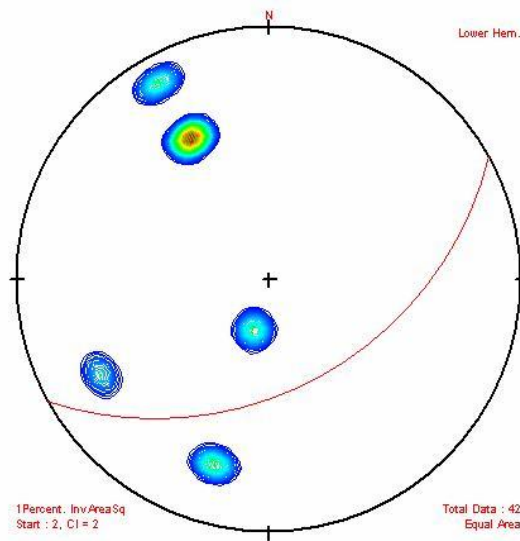
Site 46



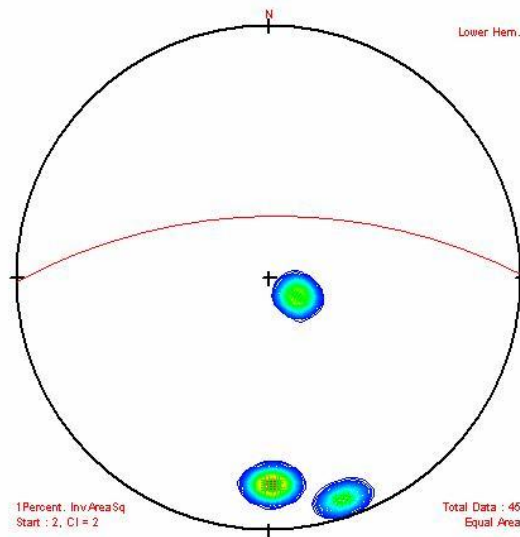
Site 47



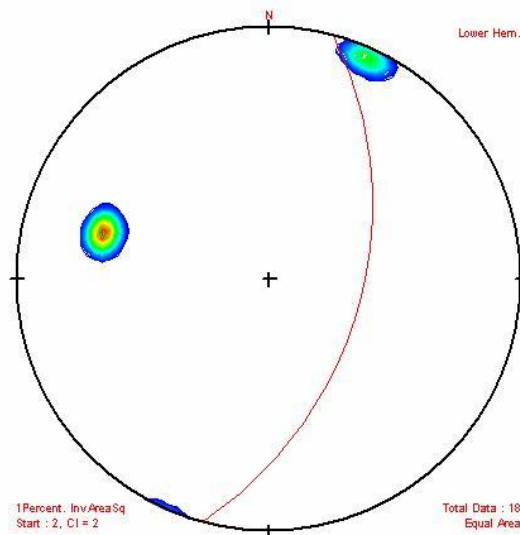
Site 48



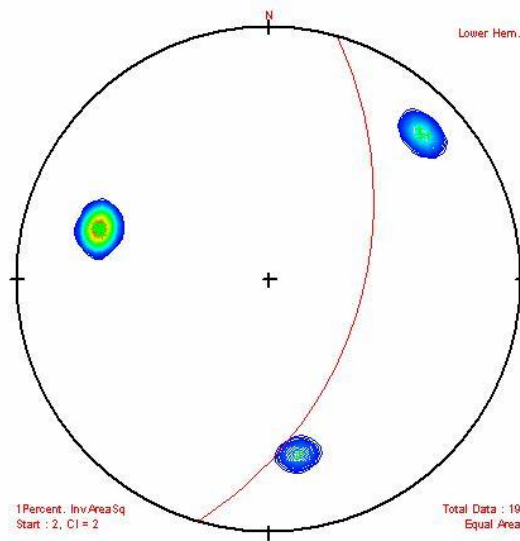
Site 49



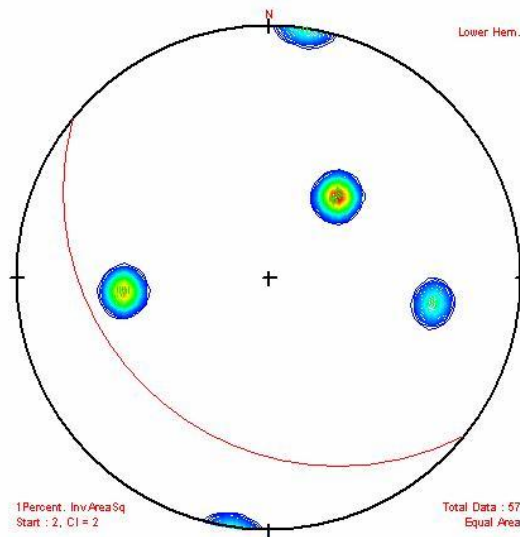
Site 50



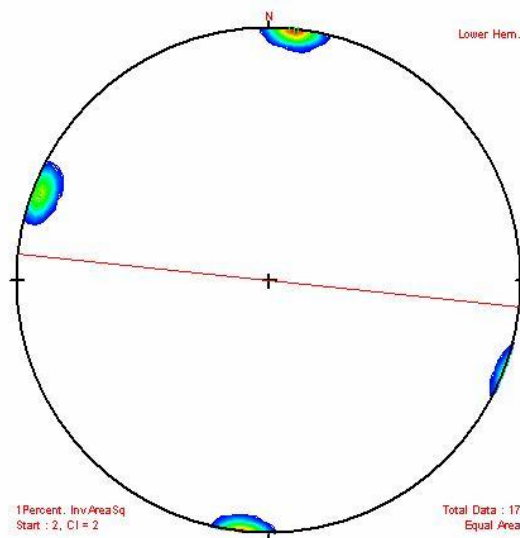
Site 51



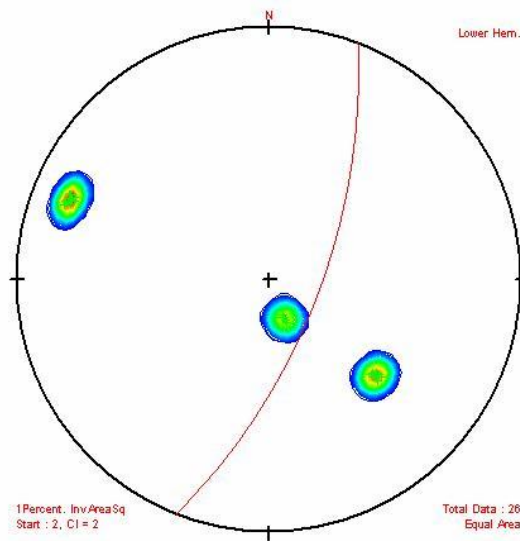
Site 52



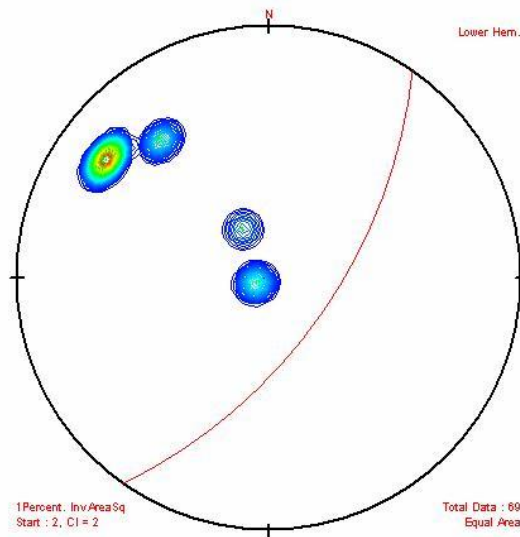
Site 53



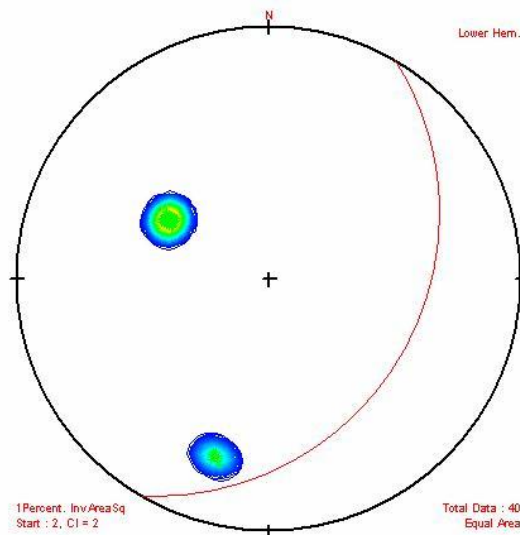
Site 54



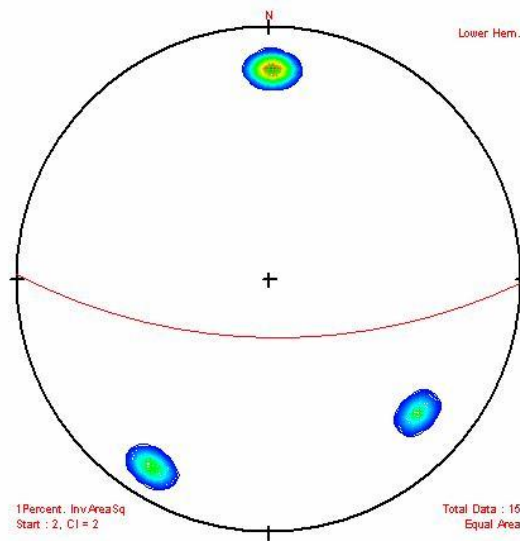
Site 55



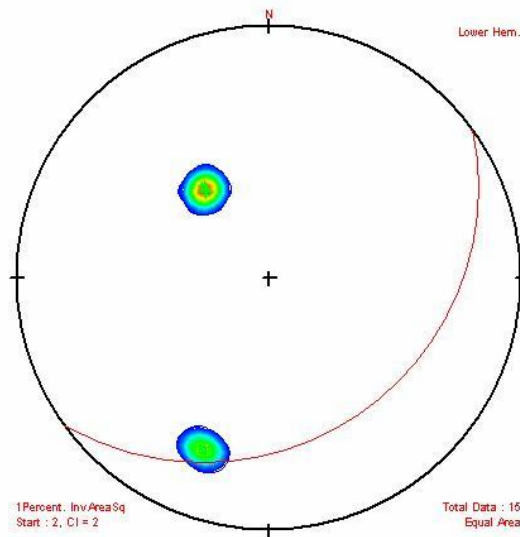
Site 56



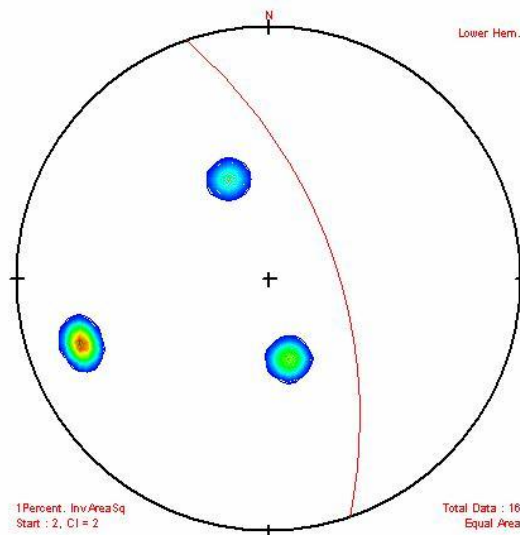
Site 57



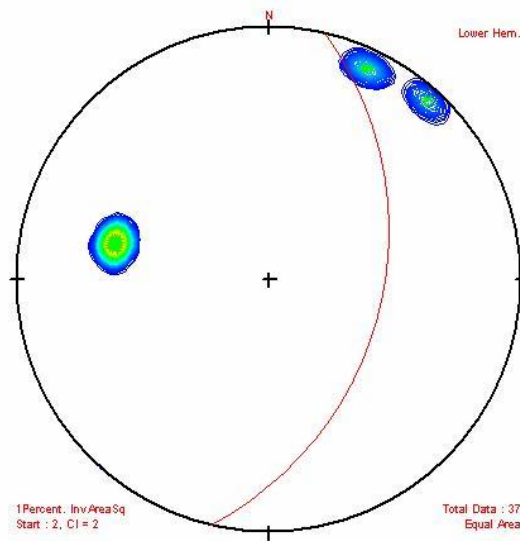
Site 58



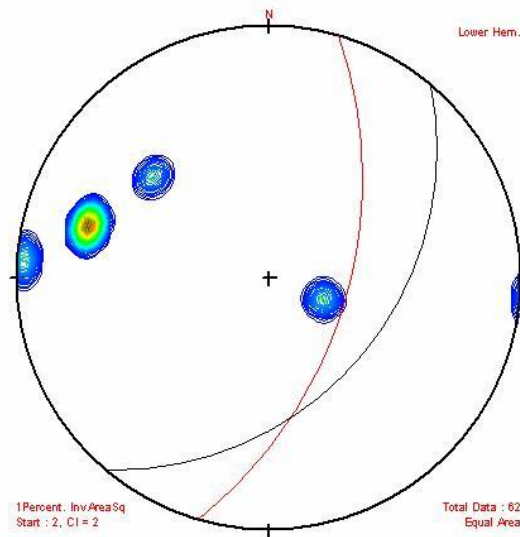
Site 59



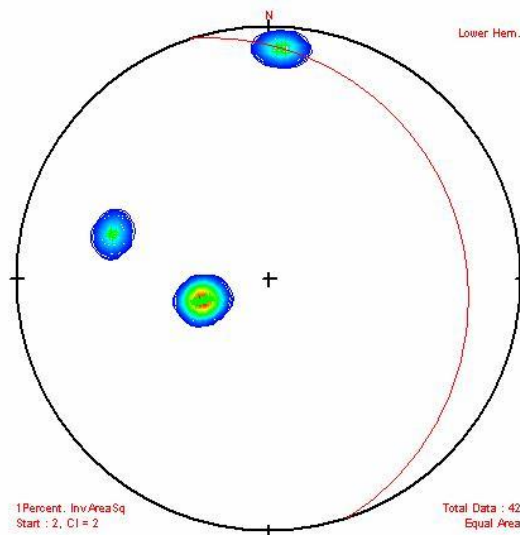
Site 60



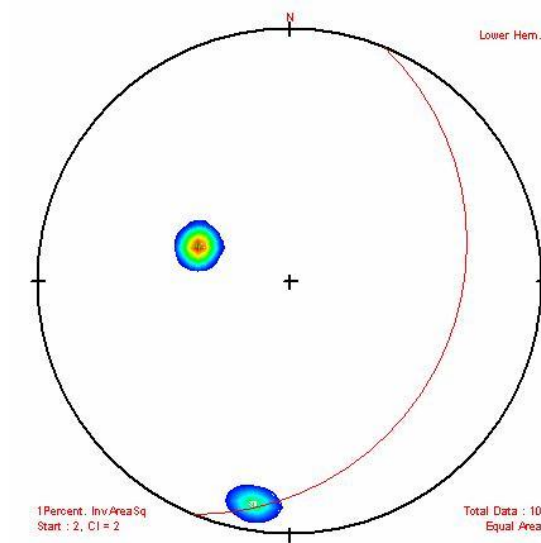
Site 61



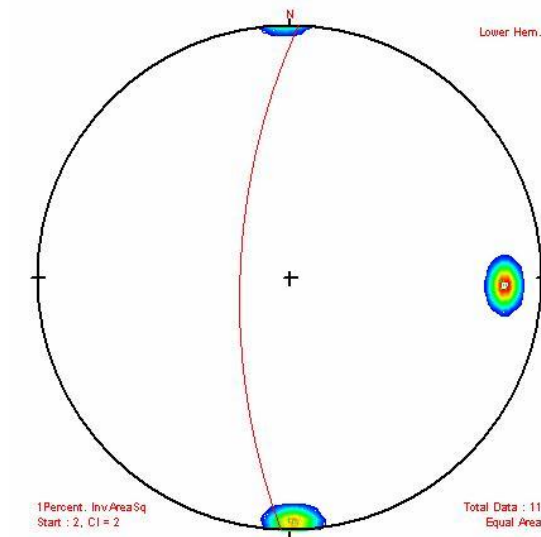
Site 62



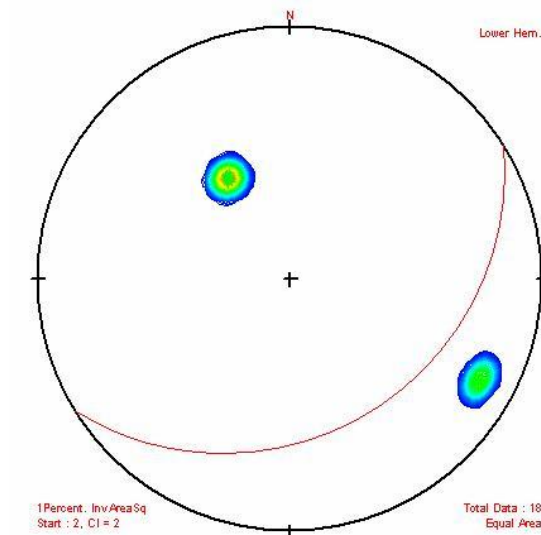
Site 63



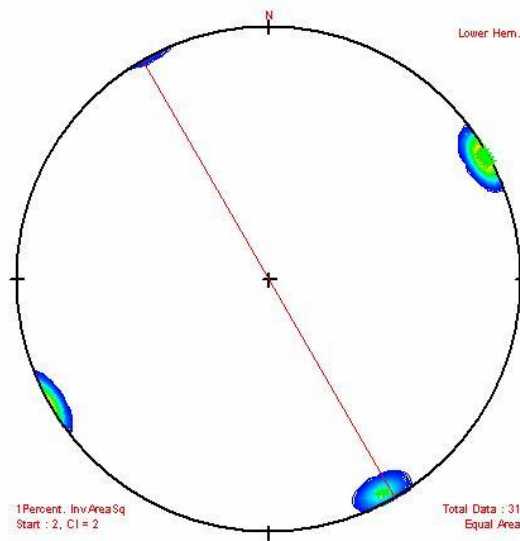
Site 64



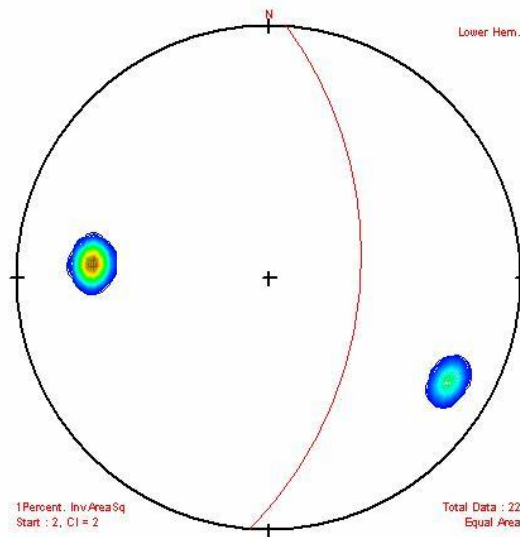
Site 65



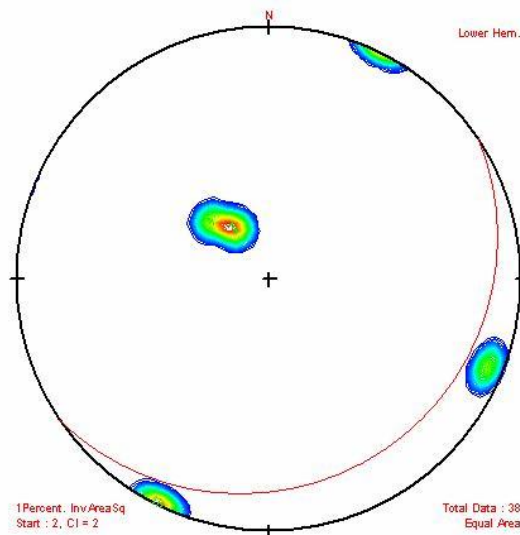
Site 66



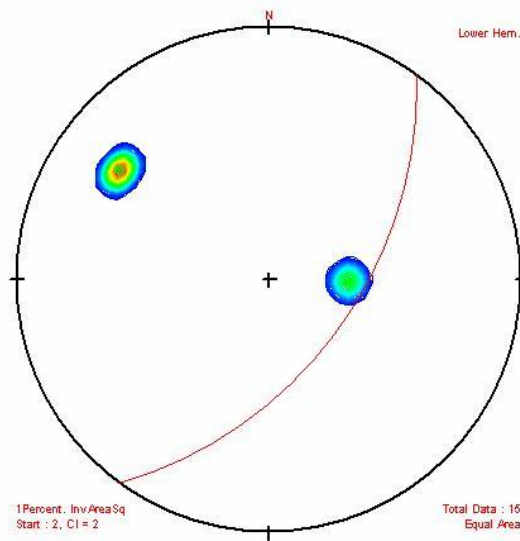
Site 67A



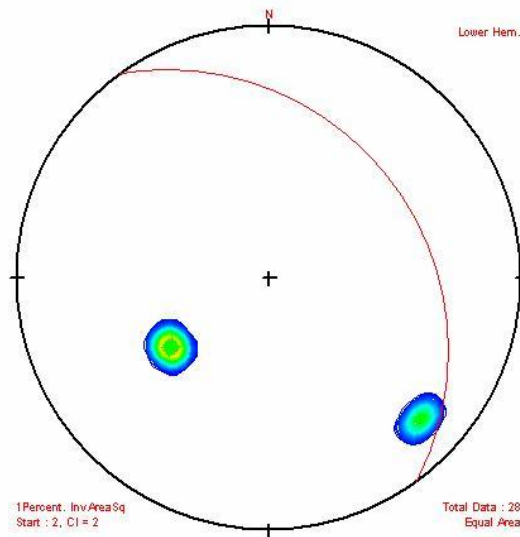
Site 67B



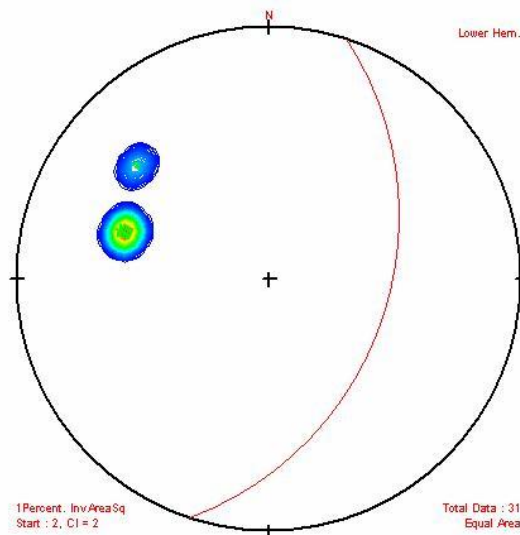
Site 68



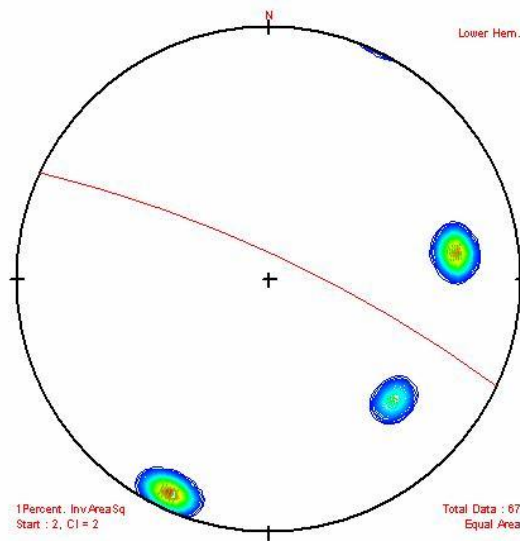
Site 69



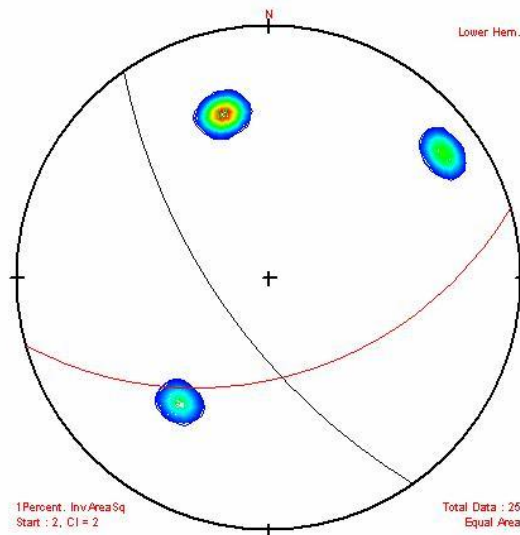
Site 70



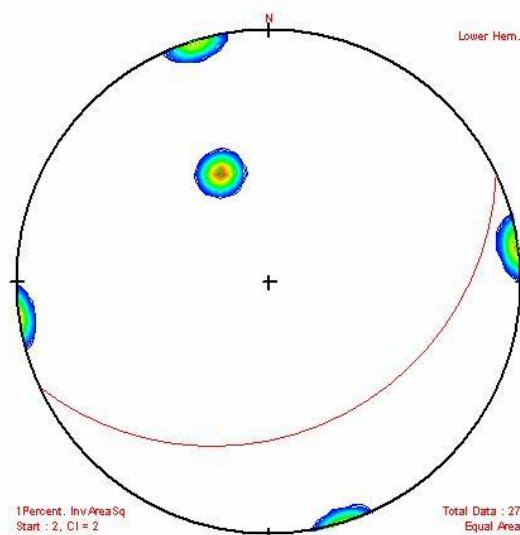
Site 71



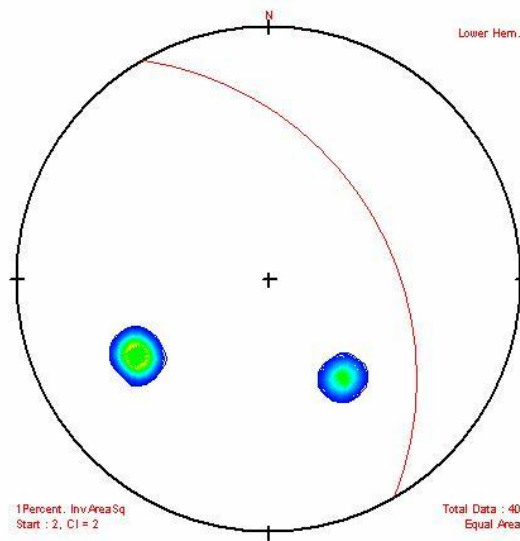
Site 72



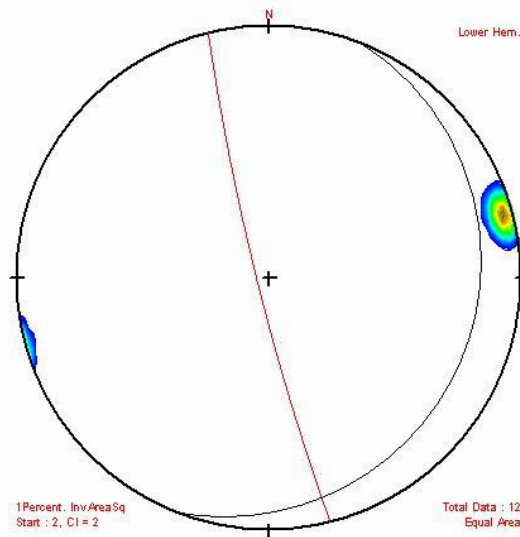
Site 73



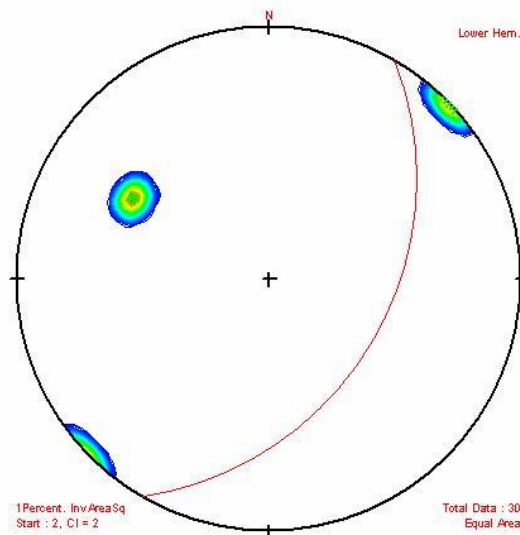
Site 74



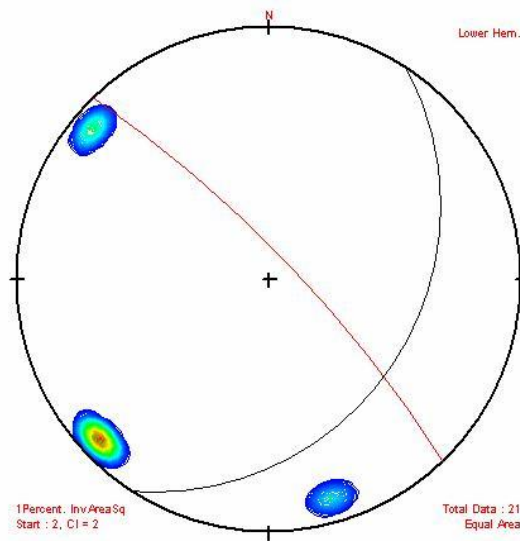
Site 75



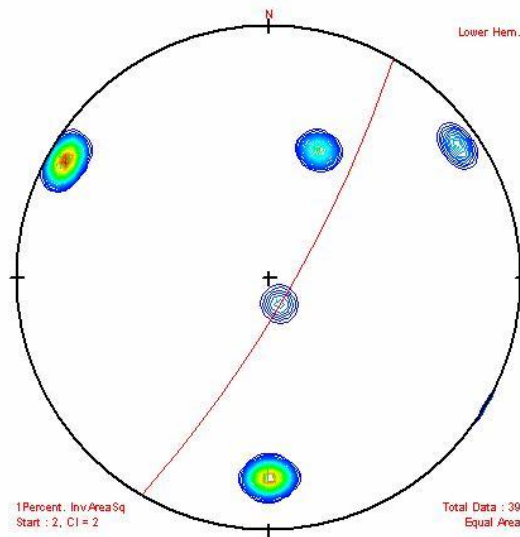
Site 76



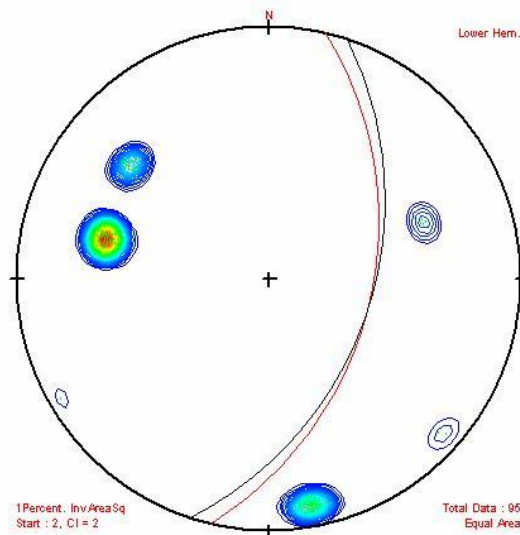
Site 77



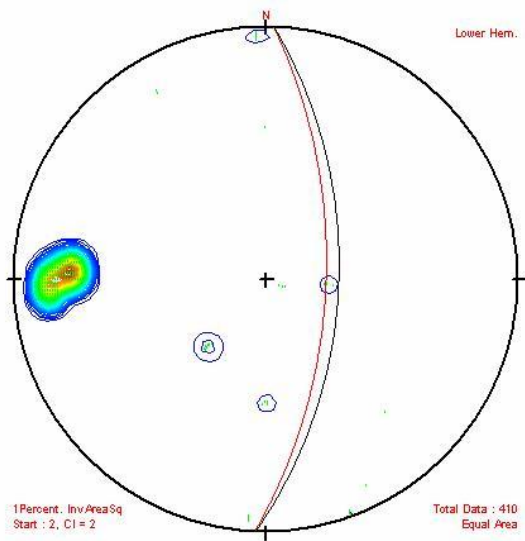
Site 78



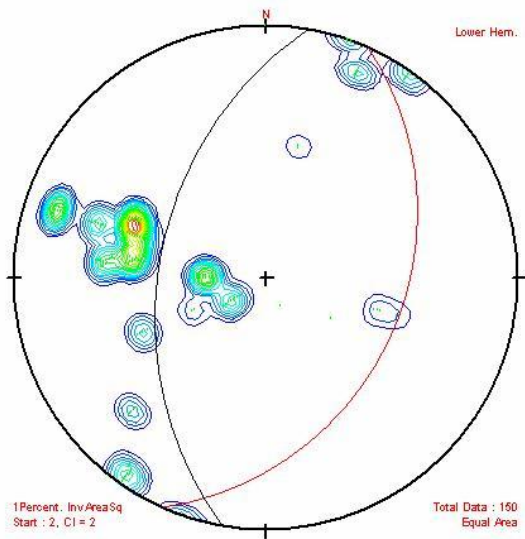
Site 79



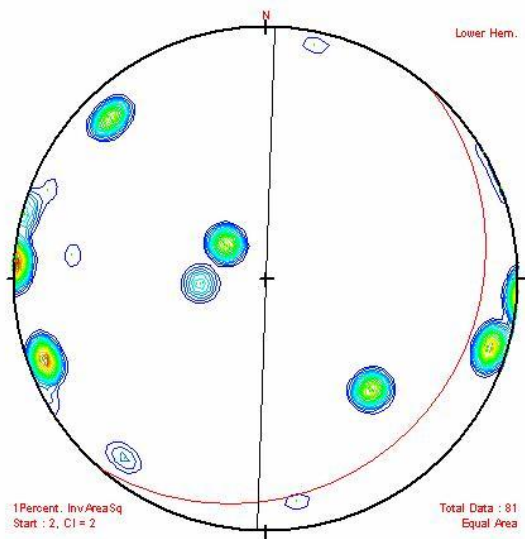
Site 80



Site 81

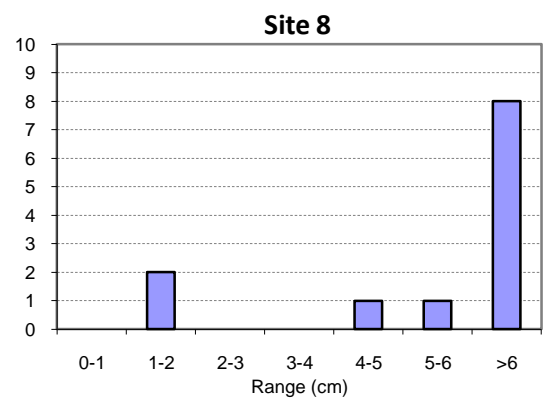
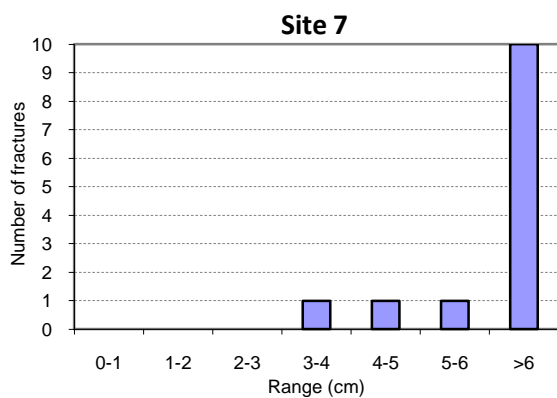
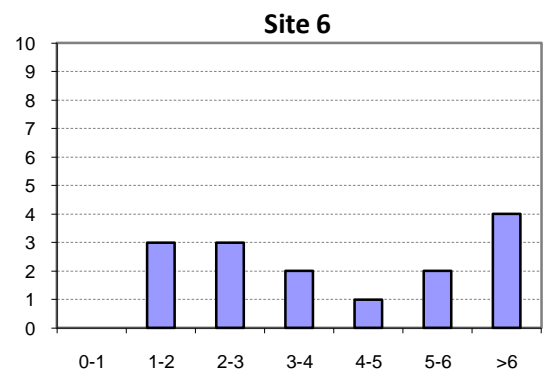
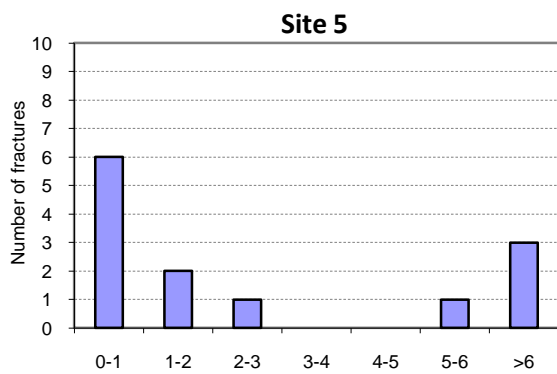
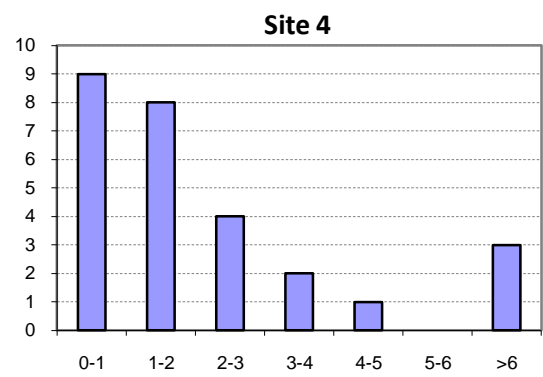
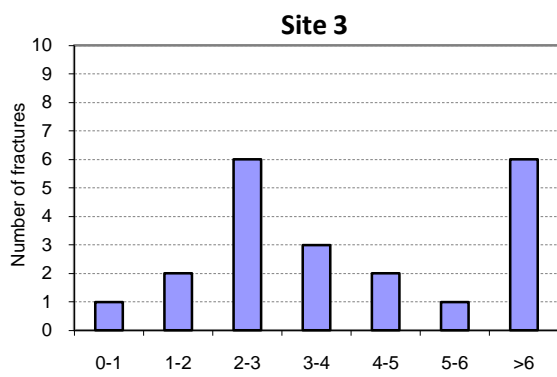
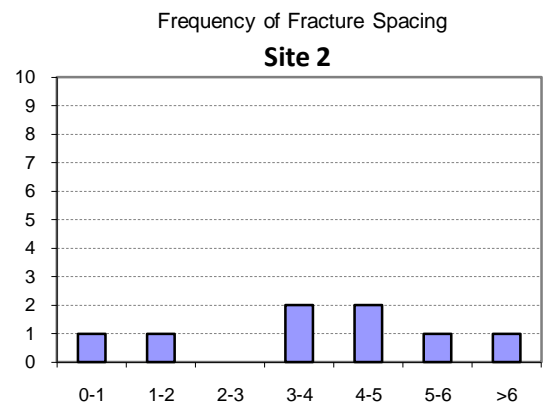
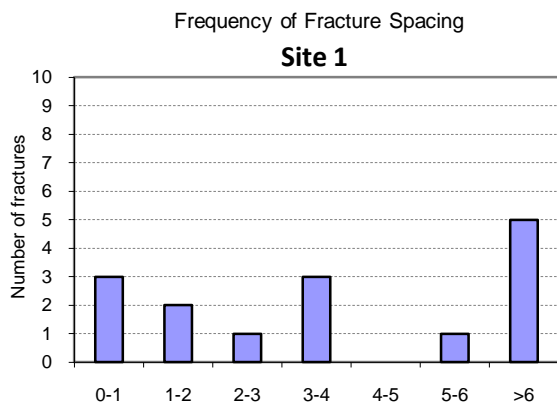


Site 82



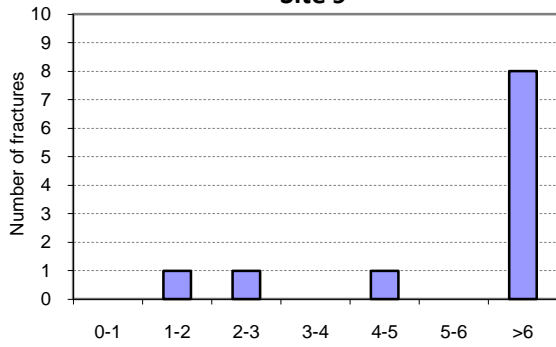
Site 83

***B. FRACTURE SPACING ANALYSIS***



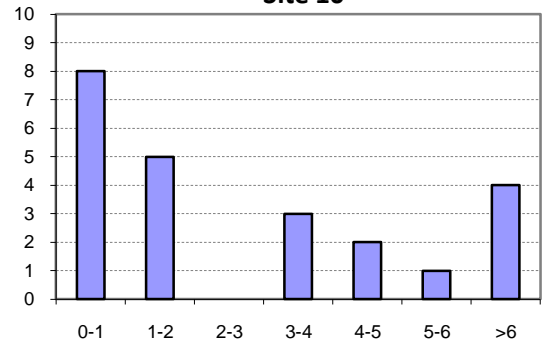
Frequency of Fracture Spacing

Site 9

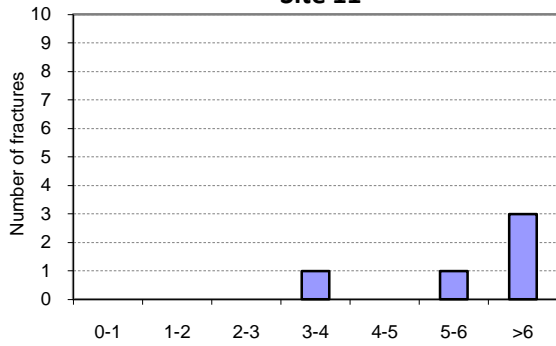


Frequency of Fracture Spacing

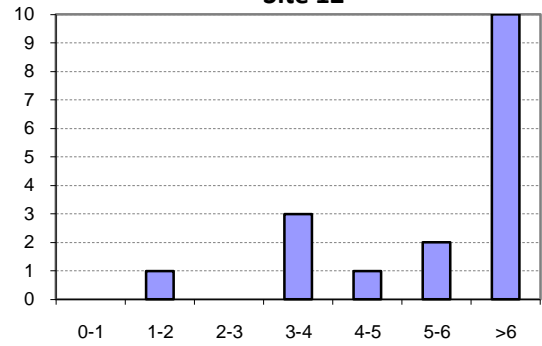
Site 10



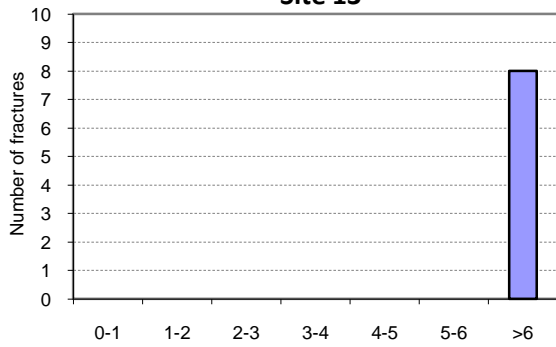
Site 11



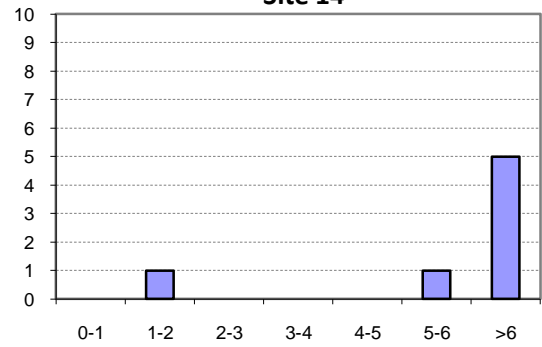
Site 12



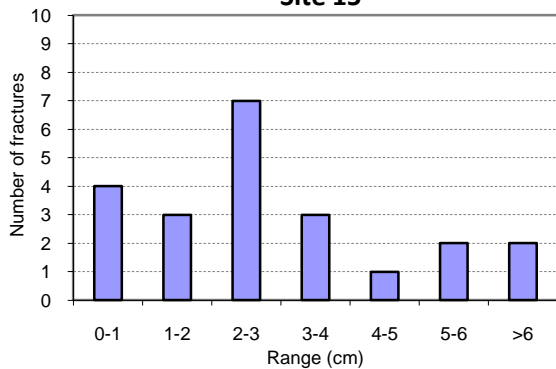
Site 13



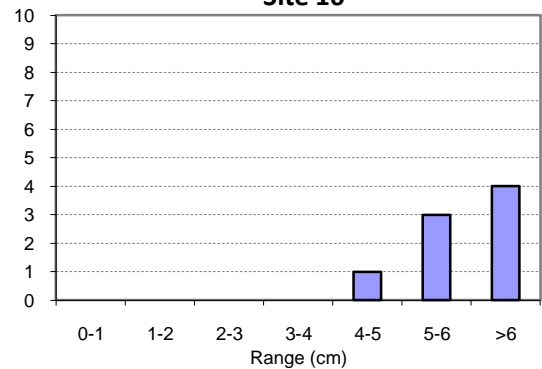
Site 14



Site 15

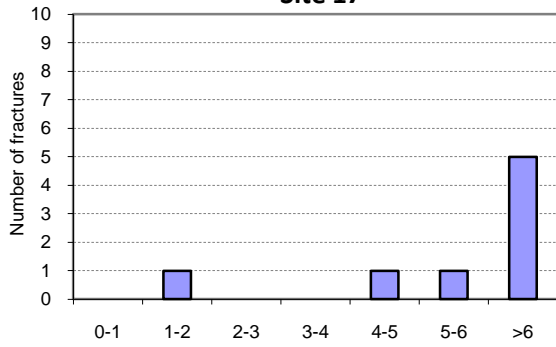


Site 16



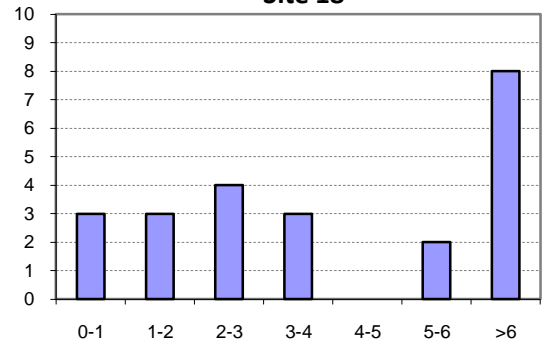
Frequency of Fracture Spacing

Site 17

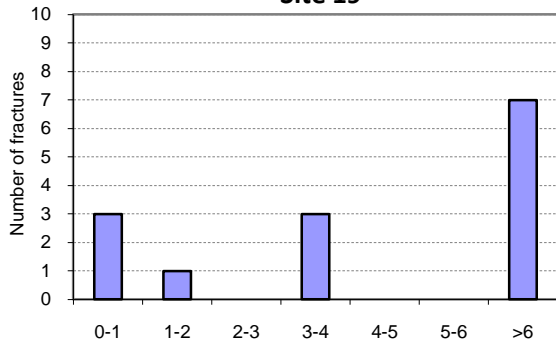


Frequency of Fracture Spacing

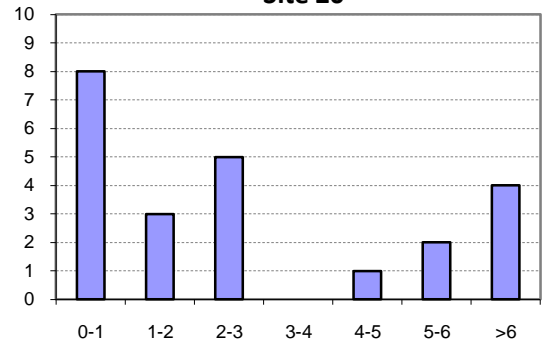
Site 18



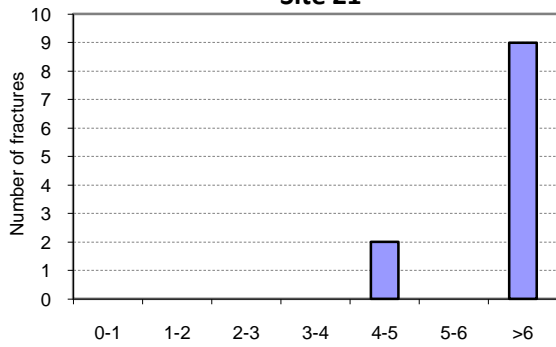
Site 19



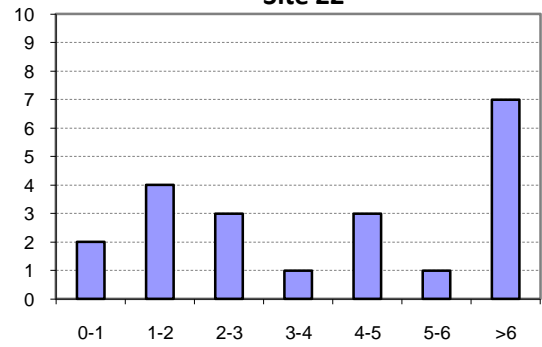
Site 20



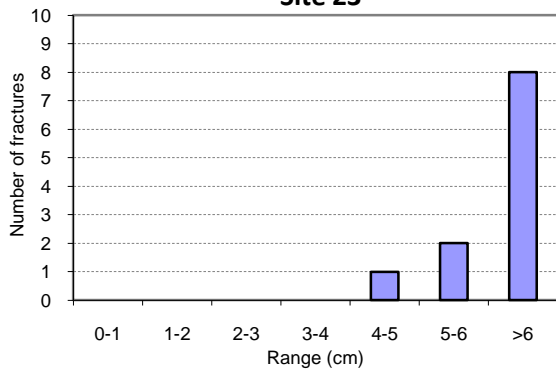
Site 21



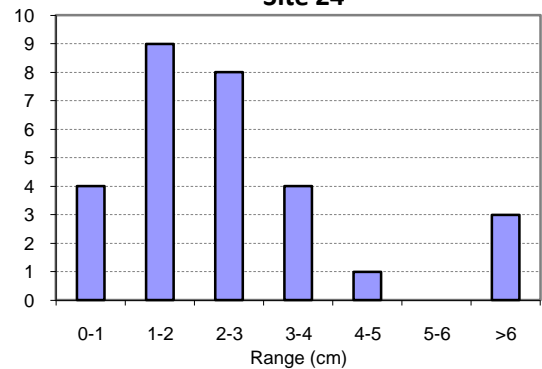
Site 22

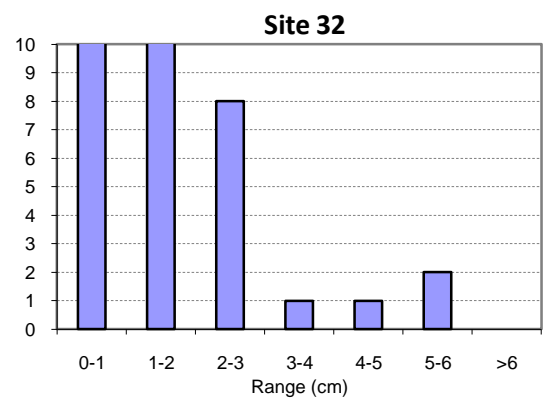
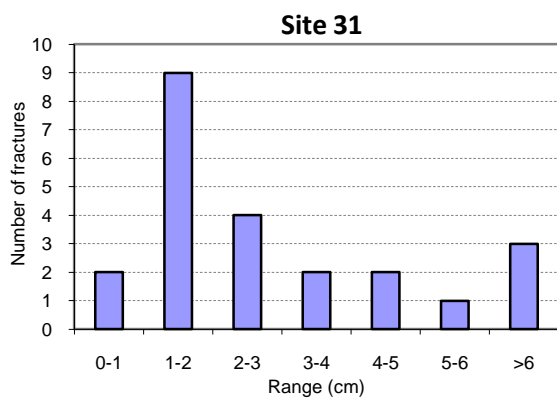
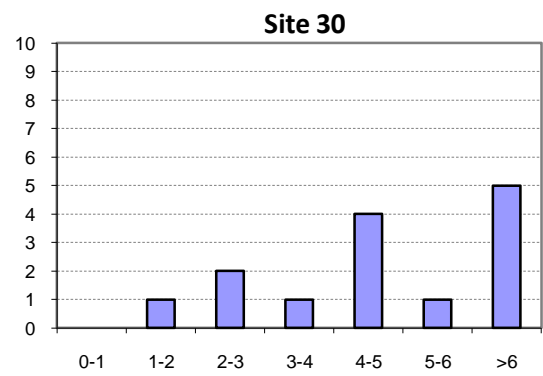
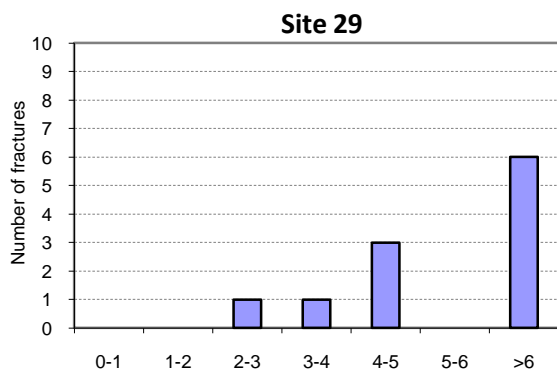
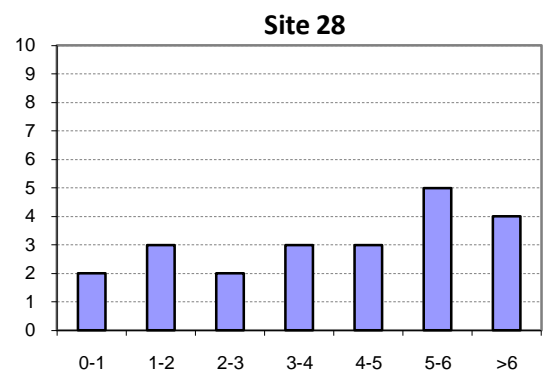
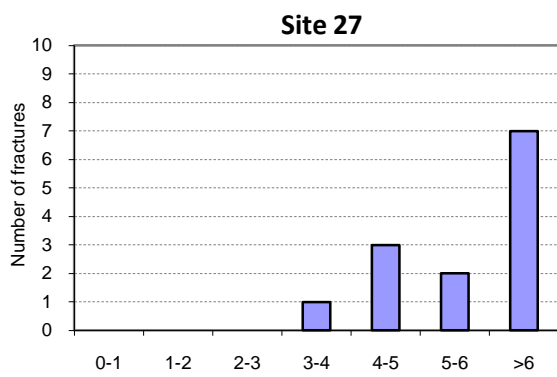
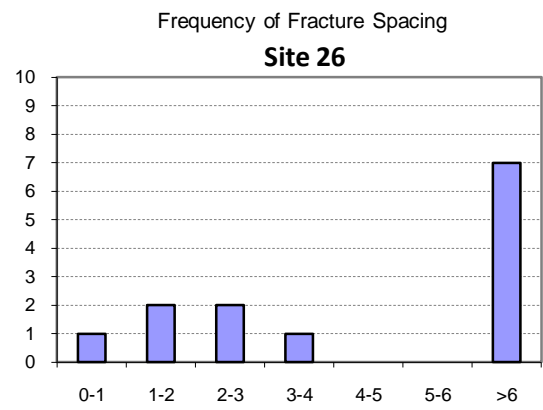
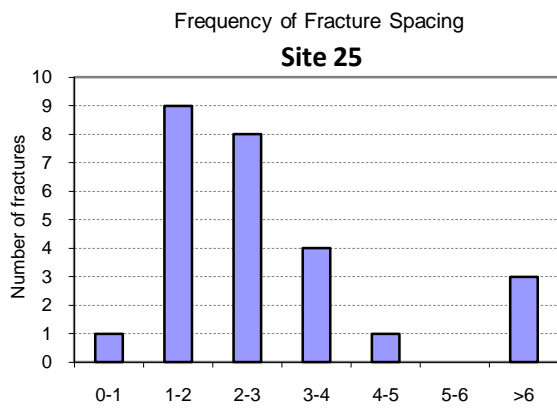


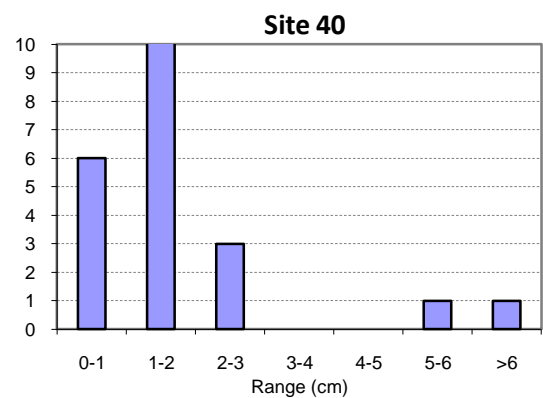
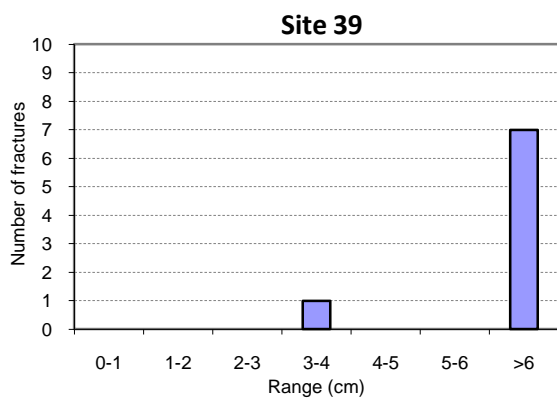
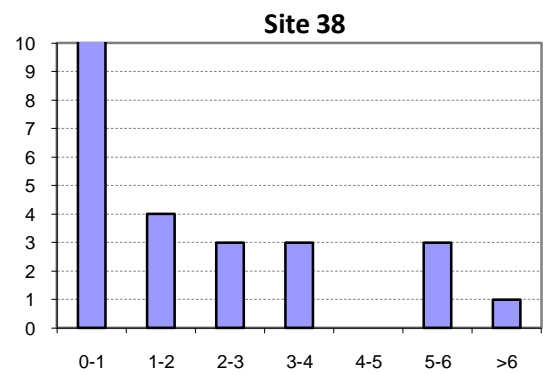
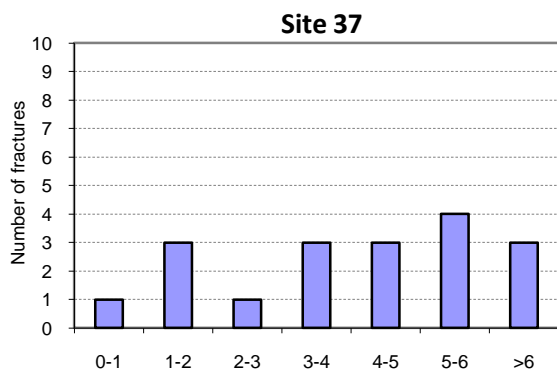
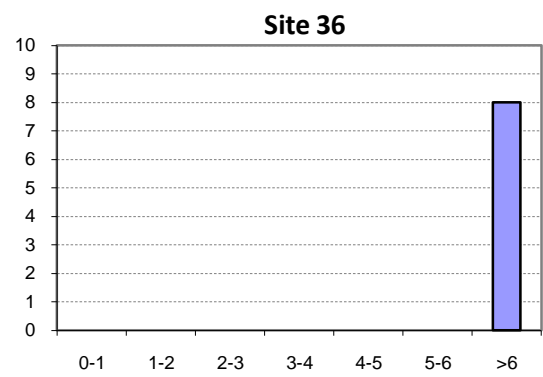
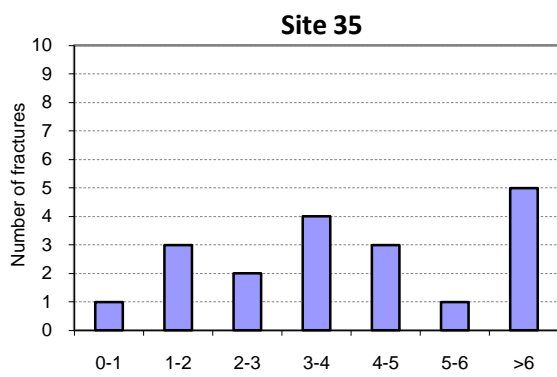
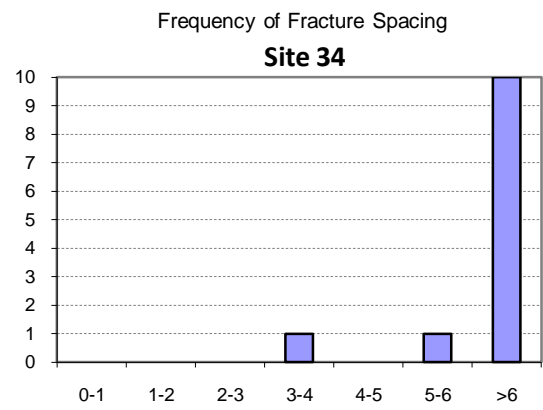
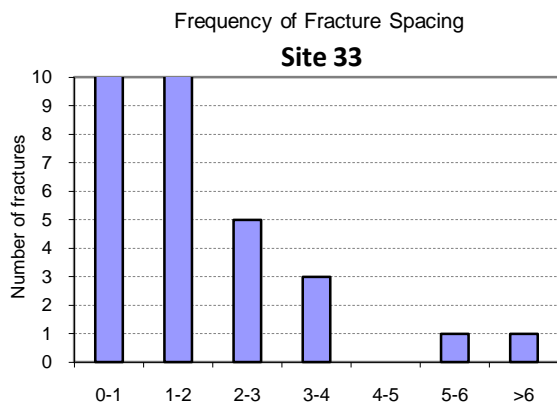
Site 23



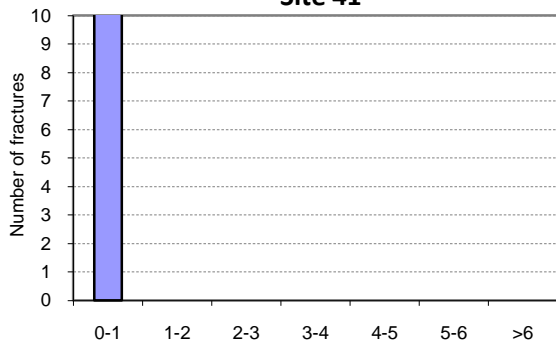
Site 24



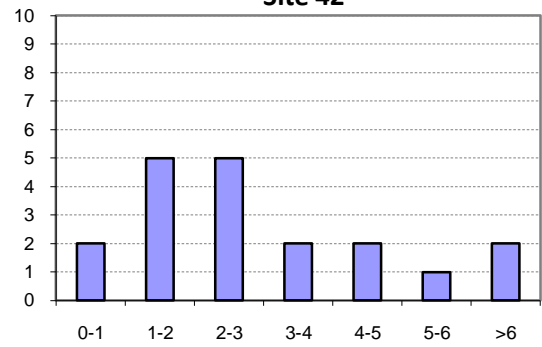




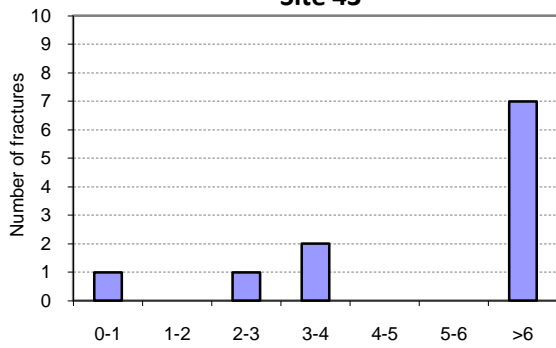
Frequency of Fracture Spacing  
**Site 41**



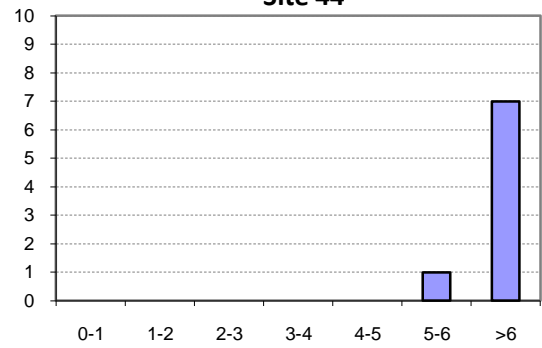
Frequency of Fracture Spacing  
**Site 42**



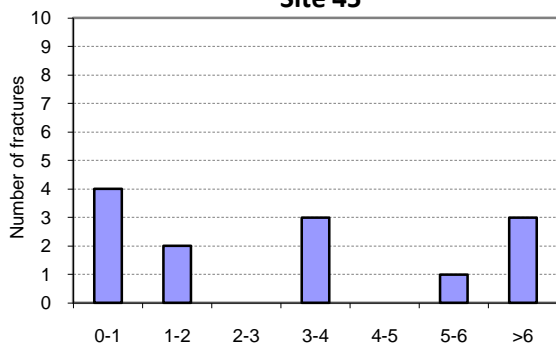
**Site 43**



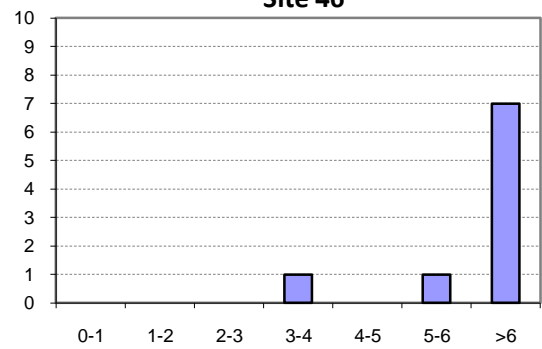
**Site 44**



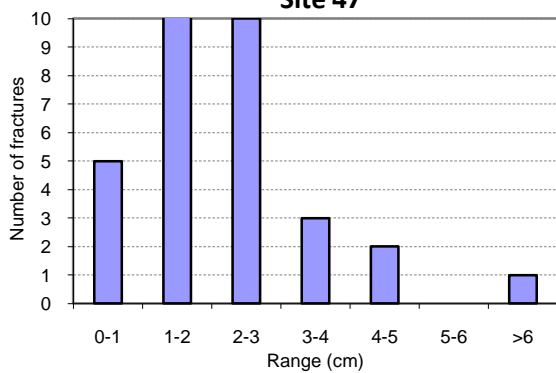
**Site 45**



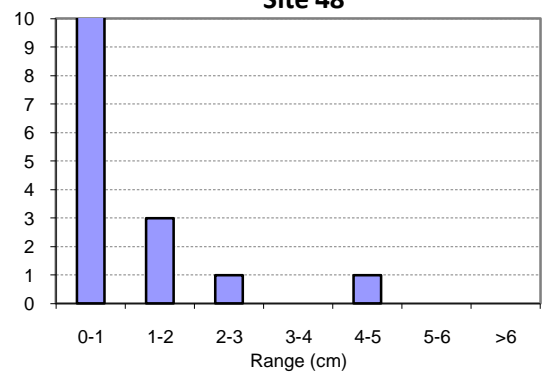
**Site 46**

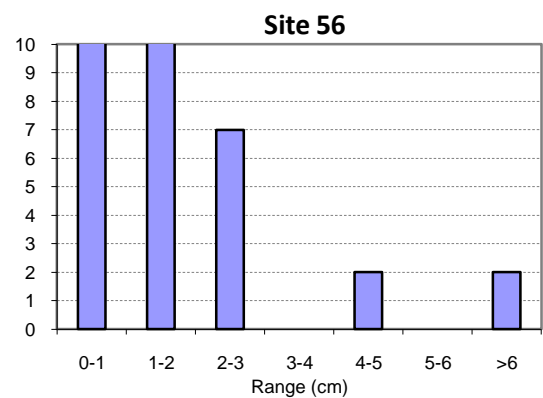
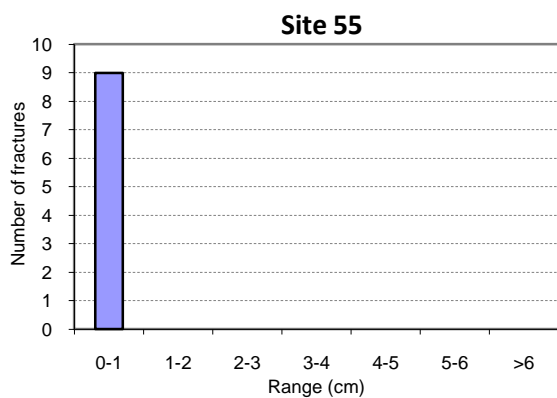
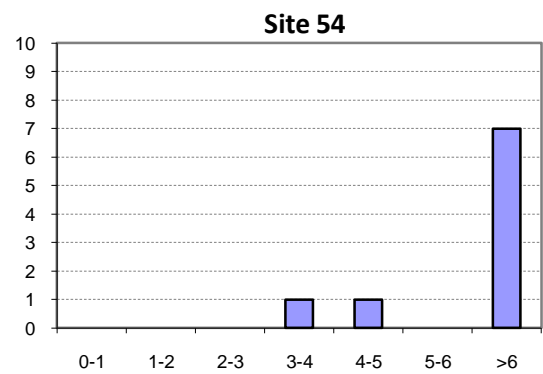
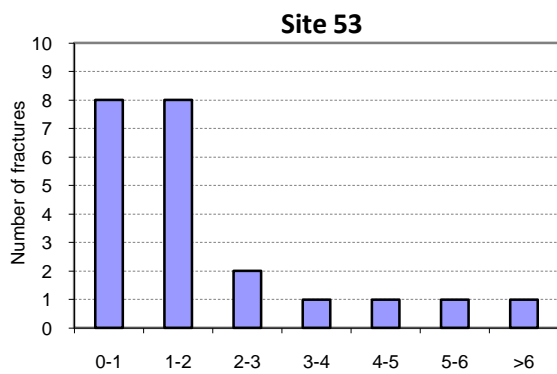
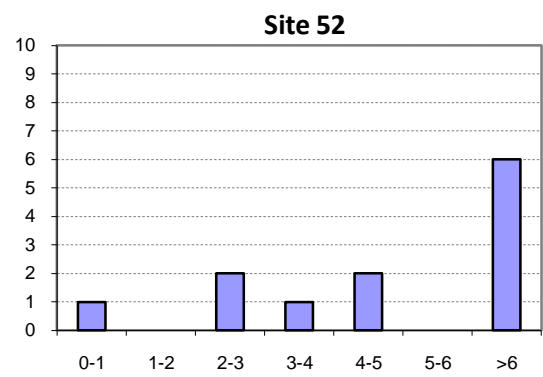
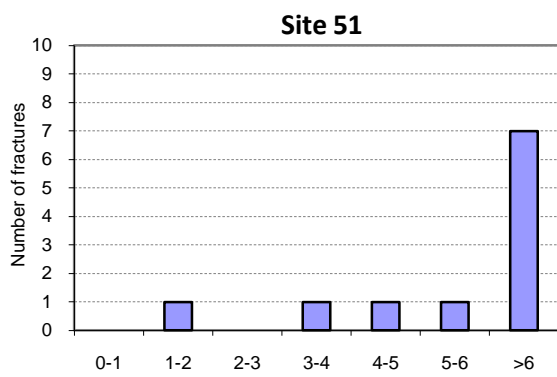
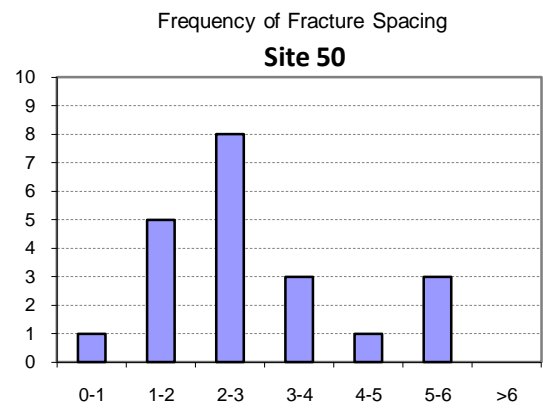
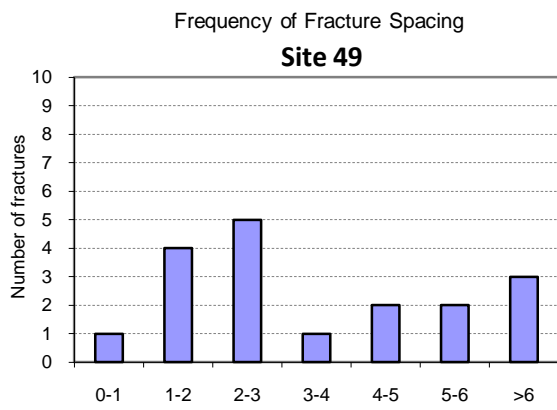


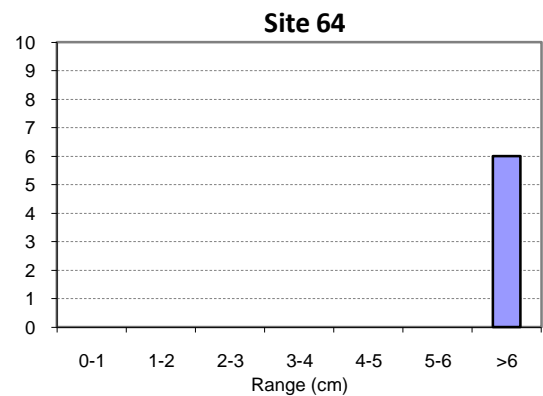
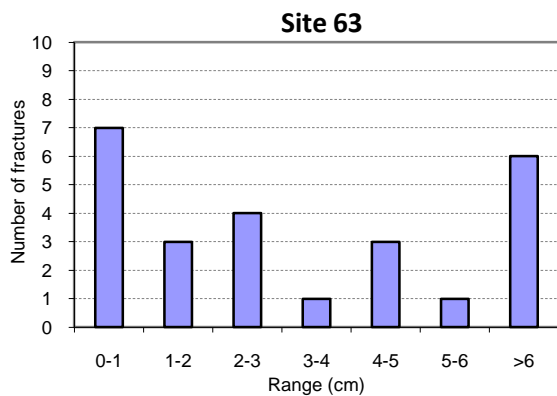
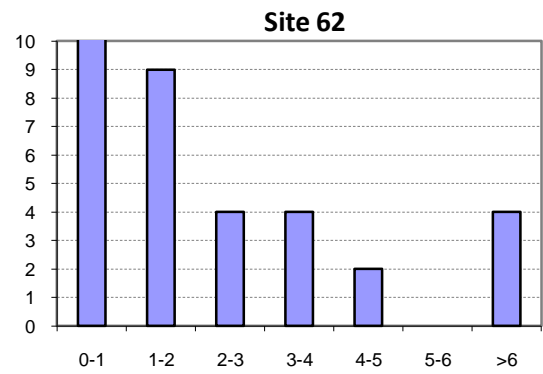
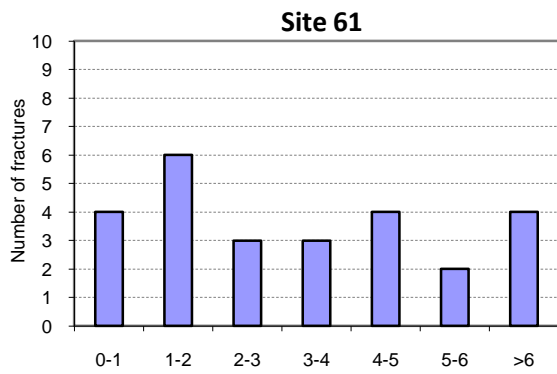
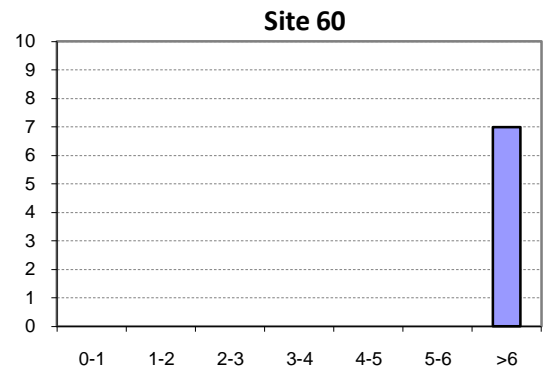
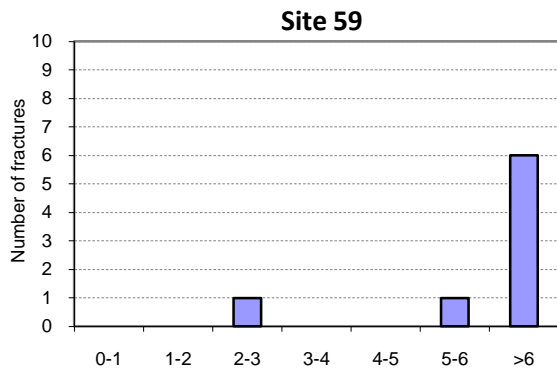
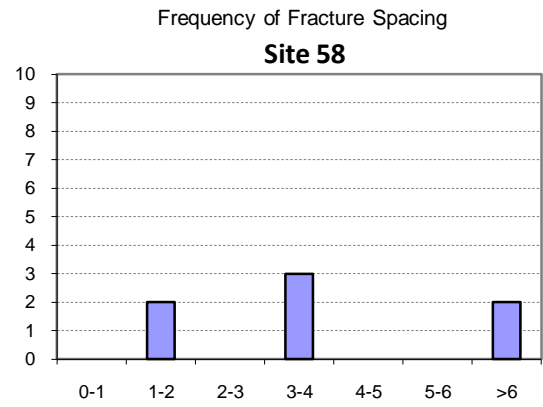
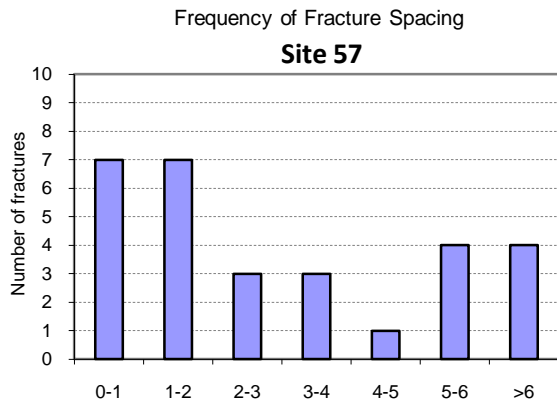
**Site 47**



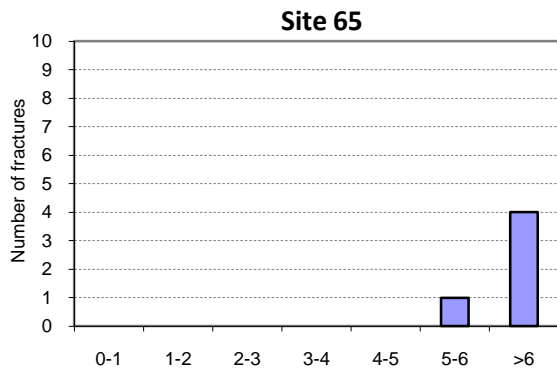
**Site 48**



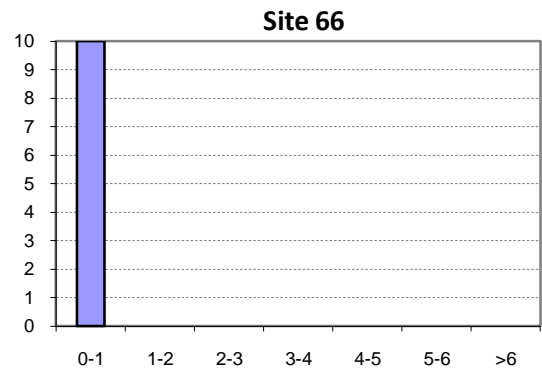




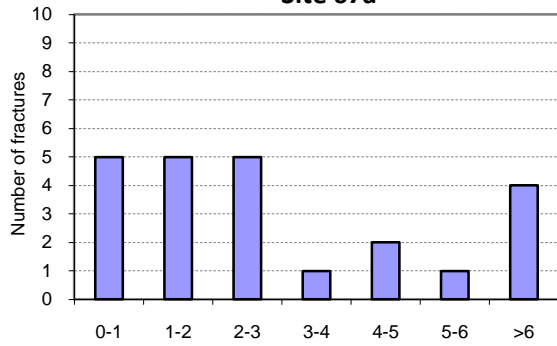
Frequency of Fracture Spacing



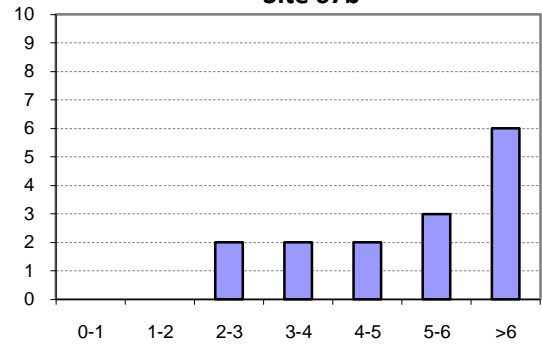
Frequency of Fracture Spacing



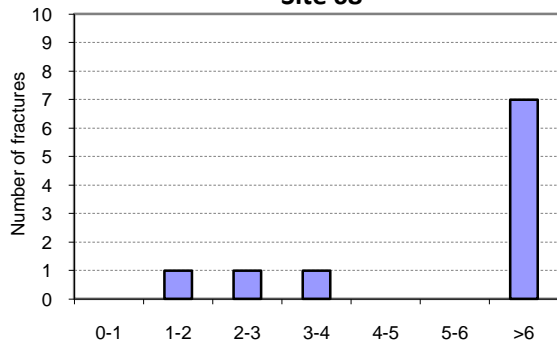
**Site 67a**



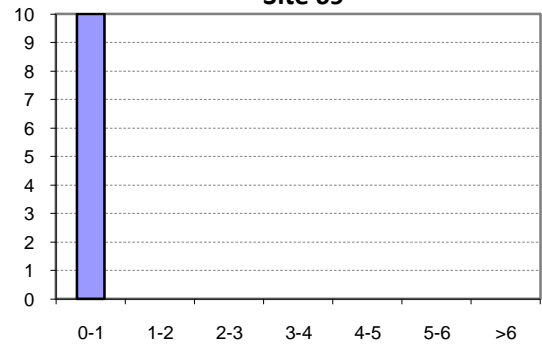
**Site 67b**



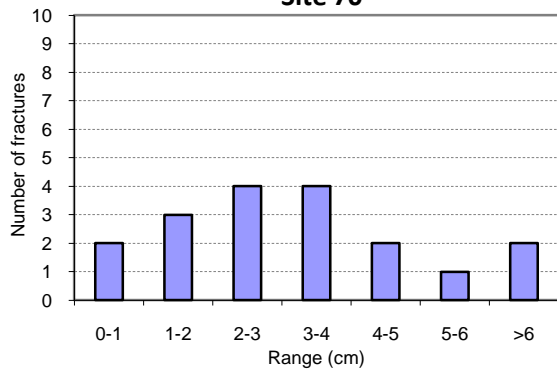
**Site 68**



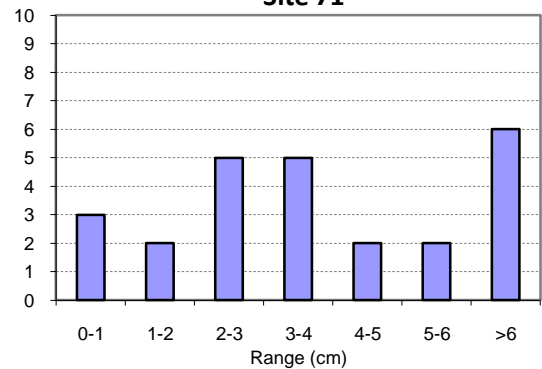
**Site 69**

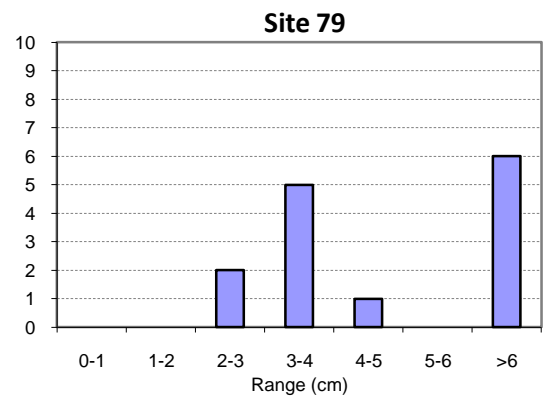
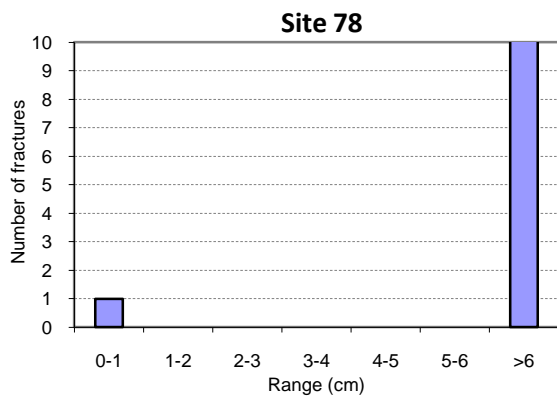
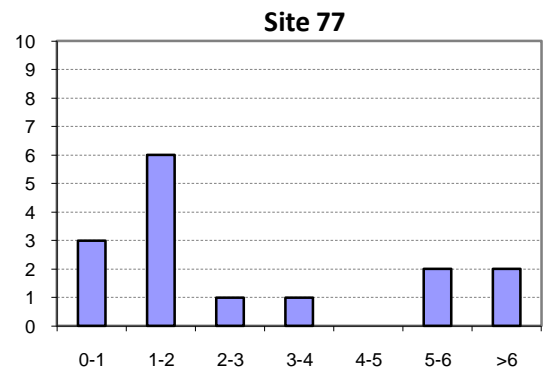
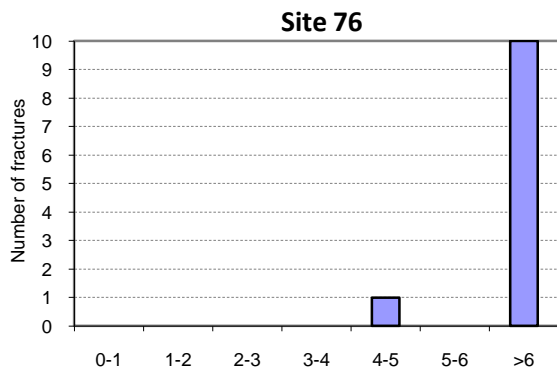
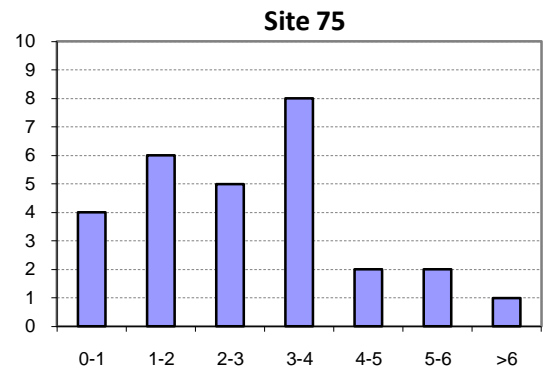
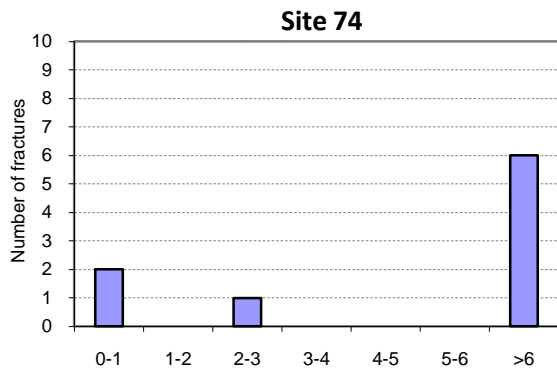
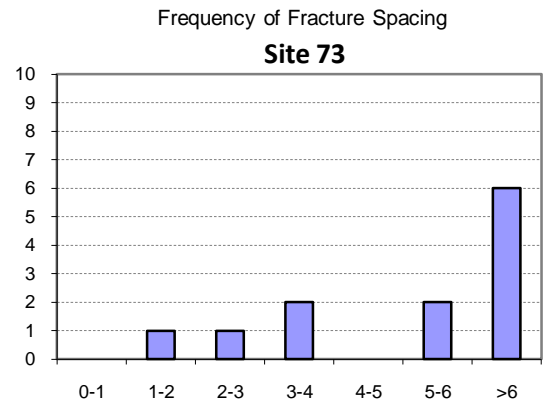
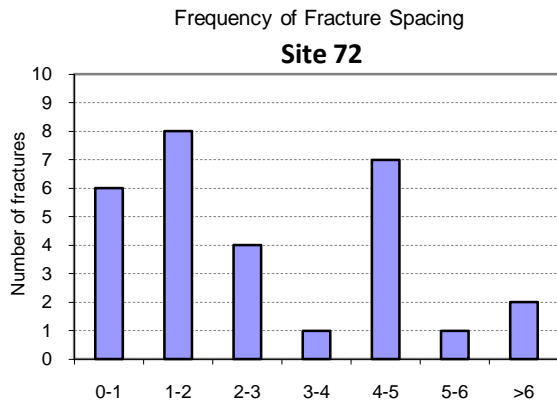


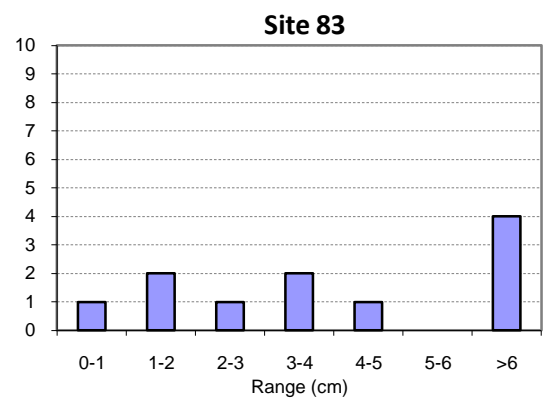
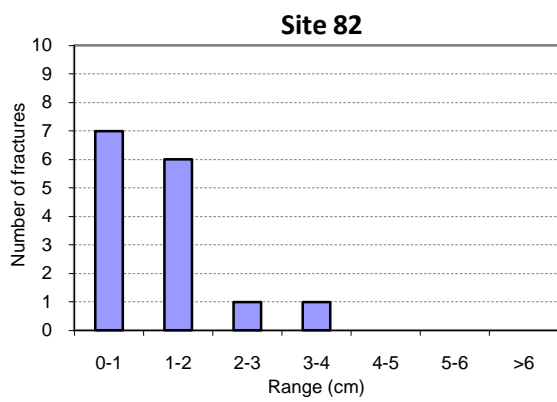
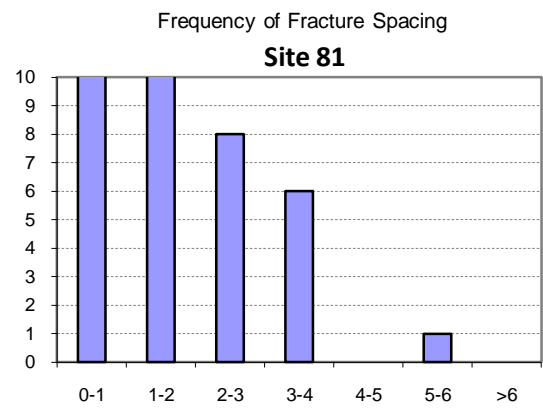
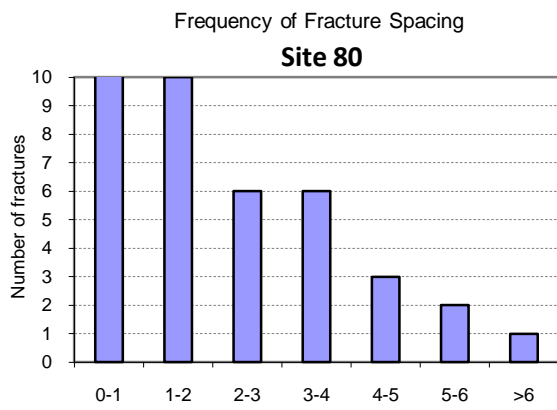
**Site 70**



**Site 71**







---

# UNITS OF MEASUREMENT

---

## Units of measurement commonly used (SI and non-SI Australian legal)

Name of unit	Symbol	Definition in terms of other metric units	Quantity
day	d	24 h	time interval
degree	°		
centimetre	cm	$10^{-2}$ m	length
hectare	ha	$10^4$ m <sup>2</sup>	area
kilometre	km	$10^3$ m	length
litre	L	$10^{-3}$ m <sup>3</sup>	volume
litres/second	L/s		
metre	m	base unit	length
millimetre	mm	$10^{-3}$ m	length
minute	min	60 s	time interval
second	s	base unit	time interval
year	Y	365 or 366 days	time interval

## Shortened forms

~      approximately equal to

---

# GLOSSARY

---

**Aquifer** — An underground layer of rock or sediment that holds water and allows water to percolate through

**Basin** — The area drained by a major river and its tributaries

**Benchmark condition** — Points of reference from which change can be measured

**Bore** — See 'well'

**Buffer zone** — A neutral area that separates and minimises interactions between zones whose management objectives are significantly different or in conflict (e.g. a vegetated riparian zone can act as a buffer to protect the water quality and streams from adjacent land uses)

**Catchment** — That area of land determined by topographic features within which rainfall will contribute to run-off at a particular point

**Conjunctive use** — The utilisation of more than one source of water to satisfy a single demand

**DWLBC** — Department of Water, Land and Biodiversity Conservation (Government of South Australia)

**EMLR** — Eastern Mount Lofty Ranges

**Erosion** — Natural breakdown and movement of soil and rock by water, wind or ice; the process may be accelerated by human activities

**Geological features** — Include geological monuments, landscape amenity and the substrate of land systems and ecosystems

**Geomorphology** — The scientific study of the landforms on the Earth's surface and of the processes that have fashioned them

**GIS** — Geographic Information System; computer software linking geographic data (for example land parcels) to textual data (soil type, land value, ownership). It allows for a range of features, from simple map production to complex data analysis

**Groundwater** — Water occurring naturally below ground level or water pumped, diverted and released into a well for storage underground; see also 'underground water'

**Hydraulic conductivity (K)** — A measure of the ease of flow through aquifer material: high K indicates low resistance, or high flow conditions; measured in metres per day

**Hydrogeology** — The study of groundwater, which includes its occurrence, recharge and discharge processes, and the properties of aquifers; see also 'hydrology'

**Hydrology** — The study of the characteristics, occurrence, movement and utilisation of water on and below the Earth's surface and within its atmosphere; see also 'hydrogeology'

**Impact** — A change in the chemical, physical, or biological quality or condition of a water body caused by external sources

**Irrigation** — Watering land by any means for the purpose of growing plants

**Metadata** — Information that describes the content, quality, condition, and other characteristics of data, maintained by the Federal Geographic Data Committee

**MLR** — Mount Lofty Ranges

**Model** — A conceptual or mathematical means of understanding elements of the real world that allows for predictions of outcomes given certain conditions. Examples include estimating storm run-off, assessing the impacts of dams or predicting ecological response to environmental change

**Monitoring** — (1) The repeated measurement of parameters to assess the current status and changes over time of the parameters measured (2) Periodic or continuous surveillance or testing to determine the level of compliance with statutory requirements and/or pollutant levels in various media or in humans, animals, and other living things

---

## GLOSSARY

---

**Natural recharge** — The infiltration of water into an aquifer from the surface (rainfall, streamflow, irrigation etc). See also recharge area, artificial recharge

**Natural resources** — Soil, water resources, geological features and landscapes, native vegetation, native animals and other native organisms, ecosystems

**NRM** — Natural Resources Management; all activities that involve the use or development of natural resources and/or that impact on the state and condition of natural resources, whether positively or negatively

**Observation well** — A narrow well or piezometer whose sole function is to permit water level measurements

**Permeability** — A measure of the ease with which water flows through an aquifer or aquitard, measured in  $\text{m}^2/\text{d}$

**Piezometer** — A narrow tube, pipe or well; used for measuring moisture in soil, water levels in an aquifer, or pressure head in a tank, pipeline, etc

**PIRSA** — Primary Industries and Resources South Australia (Government of South Australia)

**Potentiometric head** — The potentiometric head or surface is the level to which water rises in a well due to water pressure in the aquifer, measured in metres (m); also known as piezometric surface

**Prescribed water resource** — A water resource declared by the Governor to be prescribed under the Act, and includes underground water to which access is obtained by prescribed wells. Prescription of a water resource requires that future management of the resource be regulated via a licensing system.

**Recharge area** — The area of land from which water from the surface (rainfall, streamflow, irrigation, etc.) infiltrates into an aquifer.

**SA Geodata** — A collection of linked databases storing geological and hydrogeological data, which the public can access through the offices of PIRSA. Custodianship of data related to minerals and petroleum, and groundwater, is vested in PIRSA and DWLBC, respectively. DWLBC should be contacted for database extracts related to groundwater

**Sub-catchment** — The area of land determined by topographical features within which rainfall will contribute to run-off at a particular point

**Transmissivity (T)** — A parameter indicating the ease of groundwater flow through a metre width of aquifer section (taken perpendicular to the direction of flow), measured in  $\text{m}^2/\text{d}$

**Water allocation** — (1) In respect of a water licence means the quantity of water that the licensee is entitled to take and use pursuant to the licence. (2) In respect of water taken pursuant to an authorisation under s.11 means the maximum quantity of water that can be taken and used pursuant to the authorisation

**Well** — (1) An opening in the ground excavated for the purpose of obtaining access to underground water. (2) An opening in the ground excavated for some other purpose but that gives access to underground water. (3) A natural opening in the ground that gives access to underground water

**WMLR** — Western Mount Lofty Ranges

---

## REFERENCES

---

- Anderson, E.M., 1951. *The dynamics of faulting and dyke formation with application to Britain*. Oliver and Boyd, Edinburgh.
- Barton, C.A., Zoback, M.D. and Moos, D., 1995. Fluid flow along potentially active faults in crystalline rock, *Geology*, 23:683-686.
- Costar, A., Heinson, G., Wiilson, T. and Smith, Z., 2008. Hydrogeophysical mapping of fracture orientation and groundwater flow in the Eastern Mount Lofty Ranges, South Australia. Department of Water, Land and Biodiversity Conservation, Report DWLBC 2009/9.
- Costar, A., Heinson, G., and Wiilson, T., 2008. Hydrogeophysical mapping of fracture orientation and groundwater flow in the Wester Mount Lofty Ranges, South Australia. Department of Water, Land and Biodiversity Conservation, Report DWLBC 2008/32.
- Ferrill, D.A., Winterle, J., Wittmeyer, G., Sims, D., Colton, S. and Armstrong, A., 1999. Stressed rock strains groundwater at Yucca Mountain, Nevada. *GSA Today*, 9:1-8.
- Heidbach, O., Tingay, M., Barth, A., Reinecker, J., Kurfeß, D. and Müller, B., 2008. *The 2008 release of the World Stress Map* (available online at [www.world-stress-map.org](http://www.world-stress-map.org)).
- Hillis, R.R. and Reynolds, D., 2000. The Australian Stress Map. *Journal of the Geological Society, London*, 157:915-921.
- Hobbs, B.E., Means, W.D. and Williams, P.F., 1976. *An outline of structural geology*. John Wiley & Sons, New York.
- Love, A. J., 2003. Groundwater flow and solute transport dynamics in a jointed meta-sedimentary aquifer. PhD Thesis, Flinders University, South Australia (unpublished).
- Love, D., 1999. Recent Earthquakes in South Australia. Department of Primary Industries and Resources South Australia (PIRSA), MESA Journal 13. P 22-24.
- Love, D., 2001. Earthquakes in South Australia 2001: Adelaide, South Australia, Department of Primary Industries and Resources South Australia (PIRSA)
- Mortimer, L., Aydin, A., Simmons, C.T. and Love, A.J., 2008a. Primary and secondary controls on fracture and fracture permeability development. 2008 Western Pacific Geophysics Meeting Proceedings, American Geophysical Union, 29 July-1 August, Cairns, Australia
- Mortimer, L., Love, A.J., Aydin A. and Simmons, C.T., 2008b. The influence of past and present stress regimes on fracture permeability development and groundwater flow in fractured rock aquifers. Water Down Under 2008, Adelaide, South Australia, proceedings: 1855-1866.
- National Research Council (NRC), 1996. *Rock fractures and fluid flow. Contemporary understanding and applications*. National Academy of Sciences, Washington D.C.
- Preiss, W.V., 1995. Tectonic evolution of the Mid-North, South Australia: Clare Valley mid-conference excursion guide. Specialist Group in Tectonics and Structural Geology. *Geological Society of Australia Abstracts*, 40.
- Preiss, W.V., 2000. The Adelaide Geosyncline of South Australia, and its significance in continental reconstruction. *Precambrian Research*, 100:21-63.
- Quigley, M.C., Cupper, M.L. and Sandiford, M., 2006. Quaternary faults of south-central Australia: palaeoseismicity, slip rates and origin. *Australian Journal of Earth Sciences*, 53:285-301.

---

## REFERENCES

---

Sandiford, M., Wallace, M. and Coblenz, D.D., 2004. Origin of the in situ stress field of southeastern Australia. *Basin Research*, 16:325-338.

Zhang, X., Sanderson, D.J., Harkness, R.M. and Last, N.C., 1996. Evaluation of the 2-D permeability tensor for fractured rock masses. *International Journal of Rock Mechanics and Mining Sciences and Geomechanical Abstracts*, 33:17-37.